2015

Quantum Chemical Studies for the Engineering of Metal Organic Materials

Hector Javier Rivera Jacquez
University of Central Florida

QUANTUM CHEMICAL STUDIES FOR THE ENGINEERING OF METAL ORGANIC MATERIALS

by

HÉCTOR JAVIER RIVERA JACQUEZ
A.S. University of Puerto Rico, 2012
B.S. University of Puerto Rico, 2012
M.S. University of Central Florida, 2015

A dissertation submitted in partial fulfillment of the requirements
for the degree of Doctor of Philosophy
in the Department of Chemistry
in the College of Sciences
at the University of Central Florida
Orlando, Florida

Fall Term
2015

Major Professor: Artëm E. Masunov

ABSTRACT

Metal Organic Materials (MOM) are composed of transition metal ions as connectors and organic ligands as linkers. MOMs have been found to have high porosity, catalytic, and optical properties. Here we study the gas adsorption, color change, and non-linear optical properties of MOMs. These properties can be predicted using theoretical methods, and the results may provide experimentalists with guidance for rational design and engineering of novel MOMs. The theory levels used include semi-empirical quantum mechanical calculations with the PM7 Hamiltonian and, Density Functional Theory (DFT) to predict the geometry and electronic structure of the ground state, and Time Dependent DFT (TD-DFT) to predict the excited states and the optical properties.

The molecular absorption capacity of aldoxime coordinated Zn(II) based MOMs (previously measured experimentally) is predicted by using PM7 Theory level. The 3D structures were optimized with and without host molecules inside the pores. The absorption capacity of these crystals was predicted to be $8H_2$ or $3N_2$ per unit cell. When going beyond this limit, the structural integrity of the bulk material becomes fractured and microcrystals are observed both experimentally and theoretically.

The linear absorption properties of Co(II) based complexes are known to change color when the coordination number is altered. In order to understand the mechanism of this color change TD-DFT methods are employed. The chromic behavior of the Co(II) based complexes studied was confirmed to be due to a chain in coordination number that resulted in lower metal to ligand distances. These distances destabilize the occupied metal d orbitals, and as a consequence of this, the metal to ligand transition energy is lowered enough to allow the crystals to absorb light at longer wavelengths.

Covalent organic frameworks (COFs) present an extension of MOM principles to the main group elements. The synthesis of ordered COFs is possible by using predesigned structures andcarefully selecting the building blocks and their conditions for assembly. The crystals formed by these systems often possess non-linear optical (NLO) properties. Second Harmonic Generation (SHG) is one of the most used optical processes. Currently, there is a great demand for materials with NLO optical properties to be used for optoelectronic, imaging, sensing, among other applications. DFT calculations can predict the second order hyperpolarizability χ^2 and tensor components necessary to estimate NLO. These calculations for the χ^2 were done with the use of the Berry's finite field

approach. An efficient material with high χ^2 was designed and the resulting material was predicted to be nearly fivefold higher than the urea standard.

Two-photon absorption (2PA) is another NLO effect. Unlike SHG, it is not limited to acentric material and can be used development of in vivo bio-imaging agents for the brain. Pt(II) complexes with porphyrin derivatives are theoretically studied for that purpose. The mechanism of 2PA enhancement was identified. For the most efficient porphyrin, the large 2PA cross-section was found to be caused by a HOMO-LUMO+2 transition. This transition is strongly coupled to 1PA allowed Q-band HOMO-LUMO states by large transition dipoles. Alkyl carboxyl substituents delocalize the LUMO+2 orbital due to their strong π-acceptor effect, enhancing transition dipoles and lowering the 2PA transition to the desirable wavelengths range.

The mechanism 2PA cross-section enhancement of aminoxime and aldoxime ligands upon metal addition of is studied with TD-DFT methods. This mechanism of enhancement is found to be caused by the polarization of the ligand orbitals by the metal cation. After polarization an increase in ligand to ligand transition dipole moment. This enhancement of dipole moment is related to the increase in 2PA cross-sections.

ACKNOWLEDGMENTS

First of all, I would like to thank my adviser Dr. Artëm E. Masunov, for his patience and support during my graduate studies. Especially for teaching me how the academia really works, how to write papers, and for all the advices. Also I would like to state that it has been privilege of working on his group. Working this group has allow graduate school not to be only about acquiring knowledge on science but it has been in parallel to obtaining life experience and growing up.

I have to mention the unmeasured contribution of Dr. Alexander Balaeff with all his help and unmeasurable support for any idea I would present to him. Teaching me molecular dynamics, and making learning quantum mechanics a fun experience.

I specially would like to a special acknowledgement to our collaborators, Dr. Marina Fonari, Dr. Sergei Vinogradov and Dr. Fernando Uribe-Romo. I am also thankful to the members of my committee for their time and effort into increasing the quality of my research presentation. Special thanks to UCF stokes, NSF XSEDE, and NERCS for the computational resource and UCF library staff for getting all the papers not available in the database in prompt manner.

I would also like to specially acknowledge the chemistry department and Dr. Andres Campiglia for everything he has done for me during my time in this program. Dr. Campiglia has not only does his job as coordinator, but has been a voice of reason, logic and advice. Finally, I would like to thank the University of Central Florida for giving me the opportunity to join the program and perform my graduate studies.

I am thankful to Dr. Maristella Resto, Prof. Ramon Matos and for their countless support and advice when I was pursuing my undergraduate studies and graduate studies. Most importantly, I want to thank my parents for all the unconditional support, advice and knowledge they have given me all my life. Without them, this would had been nearly imposible.

TABLE OF CONTENTS

LIST OF FIGURES

LIST OF TABLES

LIST OF FORMULAS

CHAPTER 1: QUANTUM THEORY FOR THE PROPERTY PREDICTION AND ENGINEERING A NON-LINEAR OPTICAL MATERIALS PROPERTIES

1.1 Introduction

Everything in our surroundings is composed of atoms, and these atoms combine to form molecules. According to the composition and shape of these molecules, different physical and chemical properties are observed. In order to study molecular properties in a plethora of systems, quantum chemical theories are applied to predict and exploit these properties and apply them into solutions to material and engineering problems in multiple disciplines.

Quantum mechanics as a physical answer to a chemical problem, rather than something complex and abstract. The studies recompiled in this dissertation are the outcome of multidisciplinary research using quantum mechanics to answer questions in chemistry, and biology resulting in a doctoral degree formally in Chemistry. The calculations performed were done via computational methods.

The use of these methods is possible due to the constant increase of computing power, along with the recent development of new computational tools which allows molecular simulations to explore atomistic details in dept. Most of

these computational tools are commercially available packages, and have proven to be effective in the study chemically relevant problems. The main emphasis of the research recompiled here is the application of *ab initio* quantum chemical calculations into the prediction of these structures and properties.

This is important because successful analysis of the source of the materials properties can lead development of novel materials with the desired properties or the optimization of current materials. Therefore, this dissertation deals with both published and unpublished theoretical aspect of the work performed during my time during doctoral studies.

In chapter two, concerns the application of our knowledge of the coordination of bulky ligands into d^{10} metals resulting in a metal organic framework (MOF). This MOF provides a loosely packed crystal structure that possesses voids within the crystal lattice for inclusion of small guest molecules. These types of materials can be used for storage or molecules. Consequently, we focus in the study of the absorption capacity of these voids for guess molecules in the unit cell.

For this work, a Semi-Empirical Quantum Chemical method were used calculate the structure energetic changes after inserting the guess molecules into the crystal structure voids. Our calculations were in agreement with experimental data, hence we successfully predicted how many molecules could fix into the voids of the crystal structure.

Chapter three with aid our experimentalist collaborators with theoretical prediction for their recently synthesized compounds. These compounds were transformable 2D Co^{+2} coordination polymers and these polymers are based on thio-nicotinamide and 1,4-benzendicarboxylic acid. They observed significant dynamic structural changes initiated by the removal of both non-coordinated and coordinated solvent molecules, which resulted in an observed color change.

As a result of that, we had the following goals: 1) to predict the structure of a crystal which quality was not good enough for the X-Ray diffraction method but lattice parameters were measured, 2) to study the mechanism of that color change of the crystal structures by analyzing the linear optical properties.

Chapter four study a couple of acentric crystal structure to be used for second harmonic generation. For this DFT calculations are performed using CPMD software. Optimized

materials designed successfully can be used for a diverse array of applications.

Chapter five uses quantum chemical (QM) methods to understand the mechanism of non-linear optical enhancement on different ligands independently, and on a metal-organic complex. The significance of this work lies in the contribution of mechanism of enhancement to aid in the current demand for non-linear optical (NLO) materials for diverse technological applications.

In the six chapter, the electronic properties of π-extended porphyrins are study resulting in the design of novel phosphorescent sensors for oxygen imaging to study the brain. When designing these sensors, we must take into consideration that the light propagation window in biological tissues is a complex function of scattering and absorption, which in turn, is dependent on cellular structure and molecular composition.

For this reason, a beam with strong intensity could harm the biological tissue. This leads to the need to study non-linear optical properties such as two-photon absorption (2PA) materials for biological applications. 2PA is the simultaneous absorption of two photons by a molecular system. Our target molecules for the design of 2PA material were porphyrins, and during these studies we found the mechanism

of enhancement of 2PA cross-sections for the range of the wavelength desired.

In the following chapter we will review the theory and methods used to simulate the properties described in this work. This includes the basis of quantum chemistry, the corrections and approximations used to accurately and efficiently describe some the properties materials. In the latter chapters the works presented, can be applied for the rational design of chromophores and storage materials.

1.2 Wave Function Theory

Ever since Isaac Newton postulated the laws of classical mechanics in the seventeenth century, scientist and engineers have been able accurately describe the motions of many systems. The main piece of invaluable information provided by Newton's classical mechanics[1] is the precise trajectory and momentum of the system. In addition to that, the energy of the system's vibrational, translational and rotational degrees of freedom are able to be excited proportionally to the force applied to the system. When the system was excited, this transitions occurred from a state X_i to any other state X_{i+n}, without having to go through intermediate states.

However, in the nineteenth century irrefutable experimental evidence demonstrated the failure of classical mechanics to describe systems on the atomic level. This was clearly shown in multiple experiments attempting to understand the behavior of light[2-6] shown in many introductory chemistry and physics textbooks.

In order to interpret these experiments, scientist required the use of a particle model to describe the results obtained instead of the commonly accepted wave model. This led to the development of new concepts and equations which merged the postulates of the particle and wave models. These new set of concepts and equations took into account the dual particle-wave nature of atomic particles, and this later resulted in the development of quantum mechanics[7].

It is important to note that these new concepts would only work for atoms and not macroscopic system like classical mechanics. This is because if the wave model is used on an object that possesses great mass in respect to an atom, their wavelength become undetectably small due to their high momentum. Therefore their wavelength are negligible and the wave properties are not observed.

Quantum theory takes into account the dual behavior of atoms by replacing the concept of a trajectory in a definite

path for the concept of a wave being smeared through space (probabilistic). Erwin Schrödinger proposed a partial differential equation which leads to the solution of the wave function of any system[8]. In addition, this wave function contains all the information that can be known about the system it represents. Regrettably, the Schrödinger equation cannot be solved exactly for multi-electron systems. Therefore, there have been great effort from the theorist in the last decades to develop accurate approximations to the solutions of this equation.

$$\hat{H}\psi = E\,\psi \qquad (1)$$

In this equation ψ is the wave function describing the particle of interest, $\hat{H}$ is the Hamiltonian operator, and E is the energy of the system. The Hamiltonian operator describes the energy of the system by operating the wave function in respect to the kinetic and potential energy of the system. After this operation, we shall obtain an eigenvalue corresponding to the energy of the system.

In the set of these E, there must be such E that corresponds to the lowest state of our system. If we impose our system to the criteria of the variational principle. The variational principle implies there must be such function that minimizes which minimizes the values of the functions

which depends on such function. Therefore, the energy of the system must have its minimum value after the operations. Since the ground state wave function possesses the lowest energy possible, we can clearly conclude that the variational principle yields the ground state energy of our wave function.

$$E_0 \leq \frac{\langle \psi | \hat{H} | \psi \rangle}{\langle \psi | \psi \rangle} \quad (2)$$

In addition, the quality of the wave function obtained can be assessed. The main challenge in this task is that when taking into consideration multi-particle systems such as big atoms or molecules, a coupled interactions between the attraction of the nuclei and the repulsion of the electrons has to be taking into account. Therefore, this implies that all the particles are coupled to each other, or correlated.

In order to simplify this the Born-Oppenheimer approximation is applied[9]. The purpose of this approximation is to simplify the system by separating the electrons from the nuclei therefore uncoupling the system. The fundamental though of this approximation lies on the fact that the nuclei is much larger than the electron, for this reason we can assume that the nuclei is fixed and the electronic movement is instantaneous in respect to the nuclei. The Hamiltonian operator for this approximation is given by:

$$\hat{H} = \left[\hat{T} + \hat{U} + \hat{K}\right] = \left[\left[\sum_{i}^{N} -\frac{\hbar}{2m}\right]\nabla_i + \sum_{i}^{N} U(\vec{r_i}) + \sum_{i<j}^{N} K(\vec{r}_i, \vec{r}_j)\right] \quad (3)$$

Even though this approximation eliminates one factor of the correlation, the fact that electrons are correlated to each other still remains. In order to build the simplest wave function possible, the electron correlation can be ignored and the system can be considered as a nuclei and a single electron in a three dimensional space. The representation of this system must be constructed by finding an arbitrary function which can be represented by a linear combination of other functions. These other functions are called basis set, and for our purposes will represent atomic orbitals.

Noting that the square of the wave function has units of probability density, it is possible to map the most likely position of the electron to be found.

$$\psi = \sum_{i=1}^{N} \alpha_i \, \varphi_i \quad (4)$$

Therefore, the selection of our wave functions must indeed allow the electrons to be where the probability density is higher. Observing equation 4, it is possible to induct a physical meaning for the coefficient as a mechanism to allow these N basis functions to be spanned around the molecular

orbital space. This approach is the linear combination of atomic orbitals (LCAO)

In 1928 Hartree[10] proposed a theoretical approximation to solve three body problem on the Helium atom. He took the assumption that each electron feels the presence of the other electrons on its surrounding as an average (mean) field. This theory does not take into consideration the electron correlation, but it does provides the foundation of the self-consistent field method (SCF). This method guesses an initial wave function φ for all occupied orbitals, and uses this wave function to construct one electron hamiltonian operator Ћ, which in turn provides a new set of wave functions ψ after operation. This new wave functions ψ are presumed to be different and more accurate than the initial wave functions. Taking those newly guesses wave functions, the density distribution of all the electrons ρ is generate.

This process is repeated until the new wave function falls below a certain threshold criteria, thus yielding a final set of wave functions. This final process is referred as convergence of SCF orbitals and yields the optimized molecular structure of the system.

The limitation of this theory lies in the fact that quantum particles are indistinguishable from one another.

Implying that if a molecular orbital which contains two electrons, and if these particles must have unique quantum numbers, then these two electrons must be antisymmetric to one another to have a different spin quantum number[11-12].

Even though relativistic quantum mechanics provided a comprehensive mathematical treatment, in 1929 Slater[13] found a wave to simplify the construction of antisymmetric wave function by exploiting algebraic properties of matrices. One of such properties consist on taking the determinant of a matrix and, forming a permutation, as consequence the determinant changes signs. Therefore, an antisymmetric condition could be enforced for all the possible combinations of the molecular wave function. Shortly after this, Fock proposed to extend Hartree SCF theory method to include Slater's treatment into molecular wave functions. As a consequence of this the Hartree-Fock method is postulated[14-15]. One of the accomplishment of this method is that the electrons are become paired up and the correlation disappears for the ground state, but this theory leaves a very complex set of equations to be solved, leaving physicist with a desired to find an simpler alternative to wave function methods.

1.3 Density Functional Theory

Density Functional Theory[16] (DFT) is the result from the efforts of finding simpler alternatives to wave function methods. Starting from analysis of the nature of the hamiltonian operator itself, meaning that the operation performed depends on the position and the atomic numbers of our molecular system. This means that a hamiltonian operator can be built in some way that the electron density ρ will have a local maxima which depends on the nuclei coordinates acting as point charges. Therefore, this proves that information about a system molecular system (wave functions, eigenvalues etc.) could be obtained from known electronic density, suggesting possible simplifications to the wave function theory.

The way this idea work is by integrating density to obtain the number of electrons and then correlating the energy to the density. This energy can be obtained by applying an external potential (the charges and position of the nuclei) to the known density. The first theorem supporting DFT was postulated was Hohenberg-Kohn variational principle[17]. Similar to wave function theory, the process starts by guessing an initial s density which integrates to the

respective number of electrons in the system. Therefore, the density will determinate which candidate wave function and hamiltonian are the correct candidates to evaluate the energy expectation values. A main assumption to do this is that the starting point is an initial guess fictitious system of non-interacting electrons, which their ground state density is exact to some reference system. Similar to wave function theory this value must be greater or equal to the ground state energy. In order to do this the Kohn-Sham Self-consistent field methodology[17] is used to solve Kohn-Sham equations such as the one as shown in equation 5.

$$Ъ\boldsymbol{\psi}_i(\boldsymbol{r}) = \boldsymbol{\xi}_i\boldsymbol{\psi}_i \quad \textbf{(5)}$$

This methodology implies that the hamiltonian operator Ъ should be built in a way that the potentials are given for a non-interacting system of electrons. However, this system is considered as a sum of one-electron operators which in turn, possesses slater determinant based eigenfuctions. Finally, the eigenvalues ξ are the sum of the one electron eigenvalues.

In order to analyze the terms in our energy functional (which is a function which depends on other functions inside this function), as shown in equation 6.

$$E[\rho(r)] = \left(\sum_{i}^{N} \left\langle X_i \left| \frac{1}{2} \nabla_i^2 \right| X_i \right\rangle - \langle X_i | \sum_{k}^{nuclei} \frac{Z_k}{|r_i - r_k|} \right| X_i \rangle \right) + \sum_{i}^{N} \langle X_i | \frac{1}{2} \int \frac{\rho(r')}{|r_i - r'|} dr' | X_i \rangle + E_{exch}[\rho(r)] \quad (6)$$

In this equation the first term represents the kinetic energy, the second the nuclei attraction, the third the electronic repulsion, and the fourth term represent the exchange correlation energy. This exchange correlation energy is not limited to accounting for the difference between classical and quantum mechanical electron-electron repulsion, but also accounts for the difference in the kinetic energy between the guess non-interacting system and the real system. Many exchange functionals with different parameters have been developed using different approximations and amount of HF exchange energies.

Even though DFT is a powerful exact method, it is limited to the ground state, if excited states are to be considered a correction to DFT equations must be implemented. Time Dependent DFT (TD-DFT) is a correction to the DFT method which takes into account the evolution of a system after it interacts with a potential. Therefore, TD-DFT obtains their stationary ground state from the description provided by Kohn-Sham.

This density is operated by the time-evolution operator and results in a system described as a field that changes over time after a perturbation is applied. The Kohn-Sham equations for TD-DFT is shown in equation 7.

$$Ъ\boldsymbol{\psi_i}(\boldsymbol{r},\boldsymbol{t}) = \boldsymbol{i}\frac{\boldsymbol{\partial}}{\boldsymbol{\partial t}}\boldsymbol{\psi_i}(\boldsymbol{r},\boldsymbol{t}) \quad \textbf{(7)}$$

A significant portion of this dissertation consist in the use of TD-DFT for the theoretical prediction of optical materials properties such as two-photon absorption.

1.4 Two-Photon Absorption

The main concern of my studies consist in the design and optimization of non-linear optical responses, more specifically two photon absorbing materials. Two photon absorbing materials are materials that absorb two photon simultaneously as shown in figure 1. This absorption is possible in organic materials due to the nature of π conjugation. Conjugated systems can behave like semiconductors due to the π orbitals being delocalized and moving the charge across the conjugated chain. It is of considerable interest to study the charge transfer capacity of these compounds as a function of the length of conjugation,

symmetry fluctuations, and effects of external fields using theoretical methods.

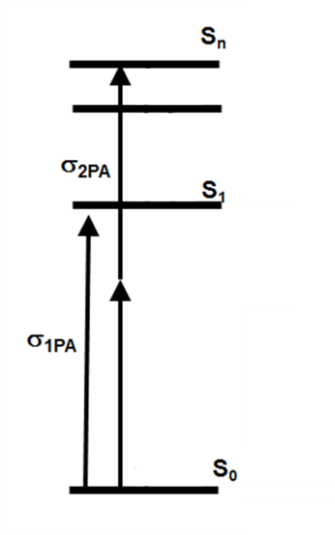

Figure 1 Jablonski Energy diagram describing 1PA and 2PA processes.

Excited state spectroscopic properties can be studied following the density change from the ground state to the excited state as consequence of the evolution of the system after an oscillating field (such as a laser) and obtain spectroscopic information about the compound. Optical properties can be described as a susceptibility tensor ξ and expressed the Taylor expansion series to obtain the polarization vector components V_i as the dipole moment as a unit of volume resultant from the electric field components E and η is the dielectric constant as shown in equation 8.

$$\boldsymbol{V_i = \eta\left(\xi_{ik}^{(1)}E_k + \frac{1}{2}\xi_{ikl}^{(2)}E_kE_{il} + \frac{1}{6}\xi_{iklm}^{(3)}E_kE_lE_m \ldots\right)} \quad \textbf{(8)}$$

In order to ease the computational cost and time this expansion is truncated according to the power of the field in which observables of interest lie in the molecular system. When only the first term is considered the method is considered as linear response DFT or just TD-DFT. In order to produce a successful prediction of non-linear photonic processes, several formalism must be employed to obtain the excitation energies and transition dipoles.[18]

In the past the perturbation theory provided a relation between non-linear properties of the ground state with a sum-over-states expression (SOS).[19] When the ground state is described by DFT with perturbation method, the linear terms from the susceptibility tensor result in a non-Hermitian eigenvalue system of equations, in which the matrixes A and B represent the basis when occupied (i, j) and vacant (a,b), when the Kohn Sham orbitals have a sub set of σ, τ (σ, τ = α , β electrons), and K is the coupling matrix expressed as the second derivative of the exchange correlation functional ω, Coulomb and exchange integral and the transition density is block diagonal with the occupied-vacant ($\hat{X} = \xi_{ia}$) and vacant-occupied ($\hat{Y} = \xi_{ai}$) blocks being nonzero as shown in equation 9-11.

$$\begin{bmatrix} \boldsymbol{A} & \boldsymbol{B} \\ -\boldsymbol{B} & -\boldsymbol{A} \end{bmatrix} \begin{bmatrix} \widehat{\boldsymbol{X}} \\ \widehat{\boldsymbol{Y}} \end{bmatrix} = \boldsymbol{\Omega_\alpha} \begin{bmatrix} \widehat{\boldsymbol{X}} \\ \widehat{\boldsymbol{Y}} \end{bmatrix} \Rightarrow \boldsymbol{A\widehat{X} + A\widehat{Y} = \Omega\widehat{X} + \Omega\widehat{Y}} \quad (9)$$

$$\boldsymbol{A_{ai\sigma,bj\tau} = \delta_{ab}\delta_{ij}\delta_{\sigma\tau}(\varepsilon_a - \varepsilon_i) + K_{ai\sigma,jb\tau}} \quad (10)$$

$$\boldsymbol{B_{ai\sigma,bj\tau} = K_{ai\sigma,jb\tau}} \quad (11)$$

In this formalism we obtain the information of matrix A and B. Matrix A consist of the interactions between singly excited states, and matrix B after indices are swapped provides information about the de-excitation from a virtual to an occupied orbital.

The perturbation treatment can also possess several corrections to the expectation values of an arbitrary operator in terms of the response functions. These additional corrections can be used to obtain transition dipole moments from the ground state into the excited states expressed through the ground state dipole moment $\mu_{0,0}$.

A well-known formalism is the Tamm-Dancoff Approximation (TDA)[20-21] is used to obtain the state-state transition dipoles $\mu_{\alpha,\beta}$, difference between permanent ground state dipole moments, state-state transition dipole moments and permanent dipole moments of the excited states. This formalism consist of in neglecting the de-excitation matrix B in the non-Hermitian eigenvalue equation (equation 9) as consequence doubly excited states and exchange-correlation coupling terms disappear and other formalism must be employed.

In order to correct the TDA deficiencies the coupled electronic oscillator (CEO) formalism is applied as used by Masunov and Tetriak et al[22]. This formalism solves the Hamiltonian-Liouville classical equations of motions for the density matrix. When first order terms in the external field are conserved this formalism is equivalent to linear response, but when the second order is considered, the solutions are found in the linear response transition densities. Therefore, the linear excitations remain unchanged in the quadratic formalism and the combined states retain their double-excited nature.

As a consequence of this, the excitation energy for each of these new states is equal to the sum of single excitations ($\Omega_{\alpha\beta} = \Omega_\alpha + \Omega_\beta$) and the an-harmonic coupling terms in the linear response excitation which constitute the transition dipoles between the excited states as product of single excitation densities $\xi_\alpha \xi_\beta$. The second order CEO yields the transition dipole moments between the ground state and the doubly excited state expressed as summations over all the states as shown in equation 12.

$$\boldsymbol{\mu_{0,\alpha\beta}} = \sum_{\boldsymbol{\alpha\beta}}^{\boldsymbol{perm}} \boldsymbol{tr}(\hat{\boldsymbol{\mu}}(\hat{\boldsymbol{I}} - \boldsymbol{2\rho})\boldsymbol{\xi_\alpha}\boldsymbol{\xi_\beta} + \sum_{\boldsymbol{\gamma>0}} \left(\frac{\boldsymbol{V_{\alpha\beta-\gamma}\mu_\gamma}}{\boldsymbol{\Omega_\alpha + \Omega_\beta - \Omega_\gamma}} - \frac{\boldsymbol{V_{\alpha\beta\gamma}\mu_{-\gamma}}}{\boldsymbol{\Omega_\alpha + \Omega_\beta + \Omega_\gamma}} \right) \quad \textbf{(12)}$$

The first summation considers symmetrized permutations of the indices, the second summation runs to all excited states, $\hat{I}$ is the identity matrix, ρ is the ground-state density matrix, and $V_{\alpha\beta\mp\gamma}$ correspond to the exchange-correlation coupling term expressed via Kohn-Sham operators V(ξ) on transition densities as shown in equation 13.

$$\boldsymbol{V_{\alpha\beta-\gamma} = \sum_{\alpha\beta\gamma}^{perm} tr((\hat{I} - 2\rho)\xi_\alpha \xi_\beta V(\xi_\gamma)} \quad \textbf{(13)}$$

When the Tamm-Dancoff Approximation is executed *a posteriori* as introduced by Mikhailov et al[23] preventing the loss the manifold of the excited states between non related transition dipoles and ground state dipole moment available as shown in equation 14.

$$\boldsymbol{\mu_{\alpha,\beta} = tr(\hat{\mu}(\hat{I} - 2\rho)\xi_\alpha^* \xi_\beta)}$$
$$\boldsymbol{\Delta\mu_\alpha = tr(\hat{\mu}(\hat{I} - 2\rho)\xi_\alpha^* \xi_\alpha)} \quad \textbf{(14)}$$

Therefore, after eliminating the B de de-excitation matrix and $\hat{Y}$ terms from equation 9 *a posteriori*, neglects the exchange correlation coupling terms as an approximation to the second order CEO yielding the excitation energies ξ as $\begin{bmatrix} \hat{X} \\ 0 \end{bmatrix}$.and the double-excited states are introduced with the following excitation energies and transition dipoles as shown in equation 15.

$$(\boldsymbol{\Omega_{\alpha\beta} = \Omega_{\alpha} + \Omega_{\beta}})$$

$$\boldsymbol{\mu_{0,\alpha\beta} = tr(\hat{\mu}(\hat{I} - 2\rho)\xi_{\alpha}^{*}\xi_{\beta})}$$

$$\boldsymbol{\mu_{\alpha,\alpha\beta} = \mu_{\beta}\,, \mu_{\alpha,\alpha\beta} = 0} \qquad \textbf{(15)}$$

After applying this treatment a hybrid between the TDA and CEO is obtained, allowing the calculation of second-order properties using simple modifications to current exiting linear response codes to predict 2PA cross-sections.

The probability of absorption of two photon from a given material is quadratically proportional to the intensity of the beam and the cross section is dependent on the imaginary part of the susceptibilities therefore we can obtain the following set of simplified equations for the cross section of one-photon absorption (equation 16) and two-photon absorption (equation17)

$$\boldsymbol{\sigma_{1PA} = \frac{4\pi\hbar\omega}{\eta c}\, Im\, \langle \xi^{(1)}(-\omega, \omega)\rangle} \qquad \textbf{(16)}$$

$$\boldsymbol{\sigma_{2PA} = \frac{4\pi^2\hbar\omega}{\eta^2 c^2}\, Im\, \langle \xi^{(3)}(-\omega, \omega, \omega, -\omega)\rangle} \qquad \textbf{(17)}$$

In which $\hbar$ is Plank's constant, η is the dielectric constant, ξ is the susceptibility, c is the speed of light and ω is the frequency of the irradiation. Using the cross-sections equation we can proceed to find probability for one and two photon absorption as shown in equation 18.

$$P_{1PA} = \sigma_{1pa} \cdot t\, x\, \frac{I}{\hbar\omega}$$

$$P_{2PA} = \sigma_{2pa} \cdot t\, x\, \frac{I^2}{\hbar\omega} \quad (18)$$

In these equations σ is the cross-section, I is the intensity, $\hbar$ is Plank's constant and ω is the frequency of the irradiation. The equations just mentioned, can be modified in order to compute the orientationally averaged 2PA cross-sections for a linearly polarized beam by using the transition dipoles previously obtained between excited states $|X\rangle$ and $|Y\rangle$, are using in a sum-over-states transition matrix elements components expression[24] $M_{\alpha\beta}^{\gamma}$ shown in equation .19 and 20.

$$\sigma_{2PA}(\omega) = \frac{16\pi^3\omega^2}{15c^2\eta^2} \sum_{\gamma} \sum_{\beta}^{x,y,z} \sum_{\alpha}^{x,y,z} \left(M_{\alpha\alpha}^{\gamma} M_{\beta\beta}^{\gamma} + 2M_{\alpha\beta}^{\gamma} M_{\alpha\beta}^{\gamma} \right) \delta_{\gamma}(2\omega) \quad (19)$$

$$M_{\alpha\beta}^{\gamma} = \frac{1}{2\hbar} \sum_{x} \frac{\langle Y|\mu_{\alpha}|X\rangle\langle X|\mu_{\beta}|0\rangle}{\left(\omega_{oX} - \frac{\omega_{0Y}}{2}\right) - i\Gamma_{X0}} + \frac{\langle Y|\mu_{\beta}|X\rangle\langle Y|\mu_{\beta}|0\rangle}{\left(\omega_{oX} - \frac{\omega_{0Y}}{2}\right) - i\Gamma_{X0}} \quad (20)$$

In these equations α and β run over the three dimensional space, the ground state is represented by $|0\rangle$, and $|X\rangle, |Y\rangle$ describe the 1PA and 2PA excited states respectively. The factor $\left(\omega_{oX} - \frac{\omega_{0Y}}{2}\right)$ expresses the detuning between the 1PA state and the 2PA state, and $i\Gamma_{X0}$ is the damping constant taken to be 0.1eV, along with $\delta_{\gamma}(2\omega)$ which accounts for the linewidths

for experimentally observed broadening and it is usually taken to be as 0.1eV.

1.5 Conclusions

In conclusion to this chapter, the evolution of the Schrödinger wave equation has been stated until the development of DFT. The methodology implemented to TD-DFT to research non-linear optical properties has been presented. This is used to understand the mechanism generating the optical properties. This is done by plotting the KS orbitals, analyzing the charge transfers and mechanism of stabilization of the excited state. After the mechanism is understood, it can be optimized with functional groups and engineered to obtain materials with the desired properties.

1.5 List of References

1. I., N., Philosophiae Naturalis Principia Mathematica. **1800**.

2. Planck, M., Ueber Das Gesetz Der Energieverteilung Im Normalspectrum. *Annalen der Physik* **1901**, *309*, 553-563.

3. Einstein, A., Über Einen Die Erzeugung Und Verwandlung Des Lichtes Betreffenden Heuristischen Gesichtspunkt. *Annalen der Physik* **1905**, *322*, 132-148.

4. Bohr, N., I. On the Constitution of Atoms and Molecules. *Philosophical Magazine Series 6* **1913**, *26*, 1-25.

5. L., d. B., Ondes Et Quanta. *Compt. Ren.* **1923**, *177*, 507.

6. Bose, S. N., Plancks Gesetz Und Lichtquantenhypothese,. *Z. Physik* **1924**, *26*, 178-181.

7. Born, M., Zur Quantenmechanik Der Stoßvorgänge. *Z. Physik* **1926**, *37*, 863-867.

8. Schrödinger, E., Quantisierung Als Eigenwertproblem. *Annalen der Physik* **1926**, *384*, 361-376.

9. Born, M.; Oppenheimer, R., Zur Quantentheorie Der Molekeln. *Annalen der Physik* **1927**, *389*, 457-484.

10. Hartree, D. R., The Wave Mechanics of an Atom with a Non-Coulomb Central Field. Part I. Theory and Methods. *Mathematical Proceedings of the Cambridge Philosophical Society* **1928**, *24*, 89-110.

11. Brown, L., Paul A.M. Dirac's the Principles of Quantum Mechanics. *Phys. perspect.* **2006**, *8*, 381-407.

12. Pauli, W., Über Den Zusammenhang Des Abschlusses Der Elektronengruppen Im Atom Mit Der Komplexstruktur Der Spektren. *Z. Physik* **1925**, *31*, 765-783.

13. Slater, J. C., The Theory of Complex Spectra. *Physical Review* **1929**, *34*, 1293-1322.

14. Fock, V., Näherungsmethode Zur Lösung Des Quantenmechanischen Mehrkörperproblems. *Z. Physik* **1930**, *61*, 126-148.

15. Froese Fischer, C., General Hartree-Fock Program. *Computer Physics Communications* **1987**, *43*, 355-365.

16. Calais, J.-L., Density-Functional Theory of Atoms and Molecules. R.G. Parr and W. Yang, Oxford University Press, New York, Oxford, 1989. Ix + 333 Pp. Price £45.00. *International Journal of Quantum Chemistry* **1993**, *47*, 101-101.

17. Hohenberg, P.; Kohn, W., Inhomogeneous Electron Gas. *Physical Review* **1964**, *136*, B864-B871.

18. Hansen, A.; Bouman, T., Chromophores in Spectroscopy: Ab Initio Studies of Localized Descriptions of Molecular Electronic Excitations. *J Math Chem* **1992**, *10*, 221-247.

19. Orr, B. J.; Ward, J. F., Perturbation Theory of the Non-Linear Optical Polarization of an Isolated System. *Molecular Physics* **1971**, *20*, 513-526.

20. Dancoff, S. M., Non-Adiabatic Meson Theory of Nuclear Forces. *Physical Review* **1950**, *78*, 382-385.

21. Taylor, J. C., Tamm-Dancoff Method. *Physical Review* **1954**, *95*, 1313-1317.

22. Masunov, A.; Tretiak, S.; Hong, J. W.; Liu, B.; Bazan, G. C., Theoretical Study of the Effects of Solvent Environment on Photophysical Properties and Electronic Structure of Paracyclophane Chromophores. *Journal of Chemical Physics* **2005**, *122*.

23. Mikhailov, I. A.; Tafur, S.; Masunov, A. E., Double Excitations and State-to-State Transition Dipoles in Pi-Pi* Excited Singlet States of Linear Polyenes: Time-Dependent Density-Functional Theory Versus Multiconfigurational Methods. *Physical Review A* **2008**, *77*.

24. Ohta, K.; Kamada, K., Theoretical Investigation of Two-Photon Absorption Allowed Excited States in Symmetrically Substituted Diacetylenes by Ab Initio Molecular-Orbital Method. *The Journal of Chemical Physics* **2006**, *124*, 124303.

CHAPTER 2: THEORETICAL STUDIES OF STORAGE MATERIALS BASED ON POLIMERIC Zd^{+2} AND Cd^{+2} DICARBOXYLATES CONTAINING OXIME AND ALDOXIME LIGANDS

2.1 Introduction

Since the seminal works by Yaghi et al., Zn(II) and Cd(II) metal–organic frameworks (MOF)[1-11] and metal organic materials (MOM)[9] in general continue to attract close attention of the scientific community interested in new materials with fascinating adsorptive,[1-9, 11-12] catalytic,[13-18] and sensor properties[19]. For these particular coordination networks, the high adsorption capacities,[1-7, 9-10, 13] luminescent,[20-22] and nonlinear optical (NLO)[23-28] properties should be mentioned first.

The NLO properties of MOMs are being investigated in relation to several technological applications, including optical communications and up conversion lazing.[26] The third order nonlinearities, such as two-photon absorption (2PA), present special interest, as they are not limited to non-centrosymmetric structures,[29] unlike the second-order nonlinearities.[30-31]

Several recent studies have indicated that 2PA properties are enhanced by metal coordination compared to

free ligands[27-28] and this enhancement by the use of approximate density functional theory (DFT) to obtain non-linear optical properties.[32-33]

From the crystal engineering viewpoint, Zn(II) and Cd(II) ions have the same d^{10} electronic configuration, yet they are dissimilar in their atomic radii and coordination capacities. This could justify the huge number of the homo-ligand, primarily carboxylate and mixed-ligand. This includes carboxylate-aromatic amine-based coordination networks (isostructural and isomorphous analogues) in addition to the supramolecular isomers as well.[20, 34-37]

The experimental efforts aimed at the forthcoming MOF materials with large pores, efficient guest uptake, and stability[37-38] continue, and theoretical studies complement experiment by predicting adsorption capacity, adsorption preference, and desired optical properties of MOMs including the Zn(II)/Cd(II)-based ones.[39-42]

It is important to note that our collaborators Fonari et al have used the mixed-ligand "blend approach"[43-44] before for decoration of coordination polymers (CP) by oxime ligands,[32, 45-49] and concluded on the following hypothesis: "The coordination of bulky neutral oxime ligands to the d^{10} metals provides the loosely packed MOMs with the voids in the crystal

lattice for inclusion of small guest molecules, such as water and dimethylformamide (DMF)."

Studies performed so far have revealed that the oxime molecules coordinated as the terminal ligands impose restrictions on the dimensionality of coordination networks. Those one and two-dimensional (1D and 2D) polymeric materials are capable of holding the guest molecules in their voids. While some of them held their coordination frameworks in the guest-free state spontaneously or after evacuation of the DMF guest molecules (resulting in the crystal-to-crystal transformation in the solid state), the others failed.[32, 50]

Recent study based on a series of 4-pyao containing 1D Zn(II)/ Cd(II) supramolecular isomers suggests several guidelines for the rational design of acentric polymeric materials for NLO applications.[51] In order to search for the new coordination networks herein, we have combined the Zn(II)/Cd(II) metal centers with two types of ligands, flexible aliphatic dicarboxylic acids of different length, HOOC-$(CH_2)_n$-COOH (n = 1, 2, 4) including malonic (H_2mal), succinic (H_2suc), and adipic acids (H_2adi), and three oxime ligands, including pyridine-2-aldoxime (2-pyao), pyridine-4-aldoxime (4-pyao), and 1,2-cyclohexanedionedioxime (Niox).

The ligands used in this study to make the crystal structures are shown in figure 2.

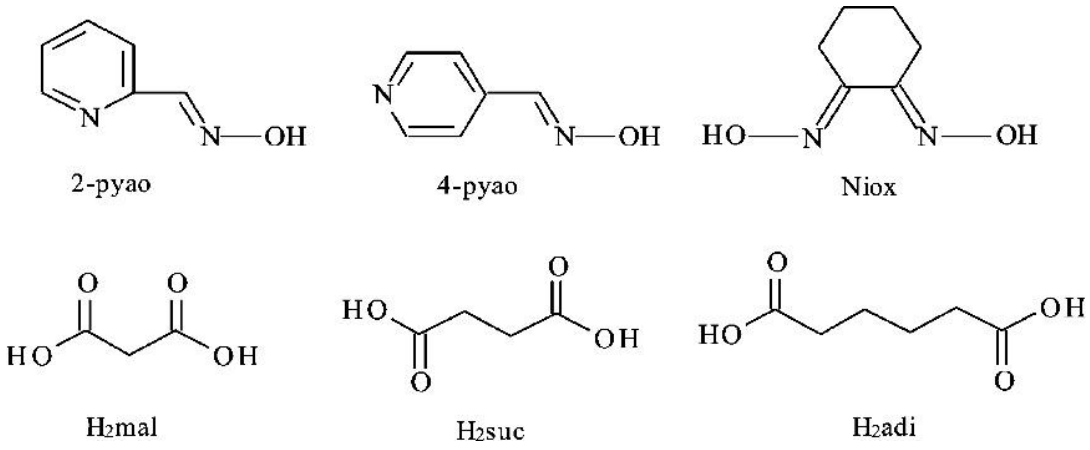

Figure 2 Structural information of the ligands used in this study.

2.2 Methods

Periodical Semi-Empirical Quantum Chemical calculations were performed on the structures with and without guest molecules using PM7 Hamiltonian,[52] which includes dispersion correction. The computer program MOPAC2012 was used for all calculations.[53-54] Although periodical DFT, HF, and semi-empirical calculations lack the dispersion component of inter-molecular interactions and may result in unbound structures,[55] the empirically added dispersion correction makes both ab initio and semi-empirical results rather accurate.[53] Another potential source of inaccuracy could be chlorine bonds,[55] or other inter-molecular interactions with a strong donor–acceptor component.[56-57] Fortunately, neither

halogen nor chalcogen atoms are present in the structure, making PM7 results reliable in this case.

The initial atomic coordinates for the crystal were taken from the CIF file containing the information from experimental measurements. The symmetry for this structure was reduced to the P1 space group. Mercury software[58] was used to display the voids in the crystal structure. The crystal structure was optimized first with the lattice parameters frozen, and then optimized relaxed. The voids of the crystal structure were filled with eight H_2 or N_2 molecules per unit cell. The resulting formation enthalpy was used to calculate the interaction enthalpy between the crystalline matrix and guest molecule.

2.3 Discussion

The structure presented in figure 3 represents the binuclear cluster built of two Zn(II) octahedra. Each Zn(II) atom adopts the distorted N_2O_4-octahedral geometry, arising from one Niox ligand coordinated in the N,N′ -chelate mode, and three symmetry-equivalent adipate anions. The Zn–O bond distances are in the range 1.977–2.119 Å, and the Zn–N bond distances are equal to 2.091(4) and 2.214 Å. The adipate anion

acts in the monodentate and mono, bidentate bridging modes. The self-association of the two Zn(II) octahedra occurs via two inversion-related adipate anions through their mono, bidentate-bridging coordination.

This coordination mode of adipate anion has not been reported in the literature so far. The Zn···Zn separation in the binuclear unit across the carboxylate bridge is equal to 3.499 Å. The binuclear metal clusters are associated in a spongy layer with the (4,4) topology being composed of the S-shaped meshes due to the bent conformation of the adipate ligand. The layers are propagated parallel to the bc crystallographic plane, and the layer thickness is estimated as 10.696 Å. The layers stack along the crystallographic a axis and meet by the cyclohexyl rings; the interpenetration is measured as 0.84 Å being minimal among the compounds discussed herein (Figure 3c).

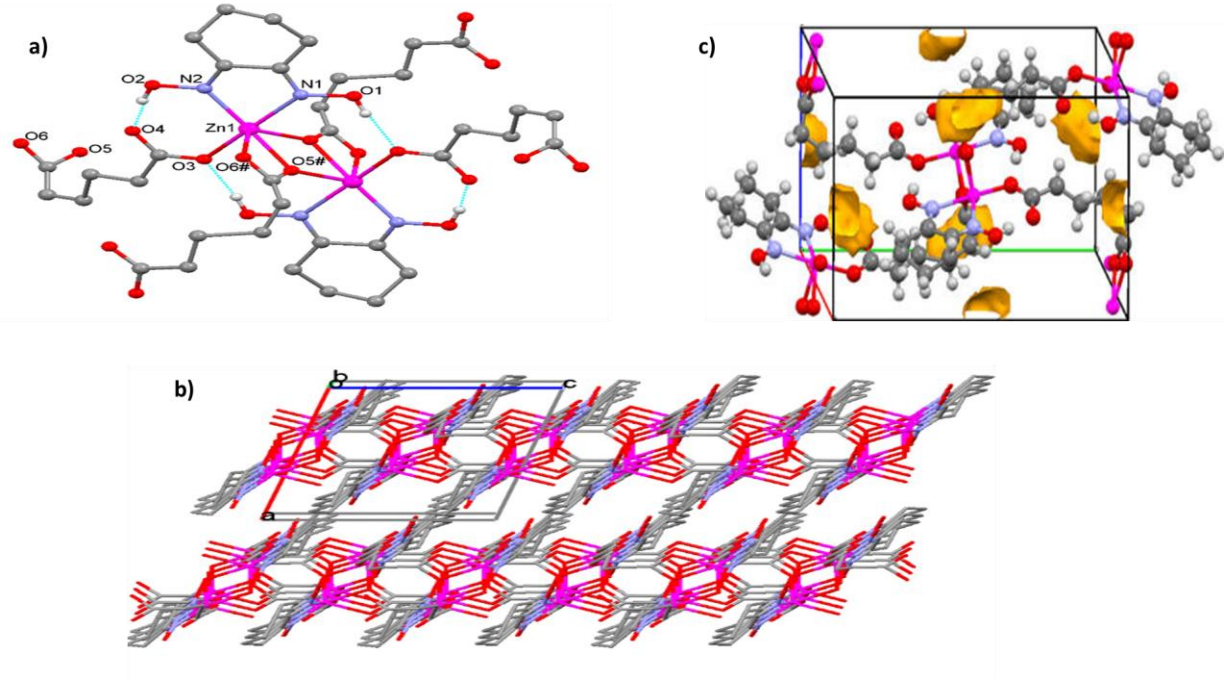

Figure 3 a) View of the crystal structure under research showing C- bound H atoms are omitted for clarity, b) Describe the stacking of the layers and c) Describes the simulated crystal structure displaying its voids.

This solid demonstrated breathing behavior indicated by the disordering of one of the carboxylate groups that adjust alternatively either bidentate- or monodentate modes of coordination, and by the commonplace disorder of the Niox cyclohexyl ring.

The conformational flexibility of the cyclohexane ring in Niox may explain its more effective crystal packing reducing the size of the voids in this crystal solid. Our analysis of the voids in the crystal after the disorder removal yields 111 $Å^3$ for 0.8 Å probe radius. Furthermore, the adsorption measurements supported by the computations revealed the developed surface acceptable for adsorption.

The examples of ultramicroporous materials that otherwise reveal excellent adsorption properties are known from the literature. For example, the so-called "SIFSIX" MOMs reported by Forrest et al.[41] with the narrow pore sizes and small Brunauer–Emmett–Teller (BET) theory surface area, yet exhibit very tight packing of CO_2 in those dense networks. The gas loading correlates with the MOM contraction and pyrazine rings tilting in the structures[59].

Similarly, the availability of the conformationally flexible components in the networks reported by us supports

the possible "breathing behavior" and "gate opening" during the adsorption processes.[60]

Our collaborators analyzed the low temperature gas adsorption isotherms with the Brunauer, Emmett, Teller (BET) method[61] and evaluated the characteristics of the solid. The BET equation is the following:

$$a = \frac{a_m \frac{K_p}{P_s}}{\left(1 - \frac{p}{P_s}\right)\left[1 + (k-1)\frac{p}{p_s}\right]} \quad (21)$$

where $\frac{p}{p_s}$ is the adsorbate relative pressure, a is the adsorption value at corresponding p/ps, am is the monolayer capacity, and K is the BET equation equilibrium constant. To determine the specific surface area of solids by this method, nitrogen is the most often used as an adsorbate at 77 K.

Building the isotherms included two stages. In the first stage, the samples were degassed for the removal of traces of moisture and carbon dioxide at 313 K in a vacuum of 2×10^{-4} mm Hg during 1 day, and in the second, the samples were subjected to nitrogen adsorption. The weight of the samples used for the analyses was 0.08 g. The resulting adsorption–desorption isotherms shown in figure 5.

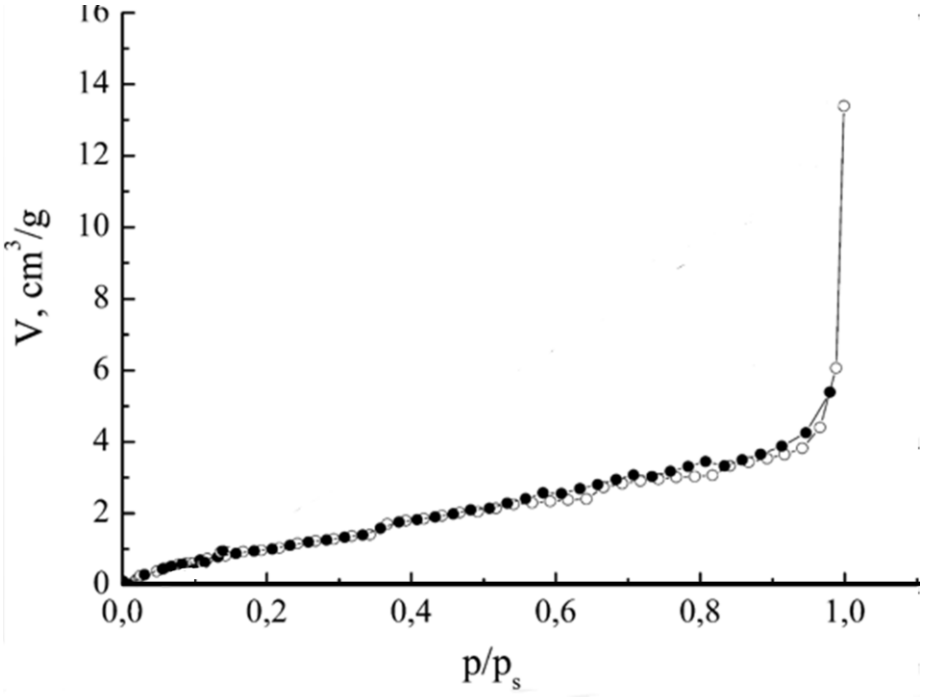

Figure 4 Experimental Diagram describing the N_2 adsorption (white circles) and desorption (black circles) at 77K for a 0.08g sample.

The isotherm in figure 4 is typical for physical adsorption and indicates the heterogeneous pores in the sample with a predominance of mesopores. The isotherm plot exhibits a slight rise of the curve at the beginning at low relative pressures of nitrogen, a monotonic increase at the relative pressure $\frac{p}{p_s}$ 0.20–0.90 and a sharp rise of the curve after the p/ps > 0.90. Initial convex section indicates the presence of a small amount of micropores; at $\frac{p}{p_s}$= 0.35 there is an inflection in the isotherm, indicating the completion of the

monolayer formation and the beginning of multilayer formation.

In order to explain why the crystal bulk is compromised in the crystal structure shown in figure 3. Optimization of the structure was performed with and without guess molecules with Semi-Empirical QM methods. The unit cell contains two types of voids, located at the centers of the a and b edges, each shared between four neighboring unit cells. Mercury software[58] was used to display the voids (0.8 Å probe radius) in the crystal structure.

The combined volume of these voids is close to 111 $Å^3$, or 7.7% of the unit cell volume. The voids of the crystal structure were filled with eight H_2 or N_2 molecules per unit cell. Relaxations of the resulting inclusion structures were distinctly different. While H_2 molecules diffused out of the cavities and did not increase the lattice parameters appreciably as shown in Table 1. The N_2 molecules remained close to the center of the cavities and increased their size so that crystal dis-integrated into non-interacting slabs (the parameter a increased by more than 1 Å).

In order to determine the capacity of the ultra-micropores with respect to the number of N_2 molecules, one

molecule was added, the structure was relaxed, then added another molecule was added and so on.

Table 1 Lattice Parameters (Å) and Interaction Enthalpies for the Crystal Structure and the Related Inclusion Compounds

System	a	B	c	β	$\Delta H\,(\frac{kcal}{mol})$
Experimental	10.239	15.342	9.652	105.727	
n=0	10.239	15.342	9.291	105.727	0
n=8, X=H2	10.645	15.531	9.73	105.122	−0.74
n=1, X=N2	10.336	15.66	9.38	104.912	−0.45
n=2, X=N2	10.328	15.652	9.364	105.111	−5.63
n=3, X=N2	10.587	15.709	9.405	104.746	−5.57
n=4, X=N2	11.49	15.671	9.839	104.788	−8.93
n=5, X=N2	11.495	15.681	9.875	104.964	−5.85

As demonstrated, the formation of the inclusion complex is energetically favorable in all cases. The addition of the first guest molecule expanded b by 0.3 Å, so that the interaction energy is largely reduced by the matrix deformation energy. The second molecule enters the matrix that is already expanded, and guest/matrix interaction results in ~5 $\frac{kcal}{mol}$ stabilization. The third molecule expanded a by extra 0.3 Å, and this deformation again is nearly compensated by the guest/matrix interaction. The fourth and fifth molecules expand a by extra 0.9 Å and c by 0.4 Å. Clearly, four N_2 molecules exceed the capacity of the voids and result in structural disintegration. Formation of the micropores is likely at this stage.

This is in agreement with adsorption experimental data reported[62] This is in agreement with experimental data, described figure 4, suggesting that the interval of relative pressures from 0.1 to 0.95 corresponds to filling of ultra-microcavities in the intact single crystal by 0.1 to 2.8 N_2 molecules per unit cell, while a steep increase at larger relative pressure corresponds to formation of the larger cavities. This implies that the crystalline structure would transform into powder (as observed experimentally) after the expansion of the ultra-micropores inside the crystal unit cell due to the guess molecules. This results in collapse of the structural integrity which is represented as an observable change in the bulk state. If the system absorbs $3N_2$ per unit cell this would cause the voids in the unit cell to expand in the molecular scale. Moreover, when most of the unit cells voids collapse the bulk solid would be compromised and turn into microcrystals.

We also predict that this material is capable of hydrogen storage, as Table 1 reports absorption of $8H_2$ molecules is energetically favorable and does not result in structural disintegration.

2.4 Conclusions

Our collaborators used the dicarboxylic acid/oxime blend approach[43-44] successfully for the fabrication of 10 new MOMs with cumulative properties. Pyridine-2-aldoxime (2-pyao), pyridine-4-aldoxime (4-pyao), and 1,2-cyclohexanedionedioxime (Niox) act as terminal ligands providing an access to the 1D, 2D, and 3D structures where aliphatic dicarboxylates act as the multidentate linkers.

The rotatable 4-pyao and flexible Niox ligands afford the extended surface areas due to the deep interpenetration of the former and the perfect accommodation of the latter within the 2D and 3D crystal solids. The selected samples demonstrate an efficient water and DMF uptake explained by the availability of the hydrophilic and hydrophobic regions in these solids.

The crystal structure simulations undertaken for one laminar sample were supported by the adsorption measurements and revealed their efficacy for the prediction of the adsorption capacity of the solids even in the absence of the registered solvent-accessible voids.[62-63] The source of the physical observables in the bulk materials were found and to be due expansion of the unit cell after addition of more than $3N_2$ molecules into the unit cell.

2.5 Copyright Acknowledgment

2.6 List of References

1. Eddaoudi, M.; Li, H. L.; Reineke, T.; Fehr, M.; Kelley, D.; Groy, T. L.; Yaghi, O. M., Design and Synthesis of Metal-Carboxylate Frameworks with Permanent Microporosity. *Topics in Catalysis* **1999**, *9*, 105-111.

2. Eddaoudi, M.; Li, H. L.; Yaghi, O. M., Highly Porous and Stable Metal-Organic Frameworks: Structure Design and Sorption Properties. *Journal of the American Chemical Society* **2000**, *122*, 1391-1397.

3. Eddaoudi, M.; Moler, D. B.; Li, H. L.; Chen, B. L.; Reineke, T. M.; O'Keeffe, M.; Yaghi, O. M., Modular Chemistry: Secondary Building Units as a Basis for the Design of Highly Porous and Robust Metal-Organic Carboxylate Frameworks. *Accounts of Chemical Research* **2001**, *34*, 319-330.

4. Li, H.; Eddaoudi, M.; Groy, T. L.; Yaghi, O. M., Establishing Microporosity in Open Metal-Organic Frameworks:

Gas Sorption Isotherms for Zn(Bdc) (Bdc = 1,4-Benzenedicarboxylate). *Journal of the American Chemical Society* **1998**, *120*, 8571-8572.

5. Li, H. L.; Davis, C. E.; Groy, T. L.; Kelley, D. G.; Yaghi, O. M., Coordinatively Unsaturated Metal Centers in the Extended Porous Framework of Zn-3(Bdc)(3).6ch(3)Oh (Bdc=1,4-Benzenedicarboxylate). *Journal of the American Chemical Society* **1998**, *120*, 2186-2187.

6. Pan, L.; Sander, M. B.; Huang, X. Y.; Li, J.; Smith, M.; Bittner, E.; Bockrath, B.; Johnson, J. K., Microporous Metal Organic Materials: Promising Candidates as Sorbents for Hydrogen Storage. *Journal of the American Chemical Society* **2004**, *126*, 1308-1309.

7. Husain, A.; Ellwart, M.; Bourne, S. A.; Ohrstrom, L.; Oliver, C. L., Single-Crystal-to-Single-Crystal Transformation of a Novel 2-Fold Interpenetrated Cadmium-Organic Framework with Trimesate and 1,2-Bis(4-Pyridyl)Ethane into the Thermally Desolvated Form Which Exhibits Liquid and Gas Sorption Properties. *Crystal Growth & Design* **2013**, *13*, 1526-1534.

8. Manos, M. J.; Moushi, E. E.; Papaefstathiou, G. S.; Tasiopoulos, A. J., New Zn2+ Metal Organic Frameworks with Unique Network Topologies from the Combination of Trimesic

Acid and Amino-Alcohols. *Crystal Growth & Design* **2012**, *12*, 5471-5480.

9. Perry, J. J. I. V.; Perman, J. A.; Zaworotko, M. J., Design and Synthesis of Metal-Organic Frameworks Using Metal-Organic Polyhedra as Supermolecular Building Blocks. *Chemical Society Reviews* **2009**, *38*, 1400-1417.

10. Yaghi, O. M.; Davis, C. E.; Li, G. M.; Li, H. L., Selective Guest Binding by Tailored Channels in a 3-D Porous Zinc(Ii)-Benzenetricarboxylate Network. *Journal of the American Chemical Society* **1997**, *119*, 2861-2868.

11. Yang, W.; Lin, X.; Blake, A. J.; Wilson, C.; Hubberstey, P.; Champness, N. R.; Schroeder, M., Self-Assembly of Metal-Organic Coordination Polymers Constructed from a Bent Dicarboxylate Ligand: Diversity of Coordination Modes, Structures, and Gas Adsorption. *Inorganic Chemistry* **2009**, *48*, 11067-11078.

12. Fang, Q. R.; Zhu, G. S.; Jin, Z.; Xue, M.; Wei, X.; Wang, D. J.; Qiu, S. L., A Multifunctional Metal–Organic Open Framework with a Bcu Topology Constructed from Undecanuclear Clusters. *Angewandte Chemie International Edition* **2006**, *45*, 6126-6130.

13. Lee, J.; Farha, O. K.; Roberts, J.; Scheidt, K. A.; Nguyen, S. T.; Hupp, J. T., Metal-Organic Framework Materials as Catalysts. *Chemical Society Reviews* **2009**, *38*, 1450-1459.

14. Corma, A.; Garcia, H.; Llabres i Xamena, F. X. L. I., Engineering Metal Organic Frameworks for Heterogeneous Catalysis. *Chemical Reviews* **2010**, *110*, 4606-4655.

15. Meng, W.; Xu, Z.; Ding, J.; Wu, D.; Han, X.; Hou, H.; Fan, Y., A Systematic Research on the Synthesis, Structures, and Application in Photocatalysis of Cluster-Based Coordination Complexes. *Crystal Growth & Design* **2014**, *14*, 730-738.

16. Shin, J. W.; Bae, J. M.; Kim, C.; Min, K. S., Three-Dimensional Zinc(Ii) and Cadmium(Ii) Coordination Frameworks with N,N,N ',N '-Tetrakis(Pyridin-4-Yl)Methanediamine: Structure, Photoluminescence, and Catalysis. *Inorganic Chemistry* **2013**, *52*, 2265-2267.

17. Kan, W.-Q.; Liu, B.; Yang, J.; Liu, Y.-Y.; Ma, J.-F., A Series of Highly Connected Metal-Organic Frameworks Based on Triangular Ligands and D(10) Metals: Syntheses, Structures, Photoluminescence, and Photocatalysis. *Crystal Growth & Design* **2012**, *12*, 2288-2298.

18. Dai, M.; Su, X.-R.; Wang, X.; Wu, B.; Ren, Z.-G.; Zhou, X.; Lang, J.-P., Three Zinc(Ii) Coordination Polymers Based

on Tetrakis(4-Pyridyl)Cyclobutane and Naphthalenedicarboxylate Linkers: Solvothermal Syntheses, Structures, and Photocatalytic Properties. *Crystal Growth & Design* **2014**, *14*, 240-248.

19. Kreno, L. E.; Leong, K.; Farha, O. K.; Allendorf, M.; Van Duyne, R. P.; Hupp, J. T., Metal-Organic Framework Materials as Chemical Sensors. *Chemical Reviews* **2012**, *112*, 1105-1125.

20. Chen, D.-S.; Sun, L.-B.; Liang, Z.-Q.; Shao, K.-Z.; Wang, C.-G.; Su, Z.-M.; Xing, H.-Z., Conformational Supramolecular Isomerism in Two-Dimensional Fluorescent Coordination Polymers Based on Flexible Tetracarboxylate Ligand. *Crystal Growth & Design* **2013**, *13*, 4092-4099.

21. Guo, H.-D.; Guo, X.-M.; Batten, S. R.; Song, J.-F.; Song, S.-Y.; Dang, S.; Zheng, G.-L.; Tang, J.-K.; Zhang, H.-J., Hydrothermal Synthesis, Structures, and Luminescent Properties of Seven D(10) Metal-Organic Frameworks Based on 9,9-Dipropylfluorene-2,7-Dicarboxylic Acid (H(2)Dfda). *Crystal Growth & Design* **2009**, *9*, 1394-1401.

22. Wang, X. L.; Chao, Q.; Wang, E. B.; Lin, X.; Su, Z. M.; Hu, C. W., Interlocked and Interdigitated Architectures from Self-Assembly of Long Flexible Ligands and Cadmium Salts. *Angewandte Chemie-International Edition* **2004**, *43*, 5036-5040.

23. Evans, O. R.; Lin, W. B., Crystal Engineering of Nlo Materials Based on Metal-Organic Coordination Networks. *Accounts of Chemical Research* **2002**, *35*, 511-522.

24. Lin, W. B.; Wang, Z. Y.; Ma, L., A Novel Octupolar Metal-Organic Nlo Material Based on a Chiral 2d Coordination Network. *Journal of the American Chemical Society* **1999**, *121*, 11249-11250.

25. Zang, S. Q.; Su, Y.; Li, Y. Z.; Ni, Z. P.; Meng, Q. J., Assemblies of a New Flexible Multicarboxylate Ligand and D(10) Metal Centers toward the Construction of Homochiral Helical Coordination Polymers: Structures, Luminescence, and Nlo-Active Properties. *Inorganic Chemistry* **2006**, *45*, 174-180.

26. Yu, J.; Cui, Y.; Xu, H.; Yang, Y.; Wang, Z.; Chen, B.; Qian, G., Confinement of Pyridinium Hemicyanine Dye within an Anionic Metal-Organic Framework for Two-Photon-Pumped Lasing. *Nature Communications* **2013**, *4*.

27. Nie, C.; Zhang, Q.; Ding, H.; Huang, B.; Wang, X.; Zhao, X.; Li, S.; Zhou, H.; Wu, J.; Tian, Y., Two Novel Six-Coordinated Cadmium(Ii) and Zinc(Ii) Complexes from Carbazate Beta-Diketonate: Crystal Structures, Enhanced Two-Photon Absorption and Biological Imaging Application. *Dalton Transactions* **2014**, *43*, 599-608.

28. Xu, D.; Yang, M.; Wang, Y.; Cao, Y.; Fang, M.; Zhu, W.; Zhou, H.; Hao, F.; Wu, J.; Tian, Y., New Dyes with Enhanced Two-Photon Absorption Cross-Sections Based on the Cd(Ii) and 4-(4- 4-(Imidazole)Styryl Phenyl)-2,2:6,2-Terpyridine. *Journal of Coordination Chemistry* **2013**, *66*, 2992-3003.

29. Hu, H., et al., Two-Photon Absorption Spectrum of a Single Crystal Cyanine-Like Dye. *Journal of Physical Chemistry Letters* **2012**, *3*, 1222-1228.

30. Suponitsky, K. Y.; Masunov, A. E.; Antipin, M. Y., Computational Search for Nonlinear Optical Materials: Are Polarization Functions Important in the Hyperpolarizability Predictions of Molecules and Aggregates? *Mendeleev Communications* **2009**, *19*, 311-313.

31. Draguta, S.; Fonari, M. S.; Masunov, A. E.; Zazueta, J.; Sullivan, S.; Antipin, M. Y.; Timofeeva, T. V., New Acentric Materials Constructed from Aminopyridines and 4-Nitrophenol. *Crystengcomm* **2013**, *15*, 4700-4710.

32. Croitor, L.; Coropceanu, E. B.; Masunov, A. E.; Rivera-Jacquez, H. J.; Siminel, A. V.; Fonari, M. S., Mechanism of Nonlinear Optical Enhancement and Supramolecular Isomerism in 1d Polymeric Zn(Ii) and Cd(Ii) Sulfates with Pyridine-4-Aldoxime Ligands. *Journal of Physical Chemistry C* **2014**, *118*, 9217-9227.

33. Nayyar, I. H.; Masunov, A. E.; Tretiak, S., Comparison of Td-Dft Methods for the Calculation of Two-Photon Absorption Spectra of Oligophenylvinylenes. *Journal of Physical Chemistry C* **2013**, *117*, 18170-18189.

34. Moulton, B.; Zaworotko, M. J., From Molecules to Crystal Engineering: Supramolecular Isomerism and Polymorphism in Network Solids. *Chemical Reviews* **2001**, *101*, 1629-1658.

35. Tian, Z.; Lin, J.; Su, Y.; Wen, L.; Liu, Y.; Zhu, H.; Meng, Q.-J., Flexible Ligand, Structural, and Topological Diversity: Isomerism in Zn(No3)(2) Coordination Polymers. *Crystal Growth & Design* **2007**, *7*, 1863-1867.

36. Mukherjee, G.; Biradha, K., Modulation of Breathing Behavior of Layered Coordination Polymers Via a Solid Solution Approach: The Influence of Metal Ions on Sorption Behavior. *Chemical Communications* **2014**, *50*, 670-672.

37. Furukawa, H.; Gandara, F.; Zhang, Y.-B.; Jiang, J.; Queen, W. L.; Hudson, M. R.; Yaghi, O. M., Water Adsorption in Porous Metal-Organic Frameworks and Related Materials. *Journal of the American Chemical Society* **2014**, *136*, 4369-4381.

38. Luebke, R.; Weselinski, L. J.; Belmabkhout, Y.; Chen, Z.; Wojtas, L.; Eddaoudi, M., Microporous Heptazine Functionalized (3,24)-Connected Rht-Metal-Organic Framework:

Synthesis, Structure, and Gas Sorption Analysis. *Crystal Growth & Design* **2014**, *14*, 414-418.

39. Flage-Larsen, E.; Thorshaug, K., Linker Conformation Effects on the Band Gap in Metal-Organic Frameworks. *Inorganic Chemistry* **2014**, *53*, 2569-2572.

40. Pham, T.; Forrest, K. A.; Nugent, P.; Belmabkhout, Y.; Luebke, R.; Eddaoudi, M.; Zaworotko, M. J.; Space, B., Understanding Hydrogen Sorption in a Metal-Organic Framework with Open-Metal Sites and Amide Functional Groups. *Journal of Physical Chemistry C* **2013**, *117*, 9340-9354.

41. Forrest, K. A., et al., Computational Studies of Co2 Sorption and Separation in an Ultramicroporous Metal-Organic Material. *Journal of Physical Chemistry C* **2013**, *117*, 17687-17698.

42. Sarkisov, L.; Martin, R. L.; Haranczyk, M.; Smit, B., On the Flexibility of Metal-Organic Frameworks. *Journal of the American Chemical Society* **2014**, *136*, 2228-2231.

43. Papaefstathiou, G. S.; Escuer, A.; Mautner, F. A.; Raptopoulou, C.; Terzis, A.; Perlepes, S. P.; Vicente, R., Use of the Di-2-Pyridyl Ketone/Acetate/Dicyanamide "Blend" in Manganese(Ii), Cobalt(Ii) and Nickel(Ii) Chemistry: Neutral Cubane Complexes. *European Journal of Inorganic Chemistry* **2005**, 879-893.

44. Stamatatos, T. C.; Diamantopoulou, E.; Raptopoulou, C. P.; Psycharis, V.; Escuer, A.; Perlepes, S. P., Acetate/Di-2-Pyridyl Ketone Oximate "Blend" as a Source of High-Nuclearity Nickel(Ii) Clusters: Dependence of the Nuclearity on the Nature of the Inorganic Anion Present. *Inorganic Chemistry* **2007**, *46*, 2350-2352.

45. Coropceanu, E. B.; Croitor, L.; Fonari, M. S., Mononuclear Cd(Ii) and Zn(Ii) Complexes with the 1,2-Cyclohexanedionedioxime Ligand: Preparation and Structural Characterization. *Polyhedron* **2012**, *38*, 68-74.

46. Croitor, L.; Coropceanu, E. B.; Jeanneau, E.; Dementiev, I. V.; Goglidze, T. I.; Chumakov, Y. M.; Fonari, M. S., Anion-Induced Generation of Binuclear and Polymeric Cd(Ii) and Zn(Ii) Coordination Compounds with 4,4 '-Bipyridine and Dioxime Ligands. *Crystal Growth & Design* **2009**, *9*, 5233-5243.

47. Croitor, L.; Coropceanu, E. B.; Siminel, A. V.; Botoshansky, M. M.; Fonari, M. S., Synthesis, Structures, and Luminescence Properties of Mixed Ligand Cd(Ii) and Zn(Ii) Coordination Compounds Mediated by 1,2-Bis(4-Pyridyl)Ethane. *Inorganica Chimica Acta* **2011**, *370*, 411-419.

48. Croitor, L.; Coropceanu, E. B.; Siminel, A. V.; Kravtsov, V. C.; Fonari, M. S., Polymeric Zn(Ii) and Cd(Ii) Sulfates with Bipyridine and Dioxime Ligands: Supramolecular

Isomerism, Chirality, and Luminescence. *Crystal Growth & Design* **2011**, *11*, 3536-3544.

49. Croitor, L.; Coropceanu, E. B.; Siminel, A. V.; Masunov, A. E.; Fonari, M. S., From Discrete Molecules to One-Dimensional Coordination Polymers Containing Mn(Ii), Zn(Ii) or Cd(Ii) Pyridine-2-Aldoxime Building Unit. *Polyhedron* **2013**, *60*, 140-150.

50. Croitor, L.; Coropceanu, E. B.; Siminel, A. V.; Kulikova, O.; Zelentsov, V. I.; Datsko, T.; Fonari, M. S., 1,2-Cyclohexanedionedioxime as a Useful Co-Ligand for Fabrication of One-Dimensional Zn(Ii) and Cd(Ii) Coordination Polymers with Wheel-and-Axle Topology and Luminescent Properties. *Crystengcomm* **2012**, *14*, 3750-3758.

51. Liu, H.-Y.; Ma, J.-F.; Liu, Y.-Y.; Yang, J., A Series of Zn(Ii) and Cd(Ii) Coordination Polymers Based on Flexible Bis- (Pyridyl)-Benzimidazole Ligand and Different Carboxylates: Syntheses, Structures, and Photoluminescent Properties. *Crystengcomm* **2013**, *15*, 2699-2708.

52. Stewart, J. J. P., Optimization of Parameters for Semiempirical Methods Vi: More Modifications to the Nddo Approximations and Re-Optimization of Parameters. *Journal of Molecular Modeling* **2013**, *19*, 1-32.

53. Stewart, J. J. P., Mopac2012, Stewart Computational Chemistry Version 14.083l. **2012**.

54. Maia, J. D. C.; Urquiza Carvalho, G. A.; Mangueira, C. P.; Santana, S. R.; Cabral, L. A. F.; Rocha, G. B., Gpu Linear Algebra Libraries and Gpgpu Programming for Accelerating Mopac Semiempirical Quantum Chemistry Calculations. *Journal of Chemical Theory and Computation* **2012**, *8*, 3072-3081.

55. Cardenas-Jiron, G. I.; Masunov, A.; Dannenberg, J. J., Molecular Orbital Study of Crystalline P-Benzoquinone. *Journal of Physical Chemistry A* **1999**, *103*, 7042-7046.

56. Masunov, A. E.; Zorkii, P. M., Geometric Characteristics of Halogen-Halogen Intermolecular Contacts in Organic-Crystals. *Zhurnal Fizicheskoi Khimii* **1992**, *66*, 60-69.

57. Masunov, A. E.; Zorkii, P. M., Donor-Acceptor Nature of Specific Nonbonded Interactions of Sulfur and Halogen Atoms - Influence on the Geometry and Packing of Molecules. *Journal of Structural Chemistry* **1992**, *33*, 423-435.

58. Edgington, P. R.; McCabe, P.; Macrae, C. F.; Pidcock, E.; Shields, G. P.; Taylor, R.; Towler, M.; Van De Streek, J., Mercury: Visualization and Analysis of Crystal Structures. *Journal of Applied Crystallography* **2006**, *39*, 453-457.

59. Nugent, P., et al., Porous Materials with Optimal Adsorption Thermodynamics and Kinetics for Co2 Separation. *Nature* **2013**, *495*, 80-84.

60. Alhamami, M.; Doan, H.; Cheng, C.-H., A Review on Breathing Behaviors of Metal-Organic-Frameworks (Mofs) for Gas Adsorption. *Materials* **2014**, *7*, 3198-3250.

61. Brunauer, S.; Emmett, P. H.; Teller, E., Adsorption of Gases in Multimolecular Layers. *Journal of the American Chemical Society* **1938**, *60*, 309-319.

62. Croitor, L.; Coropceanu, E. B.; Masunov, A. E.; Rivera-Jacquez, H. J.; Siminel, A. V.; Zelentsov, V. I.; Datsko, T. Y.; Fonari, M. S., Polymeric Luminescent Zn(Ii) and Cd(Ii) Dicarboxylates Decorated by Oxime Ligands: Tuning the Dimensionality and Adsorption Capacity. *Crystal Growth & Design* **2014**, *14*, 3935-3948.

63. Seo, J.; Matsuda, R.; Sakamoto, H.; Bonneau, C.; Kitagawa, S., A Pillared-Layer Coordination Polymer with a Rotatable Pillar Acting as a Molecular Gate for Guest Molecules. *Journal of the American Chemical Society* **2009**, *131*, 12792-12800.

CHAPTER 3: QUANTUM CHEMICAL STUDIES OF CRYSTALLOCHROMISM UPON CHANGING THE TWO DIMESIONAL COORDINATION NETWORK OF Co(II) AFTER DESOLVATION

3.1 Introduction

Porous coordination polymers (PCPs)[1-3] including metal organic-frameworks (MOFs)[4-6] became rapidly growing area of chemistry in the past decades[7-9]. This is mainly due to the intriguing topological architectures and potential applications of MOFs in such fields as gas storage, catalysis, separations, ion exchange and molecular magnetism [10-17].

These solids not only possess regular porosity with high pore volume, but contain tunable organic groups within the molecular framework, which allow an easy modulation of the pore size. MOFs that show a structural response upon external stimuli such as guest sorption, temperature or mechanical pressure are of particular interest[18]. In addition to the rigid three-dimensional (3D) polymeric coordination networks, the flexible two-dimensional (2D) structures nowadays attract growing attention[19]. Many fascinating examples had been documented since Zaworotko's seminal work [20] highlighted the super structural diversity in the laminated solids.

They opened the possibilities of the rational design of both hydrophilic and hydrophobic surfaces, and their common inherent ability to mimic clays by intercalation of a wide range of organic guest molecules. The breezing behavior, ability of the metal sites in the regular grids work as catalytically active ones, preference in the CO_2 gas capture and gas stepwise adsorption were reported[21-23]. Coordination layers were proposed as a source of crystalline sheets with nanometer thickness for molecular sieving.

Their ability to achieve high proton conductivity and high water sorption under low humidity conditions was demonstrated. A novel strategy to design and synthesize homochiral phencyclidine (PCP)[24-25] and non-linear optical (NLO) materials by layered PCPs was reported[26]. Unusual properties of 2D coordination networks prompted us to introduce pyridine-n-aldoxime/dioxime ligands as pillars or chelate agents. These bulky metallo-chelate corner fragments in carboxylic networks can afford potentially porous structures which are able to accommodate, the small molecules in the crystal lattices[26-35].

Here we combine the 1,4-benzene-dicarboxylic acid (H2bdc) with thionicotinamide (S-nia), resulting in the Co(II)-based 2D coordination network that undergoes single-

crystal-to-single-crystal (SC-SC) transition in the solid state upon desolvation. Our choice is based on the following: (1) structural similarity of S-nia to the pyridine-n-aldoximes, previously explored by us[26, 32]; (2) all reported data are restricted to organic solids [36-38]; (3) this molecule is one of the commercially available analogs of nicotinamide; and (4) it presents opportunities for the generation of hydrogen-bonded network for 2D stacked layers. The latter would support Kitagawa's idea of inventing "metallo-amino acids" ensembles.[39]

3.2 Methods

3.2.1 Periodical predictions

The periodical structures were optimized with MOPAC2012 computer program[40] at PM7 semi-empirical theory level[41]. The PM7 Hamiltonian contains empirical dispersion correction which is important for molecular crystals.[42] The initial atomic coordinates for the crystals were taken from experiment, with the symmetry reduced to the P1 group. The electronic structure was assumed to have four unpaired electrons per unit cell, describing four low spin Co(II) ions.

In order to predict the unknown structure, the experimental structure of crystal structure **1** was modified by substituting each DMF molecule with three methanol molecules and each water molecule with one methanol.

3.2.2 Spectral Predictions

All TDDFT calculations were performed using the Gaussian 2009 suite of programs.[43] Density Functional Theory with M05-QX exchange-correlation functional[44] and full-electron 6-31G basis set were used.[45] In order to avoid the artificial negative excitation energies, the KS orbitals were re-optimized after stability analysis (keyword Stable=**Opt**) to obtain the most stable ground states. The prediction of the absorption spectra was performed using time dependent density functional theory[46] (TD-DFT), from these grounds states.

3.3 Discussion

Compound 1 crystallizes in the triclinic centrosymmetric P-1 space group and adopts layered structure with the binuclear $[Co_2(\mu 2\text{-}OH_2)(COO)_2]$ metal cluster as a secondary building unit (SBU).[4-6] The SBU contains two crystallographically distinct

Co(II) ions that are both found in the distorted NO_5-octahedral environments.

The triple bridge between the metal centers is provided by two syn,syn-bidentate bridging carboxylato groups, and one water molecule as shown in figure 5a. For Co(1), the coordination core comprises oxygen atoms from two bis-bidentate bridging bdc2- anions, one bridging and one terminal water molecules, and one DMF molecule, the pyridine nitrogen atom goes from the S-nia ligand. For Co(2), the coordination core comprises four bdc2- anions, two bis-bidentate bridging and two bis-monodentate, the bridging water molecule, and the pyridine nitrogen atom of the S-nia ligand. The Co···Co separation within the SBU is 3.579 Å.

The aggregation of the SBU in the (4,4) 2D network with sql topology occurs via the bdc2- bridges being resulted in rhombohedral patterns with the diagonal dimensions of 14.362 × 17.837 Å (Fig. 5b).

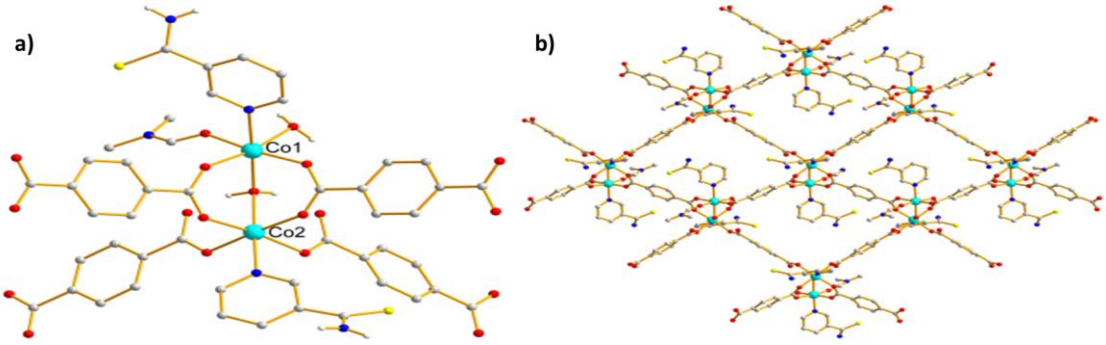

Figure 5 View of the fragment of: (a) binuclear Co(II) SBU and (b) 2D coordination network in 1, solvent molecules and C-bound H-atoms are omitted for clarity.

The are two terminal S-nia ligands, one is situated in dangling position being inclined to the layer plane, while the second S-nia ligand upraises perpendicular to the layer coordination skeleton. The layers stack along the crystallographic a axis, each rhombohedral window in the layer being partially closed by the $NH(NH_2)\cdots O(COO)$ hydrogen bonds going from the dangling S-nia ligands from the adjacent layer. Despite this partial blocking, the solvent molecules (H_2O and DMF) occupy the hydrophilic and hydrophobic regions in the intra- and inter-layer space, and are held in place by OH…O hydrogen bonds and stacking interactions between the solvated dmf and coordinated bdc residues. The volume occupied[47] by solvent molecules was calculated by PLATON[48] and it comprises 735 $Å^3$ or 31.5 % of the total unit cell volume.

The delicate heating of 1 at 105 °C for 4 h in vacuum resulted in the desolvated product, [Co(bdc)(S-nia)]n (dry_1). The SC-SC transition was accompanied by the color change from pink to dark-blue. It involved rearrangement of the coordination environment and substitution of solvent molecules with a less volatile ligand, similar to one reported previously[47, 49-61].

In the case of Co(II) SC-SC is often accompanied by the color change due to variation in the Co(II) coordination polyhedron which was not always supported by single crystal data[168-180]. Fortunately, dry_1 retained its crystallinity despite some deterioration of the crystal quality, therefore our collaborators were able to collect the diffraction data for an acceptable structural model.

The structure of dry_1 as shown in figure 6 was solved in the triclinic P-1 space group with the unit cell volume reduced by ~10% compared to 1 (2124 $Å^3$ vs. 2333 $Å^3$). The b axis contracted, while a and c elongated slightly. The unit cell shape changed from the oblique to nearly orthogonal. All solvent molecules were removed, including those coordinated to the metal centers in 1. The Co(II) coordination sphere changed from octahedral to square pyramidal shape, although SBU remained binuclear. Thus, the binuclear complex

transformed from $[Co_2(\mu2\text{-}OH_2)(dmf)(COO)_2]$ into the paddle-wheel $[Co2(\mu2\text{-}COO)_4]$.

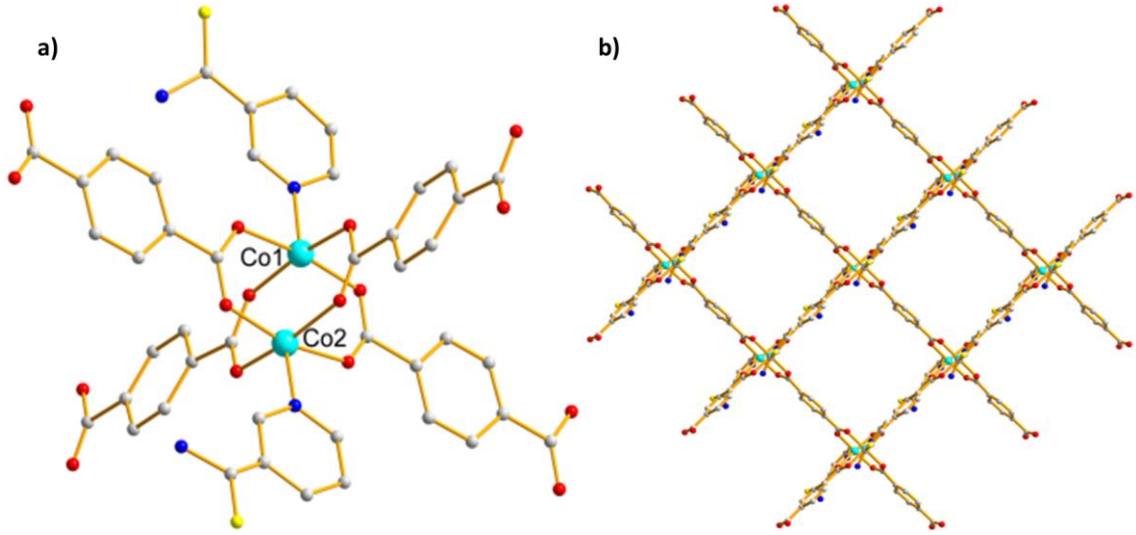

Figure 6 View of the fragment of: (a) paddle-wheel binuclear SBU and (b) 2D coordination network in dry_1. H-atoms are omitted for clarity

Each Co(II) atom is coordinated by four oxygen atoms from four bidentate bridging bdc2- residues, and one nitrogen atom from the terminal S-nia ligand. The Co···Co separations within the paddle-wheel SBUs are 2.784 and 2.735 Å. The crystal retains the 2D network, but its structure is modified. Two nearly identical layered motifs have almost ideal square-grid (4,4) sql topology with diagonal dimensions of 15.513 Å × 15.586 Å (Fig. 7a). All the S-nia ligands appear perpendicular to the layer plane as the pillars. Thus, the absence of solvent molecules modifies both coordination geometry and local connectivity of the SBUs

After blue dry_1 was soaked in methanol for one day at room temperature, the color changed back to pink, producing dry_1s. The unit cell for dry_1s was found to be triclinic, with a = 11.11 Å, b = 15.73 Å, c = 18.08 Å; α = 73.81°, β = 86.67°, γ = 76.43°; V = 2955.16 Å3. The three crystals obtained by our collaborators are shown in figure 7.

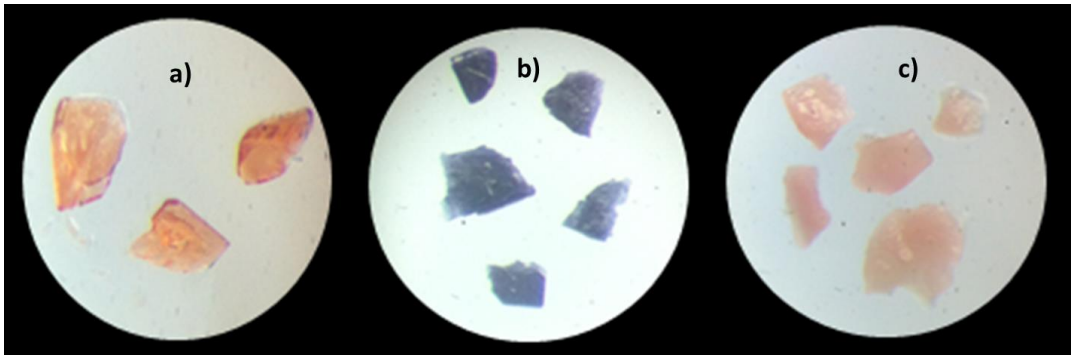

Figure 7 Photographs of single crystals of compound a) 1, b) dry_1, and c) dry_1s

The semi empirical QM calculations of dry_1s were performed starting from the solved structure of crystal 1 and both water and dmf were replaced with methanol molecules. As the methanol molecules were added the structure was optimized, and the resulting lattice parameters are shown in table 2. There is a range of potential structures in acceptable agreement with the experimental lattice parameters. This agreement lies in the range of 10-18 methanol molecules per unit cell.

The structures with other methanol content (6, 10, 12, and 14 molecules per unit cell) were also considered by deleting two methanol molecules from the unit cell. Their lattice parameters of dry_1s are also reported in table 2. All versions with 10-18 methanol molecules were found in fair agreements with experiment. The optimized lattice parameters for crystals 1 and dry_1 are also reported in table 2 for validation purposes.

Table 2 PM7 optimized vs. experimental lattice parameters for crystals 1, dry_1 and dry_1s.

System	a	b	c	α	β	γ
Crystal 1, experimental	**10.61**	**13.43**	**17.84**	**78.86**	**76.42**	**72.3**
Crystal 1, optimized	**10.76**	**13.53**	**17.96**	**73.41**	**75.17**	**74.42**
Crystal dry_1s, experimental	**11.11**	**15.73**	**18.08**	**73.81**	**86.67**	**76.43**
Crystal dry_1s, 6MeOH	**12.64**	**14.10**	**18.23**	**73.78**	**70.01**	**53.56**
Crystal dry_1s, 10MeOH	**10.85**	**13.88**	**20.17**	**77.25**	**62.39**	**55.53**
Crystal dry_1s, 12MeOH	**10.78**	**13.49**	**17.90**	**77.92**	**75.44**	**69.53**
Crystal dry_1s, 14MeOH	**10.76**	**13.65**	**18.41**	**75.14**	**73.38**	**67.28**
Crystal dry_1s, 18MeOH	**11.87**	**15.82**	**18.46**	**73.22**	**71.73**	**60.29**
Crystal dry_1, experimental	**10.95**	**11.04**	**17.92**	**99.33**	**96.76**	**90.26**
Crystal dry_1, optimized	**10.51**	**10.62**	**17.51**	**95.64**	**92.87**	**89.91**

Co(II) complexes are known to change color. For instance, the color transition for aqueous solutions of $CoCl_2$ upon rising concentration of chloride ions was interpreted[59]

as shift in equilibrium between pink $[CoCl(H_2O)_5]^{+1}$ and blue $[CoCl_2(H_2O)_2]$ complexes. The respective absorption spectra are shown in figure 8.

In order to analyze the nature of colour change in 1 and dry_1, TDDFT calculations were performed on binuclear complexes taken from the crystal structure of 1 and dry_1 (protonated to make them neutral), therefore these complexes will be referred as 1c and dry_1c.

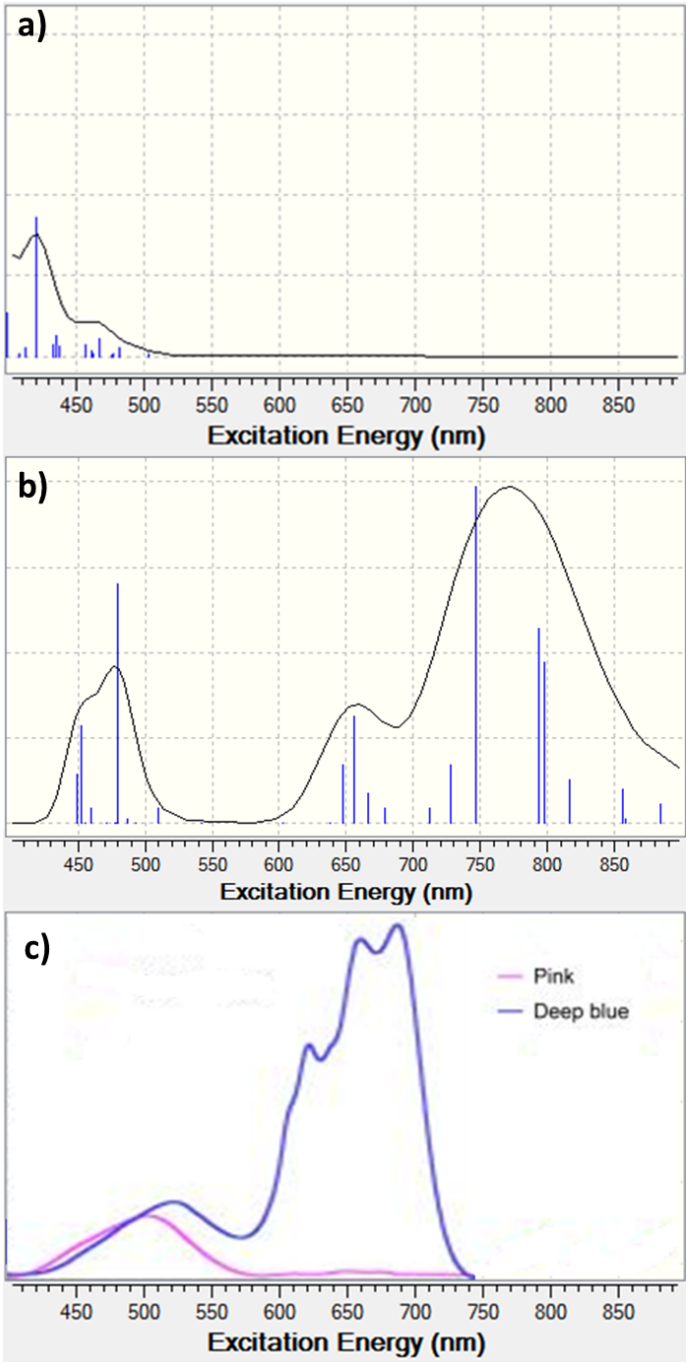

Figure 8 TDDFT predicted electronic spectra or (a) dinuclear complex from 1, and (b) dinuclear complex dry_1; (c) experimental absorption spectra for pink [CoCl(H2O)5]+1 and blue [CoCl2(H2O)2] complexes in aqueous solution (from Ref.178)are also shown.

Table 3 Leading electronic configurations for the absorbing states of the selected excited states in dinuclear complexes from structures 1 and dry_1.

Complex	Excited State	Leading configuration	Amplitude	Wavelength	Oscillator strength
1c	31	αHOMO → αLUMO+2	0.79	420nm	0.0384
dry_1c	40	αHOMO → αLUMO+7	0.87	480nm	0.0049
dry_1c	30	βHOMO-4 → βLUMO	0.84	656nm	0.0022

As shown in figure 8, 1c have an absorption peak in 450-500 nm range, and dry_1c contains three significant peaks one located near 480, 656, and 746 nm. The leading electronic configurations for the strongest absorbing states in 400-800 nm range for 1c and dry_1c are summarized in table 3. The absorption band in 1c is due to MLCT state, originating from transition between αHOMO (localized on the metal toward) and αLUMO+2 orbital (localized on the conjugated system in the bdc) as shown in figure 9.

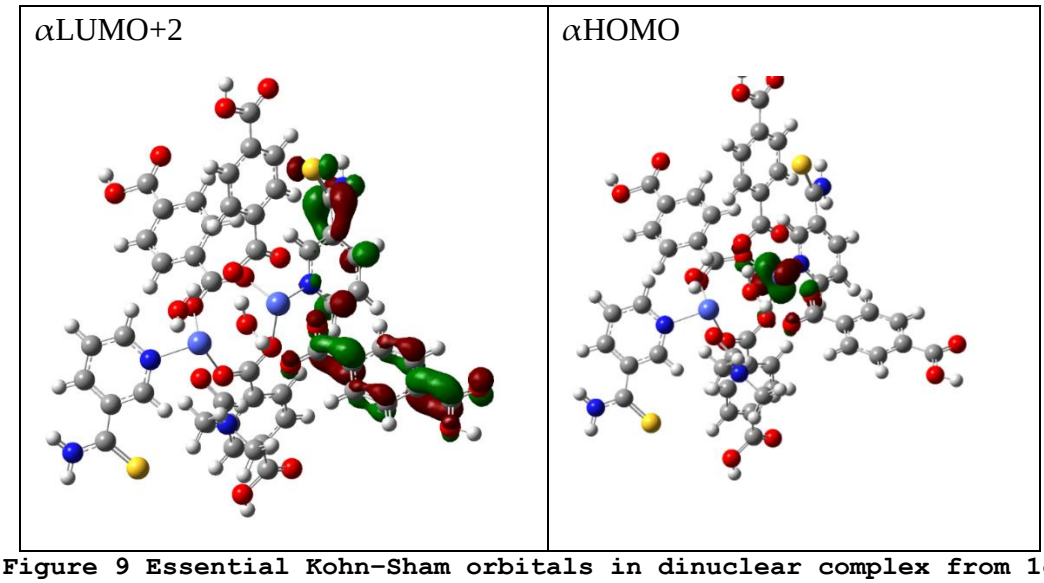

Figure 9 Essential Kohn-Sham orbitals in dinuclear complex from 1c

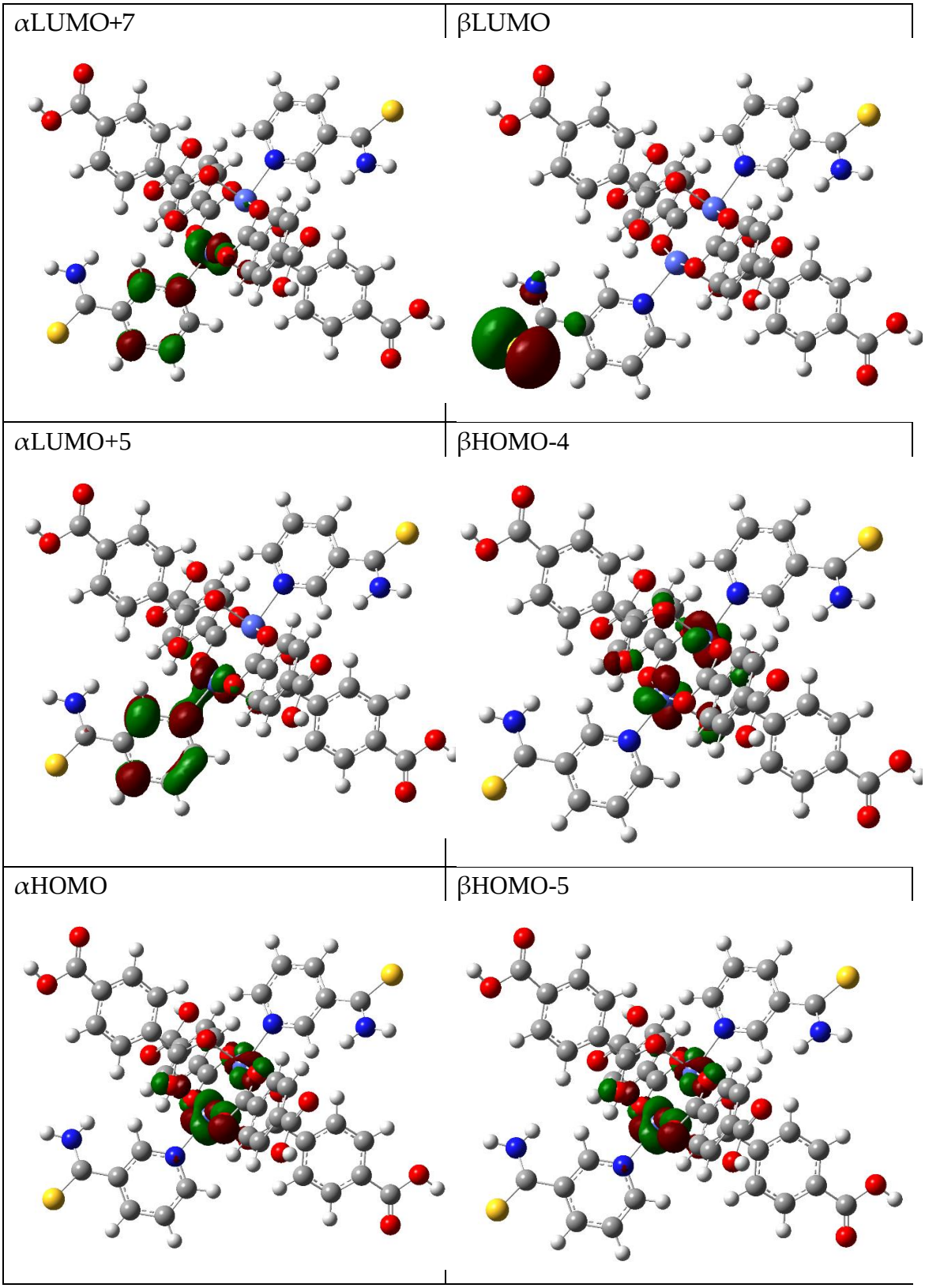

Figure 10 Essential Kohn-Sham orbitals in dinuclear complex from dry_1c

The binuclear complex dry_1c absorbs at three wavelengths. The essential Kohn-Sham orbitals are shown in figure 10. The absorption peak near 480 nm is due to LMCT state, corresponding to transition between αHOMO orbital (localized on S-nic ligand) into αLUMO+7, mostly *d*-orbital on Co(II).

The peak close to 656 nm consist of two leading configurations. The latter are composed of MLCT transitions originating from the βHOMO-4 and βHOMO-5 on Co(II) into the βLUMO orbital on S-nic. The dry_1c has another MLCT state, which has a lower excitation energy due to destabilization of *d*-orbital of Co metal by the surrounding ligands. This destabilization is due to the shorter metal to ligand distances in Co(II) complexes with lower coordination number.

In order to confirm the previous statement the average distances from the Co(II) to bdc and S-nic ligands are were measured from X-Ray experimental data. The average distances for the Co(II) to Oxygen in bdc for 1c is 2.26 Å and for dry_1c is 2.02 Å. The average distances for the Co(II) to Nitrogen are nearly constant: 2.09 Å for 1c and 2.05 Å for dry_1c. Therefore, the colour pink of dry_1s supports our hypothesis of octahedral Co(II) coordination when resolvated with methanol.

3.4 Conclusions

In summary, the compounds discussed here show dynamic behavior as consequence of the type and amount of solvent in coordinated to Co(II). The coordination geometry of the Co(II) centers, transitions of the 2D network, changes the color from pink to blue and back to pink again indicate in favor of the higher stability of Co(II) octahedral coordination against the pentagonal one.

Theoretical prediction were performed in order to find the mechanism of the solvatochromic behavior of the crystal resulting MLCT charge transfer transitions due to destabilization of *d*-orbital of Co metal by the surrounding ligands. This destabilization is due to the shorter metal to ligand distances in Co(II) complexes with lower coordination number.

3.5 List of References

1. Kitagawa, S.; Kitaura, R.; Noro, S.-i., Functional Porous Coordination Polymers. *Angewandte Chemie International Edition* **2004**, *43*, 2334-2375.

2. Kitagawa, S.; Matsuda, R., Chemistry of Coordination Space of Porous Coordination Polymers. *Coordination Chemistry Reviews* **2007**, *251*, 2490-2509.

3. Kitaura, R.; Seki, K.; Akiyama, G.; Kitagawa, S., Porous Coordination-Polymer Crystals with Gated Channels Specific for Supercritical Gases. *Angewandte Chemie International Edition* **2003**, *42*, 428-431.

4. Li, H.; Eddaoudi, M.; O'Keeffe, M.; Yaghi, O. M., Design and Synthesis of an Exceptionally Stable and Highly Porous Metal-Organic Framework. *Nature* **1999**, *402*, 276-279.

5. Eddaoudi, M.; Moler, D. B.; Li, H. L.; Chen, B. L.; Reineke, T. M.; O'Keeffe, M.; Yaghi, O. M., Modular Chemistry: Secondary Building Units as a Basis for the Design of Highly Porous and Robust Metal-Organic Carboxylate Frameworks. *Accounts of Chemical Research* **2001**, *34*, 319-330.

6. Tranchemontagne, D. J.; Mendoza-Cortes, J. L.; O'Keeffe, M.; Yaghi, O. M., Secondary Building Units, Nets and Bonding in the Chemistry of Metal-Organic Frameworks. *Chemical Society Reviews* **2009**, *38*, 1257-1283.

7. Kitagawab, H.-C. J. Z. a. S., Metal–Organic Frameworks (Mofs). *Chem. Soc. Rev.* **2014**, *43*, 5415-5418.

8. Long, J. R.; Yaghi, O. M., The Pervasive Chemistry of Metal-Organic Frameworks. *Chemical Society Reviews* **2009**, *38*, 1213-1214.

9. Moulton, B.; Zaworotko, M. J., From Molecules to Crystal Engineering: Supramolecular Isomerism and Polymorphism in Network Solids. *Chemical Reviews* **2001**, *101*, 1629-1658.

10. Lee, J.; Farha, O. K.; Roberts, J.; Scheidt, K. A.; Nguyen, S. T.; Hupp, J. T., Metal-Organic Framework Materials as Catalysts. *Chemical Society Reviews* **2009**, *38*, 1450-1459.

11. Furukawa, H.; Gandara, F.; Zhang, Y.-B.; Jiang, J.; Queen, W. L.; Hudson, M. R.; Yaghi, O. M., Water Adsorption in Porous Metal-Organic Frameworks and Related Materials. *Journal of the American Chemical Society* **2014**, *136*, 4369-4381.

12. Kurmoo, M., Magnetic Metal-Organic Frameworks. *Chemical Society Reviews* **2009**, *38*, 1353-1379.

13. Allendorf, M. D.; Bauer, C. A.; Bhakta, R. K.; Houk, R. J. T., Luminescent Metal-Organic Frameworks. *Chemical Society Reviews* **2009**, *38*, 1330-1352.

14. Morris, R. E.; Wheatley, P. S., Gas Storage in Nanoporous Materials. *Angewandte Chemie International Edition* **2008**, *47*, 4966-4981.

15. Li, J.-R.; Kuppler, R. J.; Zhou, H.-C., Selective Gas Adsorption and Separation in Metal-Organic Frameworks. *Chemical Society Reviews* **2009**, *38*, 1477-1504.

16. Ma, S.; Zhou, H.-C., Gas Storage in Porous Metal-Organic Frameworks for Clean Energy Applications. *Chemical Communications* **2010**, *46*, 44-53.

17. Dulcevscaia, G.; Liu, S.-X.; Hauser, J.; Krämer, K. W.; Frei, G.; Möller, A.; Decurtins, S., A Benzaldehyde Derivative as a Chelating Ligand: Helical Manganese(Ii) Coordination Polymers Assembling into a Porous Solid. *Crystal Growth & Design* **2013**, *13*, 4138-4144.

18. Kreno, L. E.; Leong, K.; Farha, O. K.; Allendorf, M.; Van Duyne, R. P.; Hupp, J. T., Metal-Organic Framework Materials as Chemical Sensors. *Chemical Reviews* **2012**, *112*, 1105-1125.

19. Feng, J.; Li, H.; Yang, Q.; Wei, S.-C.; Zhang, J.; Su, C.-Y., A Two-Dimensional Flexible Porous Coordination Polymer Based on Co(Ii) and Terpyridyl Phosphine Oxide. *Inorganic Chemistry Frontiers* **2015**, *2*, 388-394.

20. Zaworotko, M. J., Superstructural Diversity in Two Dimensions: Crystal Engineering of Laminated Solids. *Chemical Communications* **2001**, 1-9.

21. Yan, Q.; Lin, Y.; Wu, P.; Zhao, L.; Cao, L.; Peng, L.; Kong, C.; Chen, L., Designed Synthesis of Functionalized Two-Dimensional Metal–Organic Frameworks with Preferential Co2 Capture. *ChemPlusChem* **2013**, *78*, 86-91.

22. Kondo, A.; Noguchi, H.; Carlucci, L.; Proserpio, D. M.; Ciani, G.; Kajiro, H.; Ohba, T.; Kanoh, H.; Kaneko, K., Double-Step Gas Sorption of a Two-Dimensional Metal–Organic Framework. *Journal of the American Chemical Society* **2007**, *129*, 12362-12363.

23. Huang, W.-H.; Yang, G.-P.; Chen, J.; Chen, X.; Zhang, C.-P.; Wang, Y.-Y.; Shi, Q.-Z., Solvent Influence on Sizes of Channels in Three New Co(Ii) Complexes, Exhibiting an Active Replaceable Coordinated Site. *Crystal Growth & Design* **2013**, *13*, 66-73.

24. Peng, Y.; Li, Y.; Ban, Y.; Jin, H.; Jiao, W.; Liu, X.; Yang, W., Metal-Organic Framework Nanosheets as Building Blocks for Molecular Sieving Membranes. *Science* **2014**, *346*, 1356-1359.

25. Sadakiyo, M.; O¯kawa, H.; Shigematsu, A.; Ohba, M.; Yamada, T.; Kitagawa, H., Promotion of Low-Humidity Proton

Conduction by Controlling Hydrophilicity in Layered Metal-Organic Frameworks. *Journal of the American Chemical Society* **2012**, *134*, 5472-5475.

26. Croitor, L.; Coropceanu, E. B.; Masunov, A. E.; Rivera-Jacquez, H. J.; Siminel, A. V.; Fonari, M. S., Mechanism of Nonlinear Optical Enhancement and Supramolecular Isomerism in 1d Polymeric Zn(Ii) and Cd(Ii) Sulfates with Pyridine-4-Aldoxime Ligands. *Journal of Physical Chemistry C* **2014**, *118*, 9217-9227.

27. Croitor, L.; Coropceanu, E. B.; Siminel, A. V.; Kulikova, O.; Zelentsov, V. I.; Datsko, T.; Fonari, M. S., 1,2-Cyclohexanedionedioxime as a Useful Co-Ligand for Fabrication of One-Dimensional Zn(Ii) and Cd(Ii) Coordination Polymers with Wheel-and-Axle Topology and Luminescent Properties. *Crystengcomm* **2012**, *14*, 3750-3758.

28. Croitor, L.; Coropceanu, E. B.; Jeanneau, E.; Dementiev, I. V.; Goglidze, T. I.; Chumakov, Y. M.; Fonari, M. S., Anion-Induced Generation of Binuclear and Polymeric Cd(Ii) and Zn(Ii) Coordination Compounds with 4,4 '-Bipyridine and Dioxime Ligands. *Crystal Growth & Design* **2009**, *9*, 5233-5243.

29. Croitor, L.; Coropceanu, E. B.; Siminel, A. V.; Masunov, A. E.; Fonari, M. S., From Discrete Molecules to One-Dimensional Coordination Polymers Containing Mn(Ii), Zn(Ii)

or Cd(Ii) Pyridine-2-Aldoxime Building Unit. *Polyhedron* **2013**, *60*, 140-150.

30. Coropceanu, E. B.; Croitor, L.; Fonari, M. S., Mononuclear Cd(Ii) and Zn(Ii) Complexes with the 1,2-Cyclohexanedionedioxime Ligand: Preparation and Structural Characterization. *Polyhedron* **2012**, *38*, 68-74.

31. Croitor, L.; Coropceanu, E. B.; Masunov, A. E.; Rivera-Jacquez, H. J.; Siminel, A. V.; Zelentsov, V. I.; Datsko, T. Y.; Fonari, M. S., Polymeric Luminescent Zn(Ii) and Cd(Ii) Dicarboxylates Decorated by Oxime Ligands: Tuning the Dimensionality and Adsorption Capacity. *Crystal Growth & Design* **2014**, *14*, 3935-3948.

32. Croitor, L.; Coropceanu, E. B.; Siminel, A. V.; Kravtsov, V. C.; Fonari, M. S., Polymeric Zn(Ii) and Cd(Ii) Sulfates with Bipyridine and Dioxime Ligands: Supramolecular Isomerism, Chirality, and Luminescence. *Crystal Growth & Design* **2011**, *11*, 3536-3544.

33. Coropceanu, E. B.; Croitor, L.; Siminel, A. V.; Fonari, M. S., Preparation, Structural Characterization and Luminescence Studies of Mono- and Binuclear Zn(Ii) and Cd(Ii) Acetates with Pyridine-4-Aldoxime and Pyridine-4-Amidoxime Ligands. *Polyhedron* **2014**, *75*, 73-80.

34. Croitor, L.; Coropceanu, E. B.; Siminel, A. V.; Botoshansky, M. M.; Fonari, M. S., Synthesis, Structures, and Luminescence Properties of Mixed Ligand Cd(Ii) and Zn(Ii) Coordination Compounds Mediated by 1,2-Bis(4-Pyridyl)Ethane. *Inorganica Chimica Acta* **2011**, *370*, 411-419.

35. Coropceanu, E. B.; Croitor, L.; Siminel, A. V.; Fonari, M. S., Unique Tetranuclear Heterometallic Compound Na2zn2{(4-Py)C(H)(Noh)}(2) (Ch3coo)(6)(H2o)(4) Center Dot 2h(2)O with Luminescent Properties. *Inorganic Chemistry Communications* **2011**, *14*, 1528-1531.

36. Sharif, S.; Akkurt, M.; Khan, I. U.; Nadeem, S.; Tirmizi, S. A.; Ahmad, S., 3-Carbamothioylpyridinium Iodide. *Acta Crystallographica Section E* **2009**, *65*, o2423.

37. Jurczak, J.; Prokopowicz, P., Diastereoselectivity Control in the Ticl4-Mediated Addition Reaction of Allyltrimethylsilane to N,O-Protected (L)-Serinals. *Tetrahedron Letters* **1998**, *39*, 9835-9838.

38. Fonari, M. S.; Ganin, E. V.; Tang, S.-W.; Wang, W.-J.; Simonov, Y. A., Molecular Complexes of Thionicotinamide with 18-Membered Crown Ethers: Synthesis and Crystal Structures. *Journal of Molecular Structure* **2007**, *826*, 89-95.

39. Kitagawa, S.; Uemura, K., Dynamic Porous Properties of Coordination Polymers Inspired by Hydrogen Bonds. *Chemical Society Reviews* **2005**, *34*, 109-119.

40. Stewart, J. J. P., Mopac2012, Stewart Computational Chemistry Version 14.083l. **2012**.

41. Stewart, J. J. P., Optimization of Parameters for Semiempirical Methods Vi: More Modifications to the Nddo Approximations and Re-Optimization of Parameters. *Journal of Molecular Modeling* **2013**, *19*, 1-32.

42. Cardenas-Jiron, G. I.; Masunov, A.; Dannenberg, J. J., Molecular Orbital Study of Crystalline P-Benzoquinone. *Journal of Physical Chemistry A* **1999**, *103*, 7042-7046.

43. Frisch, M. J., et al. *Gaussian 09, Revision D.01*, Gaussian, Inc.: Wallingford CT, 2009.

44. Mikhailov, I. A.; Bondar, M. V.; Belfield, K. D.; Masunov, A. E., Electronic Properties of a New Two-Photon Absorbing Fluorene Derivative: The Role of Hartree-Fock Exchange in the Density Functional Theory Design of Improved Nonlinear Chromophores. *Journal of Physical Chemistry C* **2009**, *113*, 20719-20724.

45. Rassolov, V. A.; Pople, J. A.; Ratner, M. A.; Windus, T. L., 6-31g* Basis Set for Atoms K through Zn. *Journal of Chemical Physics* **1998**, *109*, 1223-1229.

46. Casida, M. E.; Huix-Rotllant, M., Progress in Time-Dependent Density-Functional Theory. *Annual Review of Physical Chemistry, Vol 63* **2012**, *63*, 287-323.

47. Yoshida, Y.; Inoue, K.; Kurmoo, M., On the Nature of the Reversibility of Hydration—Dehydration on the Crystal Structure and Magnetism of the Ferrimagnet [Mnii(Enh)(H2o)][Criii(Cn)6]·H2o. *Inorganic Chemistry* **2009**, *48*, 267-276.

48. Spek, A. L., Platon Squeeze: A Tool for the Calculation of the Disordered Solvent Contribution to the Calculated Structure Factors. *Acta Crystallographica Section C-Structural Chemistry* **2015**, *71*, 9-18.

49. Knichal, J. V.; Gee, W. J.; Burrows, A. D.; Raithby, P. R.; Teat, S. J.; Wilson, C. C., A Facile Single Crystal to Single Crystal Transition with Significant Structural Contraction on Desolvation. *Chemical Communications* **2014**, *50*, 14436-14439.

50. Zhang, J.-P.; Liao, P.-Q.; Zhou, H.-L.; Lin, R.-B.; Chen, X.-M., Single-Crystal X-Ray Diffraction Studies on Structural Transformations of Porous Coordination Polymers. *Chemical Society Reviews* **2014**, *43*, 5789-5814.

51. Aggarwal, H.; Bhatt, P. M.; Bezuidenhout, C. X.; Barbour, L. J., Direct Evidence for Single-Crystal to Single-

Crystal Switching of Degree of Interpenetration in a Metal–Organic Framework. *Journal of the American Chemical Society* **2014**, *136*, 3776-3779.

52. Dietzel, P. D. C.; Johnsen, R. E.; Blom, R.; Fjellvåg, H., Structural Changes and Coordinatively Unsaturated Metal Atoms on Dehydration of Honeycomb Analogous Microporous Metal–Organic Frameworks. *Chemistry – A European Journal* **2008**, *14*, 2389-2397.

53. Suh, M. P.; Cheon, Y. E.; Lee, E. Y., Reversible Transformation of Znii Coordination Geometry in a Single Crystal of Porous Metal-Organic Framework [Zn3(Ntb)2(Etoh)2]·4Etoh. *Chemistry – A European Journal* **2007**, *13*, 4208-4215.

54. Bradshaw, D.; Warren, J. E.; Rosseinsky, M. J., Reversible Concerted Ligand Substitution at Alternating Metal Sites in an Extended Solid. *Science* **2007**, *315*, 977-980.

55. Tian, Y.; Allan, P. K.; Renouf, C. L.; He, X.; McCormick, L. J.; Morris, R. E., Synthesis and Structural Characterization of a Single-Crystal to Single-Crystal Transformable Coordination Polymer. *Dalton Transactions* **2014**, *43*, 1519-1523.

56. Mehlana, G.; Bourne, S. A.; Ramon, G.; Öhrström, L., Concomitant Metal Organic Frameworks of Cobalt(Ii) and 3-(4-

Pyridyl)Benzoate: Optimized Synthetic Conditions of Solvatochromic and Thermochromic Systems. *Crystal Growth & Design* **2013**, *13*, 633-644.

57. Mehlana, G.; Ramon, G.; Bourne, S. A., Methanol Mediated Crystal Transformations in a Solvatochromic Metal Organic Framework Constructed from Co(Ii) and 4-(4-Pyridyl) Benzoate. *CrystEngComm* **2013**, *15*, 9521-9529.

58. Mehlana, G.; Bourne, S. A.; Ramon, G., A New Class of Thermo- and Solvatochromic Metal-Organic Frameworks Based on 4-(Pyridin-4-Yl)Benzoic Acid. *Dalton Transactions* **2012**, *41*, 4224-4231.

59. Koga N., K. T., Sakamoto M., and Furukawa Y., Temperature Effect on Cobalt(Ii)-Chloride Complex Equilibrium in Aqueous Solution. *Chem. Educator* **2009**, *14*, 225-228.

60. Chen, C.-L.; Goforth, A. M.; Smith, M. D.; Su, C.-Y.; zur Loye, H.-C., [Co2(Ppca)2(H2o)(V4o12)0.5]: A Framework Material Exhibiting Reversible Shrinkage and Expansion through a Single-Crystal-to-Single-Crystal Transformation Involving a Change in the Cobalt Coordination Environment. *Angewandte Chemie International Edition* **2005**, *44*, 6673-6677.

61. Su, Z.; Chen, M.; Okamura, T.-a.; Chen, M.-S.; Chen, S.-S.; Sun, W.-Y., Reversible Single-Crystal-to-Single-Crystal Transformation and Highly Selective Adsorption Property of

Three-Dimensional Cobalt(Ii) Frameworks. *Inorganic Chemistry* **2011,** *50*, 985-991.

CHAPTER 4: SECOND ORDER NONLINEAR OPTICAL PROPERTIES PREDICTIONS FOR COVALENT ORGANIC FRAMEWORKS

4.1 Introduction

Structural information of molecular complexes is crucial for the understanding of their properties and function. However, the most accurate method to obtain this structural information of these molecules is X-Ray diffraction of a crystalline structure. However, one of the main challenge in the synthesis of crystalline structures is finding the correct conditions that lead to crystallization. Rational protocols for crystallization of molecules is nonexistent and usually molecules are crystallized with a trial and error methodology. Therefore, understanding the molecular mechanism leading to crystallization is crucial for the pharmaceutical industry[1-4] and material science[5-15].

Reticular chemistry is the use of molecular building blocks to form extended structures[16-17]. This approach is often used as strategy to build crystalline materials[18-19]. A proposed to solution to aid in crystallization is to join metal ions with carbons and oxygen to produce metal organic frameworks. However, in addition to metal organic frameworks a new class of materials known as covalent organic frameworks

(COFs) are becoming a popular alternative[16-17, 20-22]. These materials are created by linking organic building units of predetermined structures which are composed entirely of covalent bonds between light elements (C, Si, B, O, N)[8, 16-17, 19, 22-24]. It has been shown not only that the synthesis of ordered COFs is possible, but also that predesigned structures and properties can be achieved by carefully selecting the building blocks and their conditions for assembly.

These COFs can be constructed from π-conjugated system with donor and acceptor molecular fragments. The crystals formed by these systems often possess non-linear optical (NLO) properties. Currently, there is a great demand for materials with NLO optical properties to be used for imaging[25-29], sensing[30-31], among other applications[31-33]. Second Harmonic Generation (SHG) is one of the most used optical processes and it is a second order NLO property. SHG is defined as the following process: 1) two photons with the same frequency ω interact with a material and these two photons are coherently interfere each other, 2) the material is excited to an excited state, 3) the two photons combine to produce one wave with exactly double the frequency 2ω, 4) the material relaxes to the ground state configuration.

In order to design an effective material with second order properties, the compound must possess a large first order molecular hyperpolarizability, and also must crystallize in a non-centrosymmetric structure[3]. In addition to that, second order properties can be enhanced by increasing the delocalization of π-electrons with strong donor and acceptor groups. Another factor that increases the hyperpolarizability is the addition of more polarizable elements inside the conjugated chain.[34]

Density functional theory (DFT) calculations can predict the hyperpolarizability tensor components[35-39]. This is done with the use of the finite field Berry phase approach. The use computational methods aids experimentally in rational design of the most efficient SHG material.

In a collaboration with Dr.Uribe-Romo[37-39] laboratory and using the continuing the work started by Yaghi et al[24] we proceed to perform theoretical calculations in order to predict and optimize current structures. In addition to this we shall propose a designs with better performance.

4.2 Methods

When a system is under influence of a field with strength $\vec{E}$, its dipole moment can be expressed a Taylor expansion series in which the orders correspond to the field strengths:

$$\mu_i = \mu_i^0 + \alpha_{ij} \cdot E_j + \beta_{ijk} \cdot E_j \cdot E_k + \gamma_{ijkl} \cdot E_j \cdot E_k \cdot E_l + \cdots,$$

Where $\mu_i^0$is the permanent dipole moment of the unperturbed system, α_{ij} is the linear polarizability,β_{ijk},and γ_{ijkl} are second and third order polarizabilities respectively. The hyperpolarizabilities tensor components are obtained by finding the rate of change of the dipole moment in respect to the applied electric field. In order to obtain the first hyper polarizability χ^2, the second derivative of the dipole moment in respect to the applied field must be taken:

$$\beta_{ijk} = \frac{\partial^2 \vec{\mu}}{\partial^2 \vec{E}}$$

The static hyperpolarizability tensor components were predicted using CPMD computer program.[40] CPMD uses the Berry phase[41] approach combined with the infinite field method[42]. This method describes the periodic system as it interacts with a homogeneous finite electric field. Considering the symmetry of the system (cubic unit cell), we applied the external field in two direction (one coordinate and one

diagonal). The strength of the field applied were $\mp 0.00005 \mp 0.0001, \mp 0.0002, \mp 0.0004, and \mp 0.0008$ atomic units. This field strength magnitude values are the minimum needed to maintain a stable numerical derivative of the unit cell dipole moments with respect to the electric field.

The wave function of the system without a field applied was optimized, and this wave function was used as basis for the ∓ 0.00005 on the axis and the diagonal calculations. The optimized wave function corresponding to the ∓ 0.00005 a.u. field strength was used for the ∓ 0.0001 and so on until reaching ∓ 0.0008 field strength.

4.3 Discussion

The compounds presented are covalent organic framework synthesized by the means of reticular chemistry. The main idea was based on using building blocks consisting on triangular nodes of 2,3,6,7,10,11-hexahydroxytriphenylene.and tetrahedral nodes of tetra(4-dihydroxyborylphenyl)silane and the synthesis and characterization on of these compounds was done as described by El Kaderi et al.[24] However our collaborator Dr.Uribe- Romo

have synthesized a new set of these crystals using Germanium and other ligands. For the purpose of this report, preliminary results are reported and the crystals studied are shown in figure 11.

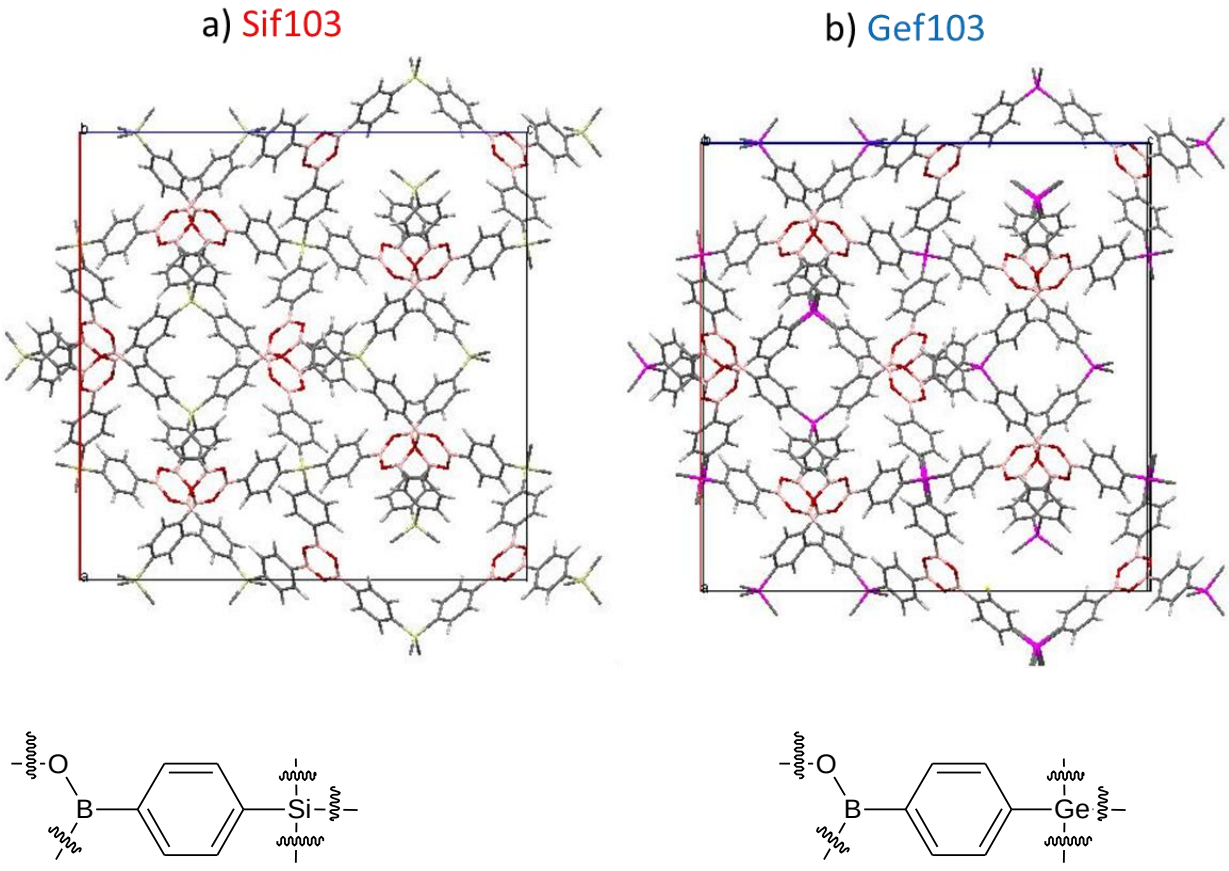

Figure 11 Crystal Structures of the compounds experimentally synthesized by our collaborators. a) Sif103 correspond to the structure based on tetrahedral nodes of (4-dihydroxyborylphenyl)silane and b) Gef103 correspond to the structure based on tetrahedral nodes of(4-dihydroxyborylphenyl)germane.

According to the crystallographic information files (cif) provided by our experimentalist collaborators, both of these structures were found to be have a cubic lattice cell

and correspond to the point group of I-43D. The crystal Sif103 has a lattice parameter of a 28.4624 and angle of 90 and Gef103 has an a of 28.7066 Å and angle of 90. An important factor to take into account is that these crystals are acentric, and this allow them to be used for SHG.

In order to analyze if these structures were good candidate as SHG materials we performed simulations using the program CPMD as described in the methods section. Starting from the experimental structure in the CIF file we applied the external field in two direction (one coordinate and one diagonal). The strength of the field applied were $\mp 0.00005 \mp 0.0001, \mp 0.0002, \mp 0.0004, and \mp 0.0008$ atomic units. The dipole moment generated as response to the field was considered against the field strength to obtain the second order hypolarizability χ^2 as shown in figure 12.

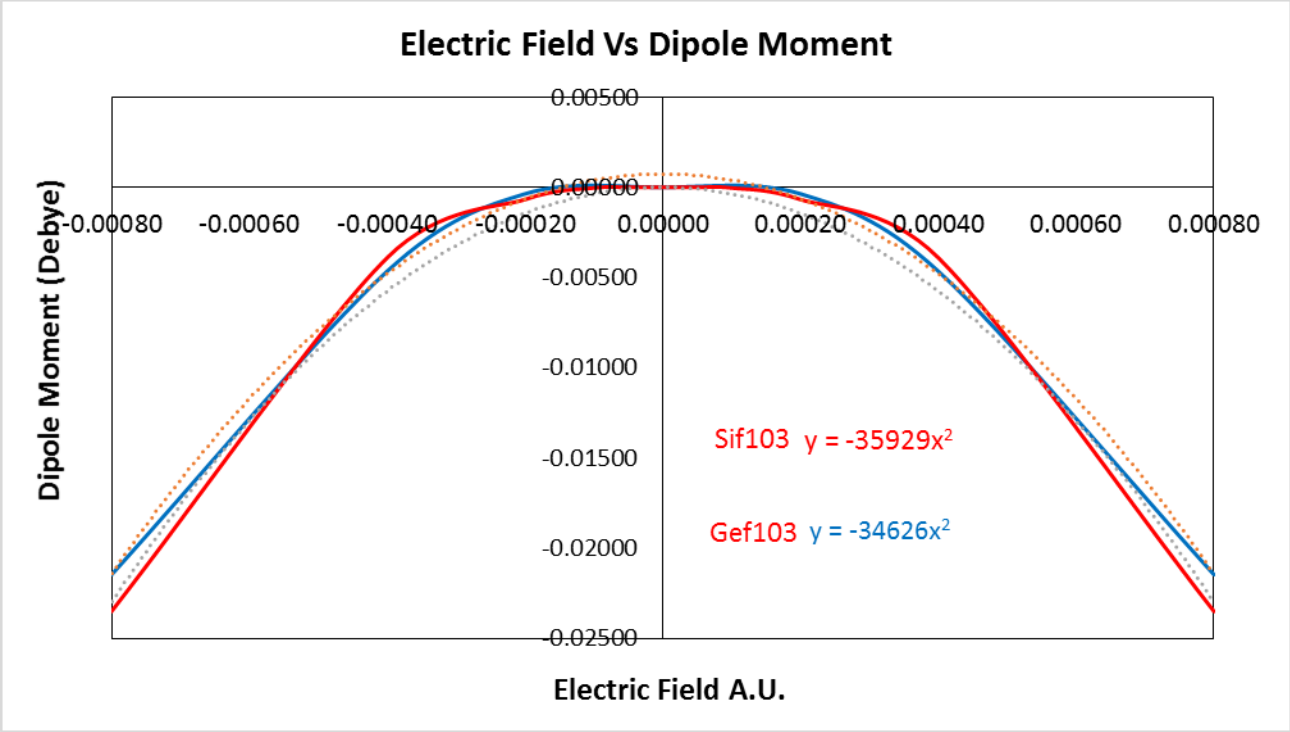

Figure 12 Plot of the electric field in atomic units versus the dipole moment in Debye for crystal sif103 and gef103. A polynomial plot is included along with the equation showing the value of the predicted χ^2

As shown in figure 12, the two structure show to have considerable χ^2. Structure sif103 is predicted to have a χ^2 of 35,929, and gef103 results to have a χ^2 of 34,626. When taking into perspective χ^2 in respect to the usual standard (Urea) these two compounds (sif103 and gef103) are 1.85 and 1.78 times better respectively.

This second order non-linear activity is observed due to the delocalization of the molecular fragments and in order to design a crystal with enhanced χ^2, two things must be taken into account: 1) increasing the charge separation of the

zwitterionic state, and 2) include into the conjugated system atoms that are more polarizable.

Based on this principle deeper analysis of the molecular structure of sif103 was performed and this structure is shown in figure 13. It is proposed to instead of using the boroxine ring, the oxygen components should be replaced by a more polarizable atom such as Sulfur.

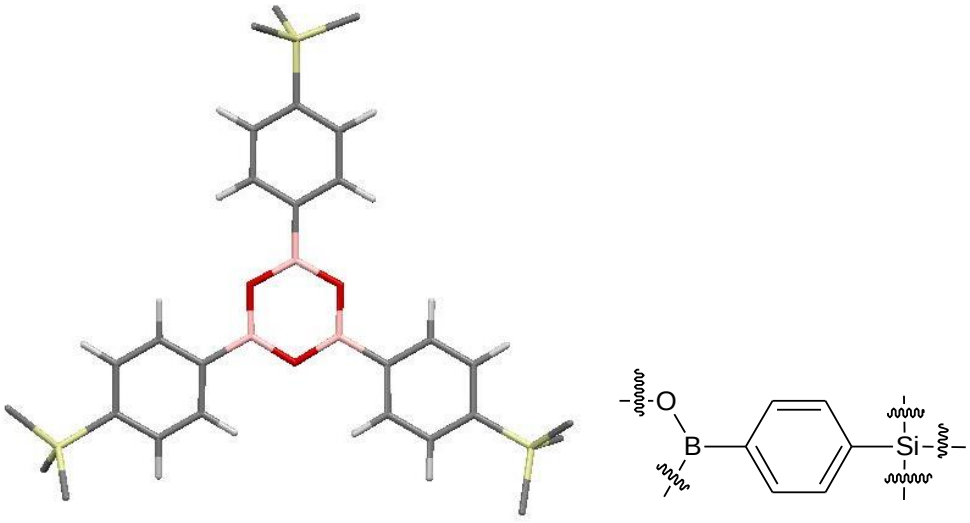

Figure 13 Molecular complex of the crystal sif103

Following this idea, theoretical calculations were performed in this new compound def107 and as shown in figure 14, and its plot of the field versus the dipole moment is in figure 15.

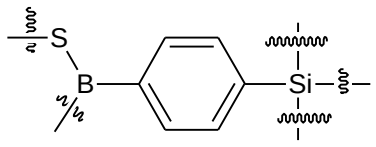

Figure 14 Molecular Formula of design 107

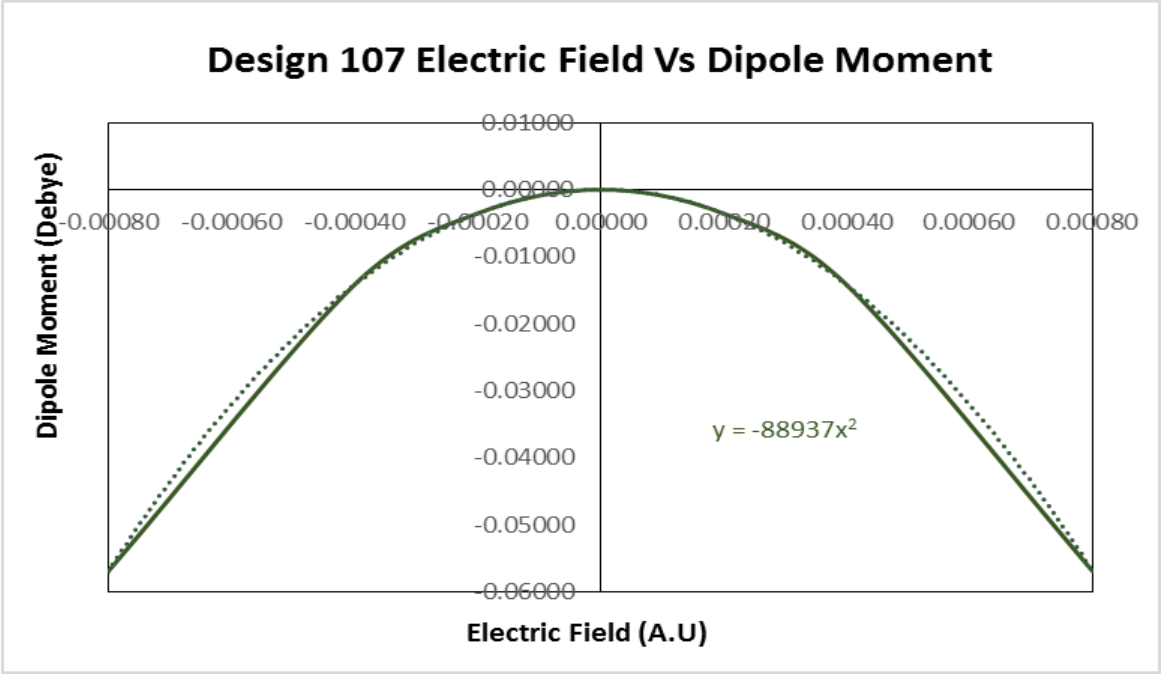

Figure 15 Plot of the electric field in atomic units versus the dipole moment in Debye for designed crystal. A polynomial plot is included along with the equation showing the value of the predicted χ^2

An enhancement of more than two times magnitude of sif103 is observed 4.6 times higher than the urea standard and this can be explained due to Sulfur polarization properties in comparison to Oxygen. The reason for this is that sulfur has a greater number of electrons and having the effect of the nuclei in the charge distribution is diminished, due to the

bigger distance of the electrons from the nuclei increases the polarization of the atom.

4.4 Conclusions

Theoretical prediction were performed and an optimized design was proposed by simply enhancing the polarization in one of the atoms in the conjugated chain. Even though this is a preliminary work, the prospective materials that can be obtained these prediction are already more multiple magnitudes higher than the urea standard.

The next design takes into consideration this and in addition to this tries to increase charge separation and include a better acceptor fragment. My hypothesis for this is to include a Phosphorus instead of silicon. The reasoning behind this, is that phosphorus is stable when it has one double bond and three single bond as observed in phosphoric acid.

4.5 List of References

1. Cunha, D.; Ben Yahia, M.; Hall, S.; Miller, S. R.; Chevreau, H.; Elkaim, E.; Maurin, G.; Horcajada, P.; Serre, C., Rationale of Drug Encapsulation and Release from

Biocompatible Porous Metal-Organic Frameworks. *Chemistry of Materials* **2013**, *25*, 2767-2776.

2. Nanev, C. N., Kinetics and Intimate Mechanism of Protein Crystal Nucleation. *Progress in Crystal Growth and Characterization of Materials* **2013**, *59*, 133-169.

3. Toth, S. J.; Schmitt, P. D.; Snyder, G. R.; Trasi, N. S.; Sullivan, S. Z.; George, I. A.; Taylor, L. S.; Simpson, G. J., Ab Initio Prediction of the Diversity of Second Harmonic Generation from Pharmaceutically Relevant Materials. *Crystal Growth & Design* **2015**, *15*, 581-586.

4. Allen, T. M.; Cullis, P. R., Drug Delivery Systems: Entering the Mainstream. *Science* **2004**, *303*, 1818-1822.

5. Janiak, C., Engineering Coordination Polymers Towards Applications. *Dalton Transactions* **2003**, 2781-2804.

6. Brunauer, S.; Emmett, P. H.; Teller, E., Adsorption of Gases in Multimolecular Layers. *Journal of the American Chemical Society* **1938**, *60*, 309-319.

7. Croitor, L.; Coropceanu, E. B.; Masunov, A. E.; Rivera-Jacquez, H. J.; Siminel, A. V.; Fonari, M. S., Mechanism of Nonlinear Optical Enhancement and Supramolecular Isomerism in 1d Polymeric Zn(Ii) and Cd(Ii) Sulfates with Pyridine-4-Aldoxime Ligands. *Journal of Physical Chemistry C* **2014**, *118*, 9217-9227.

8. **Eddaoudi, M.; Li, H. L.; Reineke, T.; Fehr, M.; Kelley, D.; Groy, T. L.; Yaghi, O. M., Design and Synthesis of Metal-Carboxylate Frameworks with Permanent Microporosity.** ***Topics in Catalysis*** **1999,** ***9,*** **105-111.**

9. Eddaoudi, M.; Li, H. L.; Yaghi, O. M., Highly Porous and Stable Metal-Organic Frameworks: Structure Design and Sorption Properties. *Journal of the American Chemical Society* **2000,** *122,* 1391-1397.

10. Furukawa, H.; Gandara, F.; Zhang, Y.-B.; Jiang, J.; Queen, W. L.; Hudson, M. R.; Yaghi, O. M., Water Adsorption in Porous Metal-Organic Frameworks and Related Materials. *Journal of the American Chemical Society* **2014,** *136,* 4369-4381.

11. Kreno, L. E.; Leong, K.; Farha, O. K.; Allendorf, M.; Van Duyne, R. P.; Hupp, J. T., Metal-Organic Framework Materials as Chemical Sensors. *Chemical Reviews* **2012,** *112,* 1105-1125.

12. Lee, J.; Farha, O. K.; Roberts, J.; Scheidt, K. A.; Nguyen, S. T.; Hupp, J. T., Metal-Organic Framework Materials as Catalysts. *Chemical Society Reviews* **2009,** *38,* 1450-1459.

13. Allendorf, M. D.; Bauer, C. A.; Bhakta, R. K.; Houk, R. J. T., Luminescent Metal-Organic Frameworks. *Chemical Society Reviews* **2009,** *38,* 1330-1352.

14. Croitor, L.; Coropceanu, E. B.; Masunov, A. E.; Rivera-Jacquez, H. J.; Siminel, A. V.; Zelentsov, V. I.; Datsko, T. Y.; Fonari, M. S., Polymeric Luminescent Zn(Ii) and Cd(Ii) Dicarboxylates Decorated by Oxime Ligands: Tuning the Dimensionality and Adsorption Capacity. *Crystal Growth & Design* **2014**, *14*, 3935-3948.

15. Crotty, A. M.; Gizzi, A. N.; Rivera-Jacquez, H. J.; Masunov, A. E.; Hu, Z.; Geldmeier, J. A.; Gesquiere, A. J., Molecular Packing in Organic Solar Cell Materials: Insights from the Emission Line Shapes of P3ht/Pcbm Polymer Blend Nanoparticles. *Journal of Physical Chemistry C* **2014**, *118*, 19975-19984.

16. O'Keeffe, M.; Peskov, M. A.; Ramsden, S. J.; Yaghi, O. M., The Reticular Chemistry Structure Resource (Rcsr) Database of, and Symbols for, Crystal Nets. *Accounts of Chemical Research* **2008**, *41*, 1782-1789.

17. Ockwig, N. W.; Delgado-Friedrichs, O.; O'Keeffe, M.; Yaghi, O. M., Reticular Chemistry: Occurrence and Taxonomy of Nets and Grammar for the Design of Frameworks. *Accounts of Chemical Research* **2005**, *38*, 176-182.

18. Holman, K. T.; Pivovar, A. M.; Ward, M. D., Engineering Crystal Symmetry and Polar Order in Molecular Host Frameworks. *Science* **2001**, *294*, 1907-1911.

19. Yaghi, O. M.; O'Keeffe, M.; Ockwig, N. W.; Chae, H. K.; Eddaoudi, M.; Kim, J., Reticular Synthesis and the Design of New Materials. *Nature* **2003**, *423*, 705-714.

20. O'Keeffe, M.; Yaghi, O. M., Deconstructing the Crystal Structures of Metal-Organic Frameworks and Related Materials into Their Underlying Nets. *Chemical Reviews* **2012**, *112*, 675-702.

21. Tranchemontagne, D. J.; Mendoza-Cortes, J. L.; O'Keeffe, M.; Yaghi, O. M., Secondary Building Units, Nets and Bonding in the Chemistry of Metal-Organic Frameworks. *Chemical Society Reviews* **2009**, *38*, 1257-1283.

22. Uribe-Romo, F. J.; Doonan, C. J.; Furukawa, H.; Oisaki, K.; Yaghi, O. M., Crystalline Covalent Organic Frameworks with Hydrazone Linkages. *Journal of the American Chemical Society* **2011**, *133*, 11478-11481.

23. Eddaoudi, M.; Moler, D. B.; Li, H. L.; Chen, B. L.; Reineke, T. M.; O'Keeffe, M.; Yaghi, O. M., Modular Chemistry: Secondary Building Units as a Basis for the Design of Highly Porous and Robust Metal-Organic Carboxylate Frameworks. *Accounts of Chemical Research* **2001**, *34*, 319-330.

24. El-Kaderi, H. M.; Hunt, J. R.; Mendoza-Cortes, J. L.; Cote, A. P.; Taylor, R. E.; O'Keeffe, M.; Yaghi, O. M.,

Designed Synthesis of 3d Covalent Organic Frameworks. *Science* **2007**, *316*, 268-272.

25. Ahn, H.-Y.; Fairfull-Smith, K. E.; Morrow, B. J.; Lussini, V.; Kim, B.; Bondar, M. V.; Bottle, S. E.; Belfield, K. D., Two-Photon Fluorescence Microscopy Imaging of Cellular Oxidative Stress Using Profluorescent Nitroxides. *Journal of the American Chemical Society* **2012**, *134*, 4721-4730.

26. Andrade, C. D.; Yanez, C. O.; Rodriguez, L.; Belfield, K. D., A Series of Fluorene-Based Two-Photon Absorbing Molecules: Synthesis, Linear and Nonlinear Characterization, and Bioimaging. *Journal of Organic Chemistry* **2010**, *75*, 3975-3982.

27. Oikawa, Y., Frontiers in Live Bone Imaging Researches. Two-Photon Excitation Microscopy, Principles and Technologies. *Clinical calcium* **2015**, *25*, 871-6.

28. Yao, S.; Belfield, K. D., Two-Photon Fluorescent Probes for Bioimaging. *European Journal of Organic Chemistry* **2012**, 3199-3217.

29. Zhang, Q., et al., Dual-Functional Analogous Cis-Platinum Complex with High Antitumor Activities and Two-Photon Bioimaging. *Biochemistry* **2015**, *54*, 2177-2180.

30. Belfield, K. D.; Bondar, M. V.; Frazer, A.; Morales, A. R.; Kachkovsky, O. D.; Mikhailov, I. A.; Masunov, A. E.;

Przhonska, O. V., Fluorene-Based Metal-Ion Sensing Probe with High Sensitivity to Zn2+ and Efficient Two-Photon Absorption. *Journal of Physical Chemistry B* **2010**, *114*, 9313-9321.

31. Masunov, A. E. M., I. A., Theory and Computations of Two-Photon Absorbing Photochromic Chromophores. *Eur. J. Chem.* **2010**, *1*, 142-161.

32. Masunov, A. E., Theoretical Spectroscopy of Carbocyanine Dyes Made Accurate by Frozen Density Correction to Excitation Energies Obtained by Td-Dft. *International Journal of Quantum Chemistry* **2010**, *110*, 3095-3100.

33. Mikhailov, I. A.; Belfield, K. D.; Masunov, A. E., Dft-Based Methods in the Design of Two-Photon Operated Molecular Switches. *Journal of Physical Chemistry A* **2009**, *113*, 7080-7089.

34. Cole, J. M., Organic Materials for Second-Harmonic Generation: Advances in Relating Structure to Function. *Philosophical Transactions of the Royal Society a-Mathematical Physical and Engineering Sciences* **2003**, *361*, 2751-2770.

35. Draguta, S.; Fonari, M. S.; Masunov, A. E.; Zazueta, J.; Sullivan, S.; Antipin, M. Y.; Timofeeva, T. V., New Acentric Materials Constructed from Aminopyridines and 4-Nitrophenol. *CrystEngComm* **2013**, *15*, 4700-4710.

36. Suponitsky, K. Y.; Masunov, A. E., Supramolecular Step in Design of Nonlinear Optical Materials: Effect of Π…Π Stacking Aggregation on Hyperpolarizability. *The Journal of Chemical Physics* **2013**, *139*, 094310.

37. Laurent, A. D.; Jacquemin, D., Td-Dft Benchmarks: A Review. *International Journal of Quantum Chemistry* **2013**, *113*, 2019-2039.

38. Nayyar, I. H.; Batista, E. R.; Tretiak, S.; Saxena, A.; Smith, D. L.; Martin, R. L., Localization of Electronic Excitations in Conjugated Polymers Studied by Dft. *Journal of Physical Chemistry Letters* **2011**, *2*, 566-571.

39. Wu, C.; Tretiak, S.; Chernyak, V. Y., Excited States and Optical Response of a Donor-Acceptor Substituted Polyene: A Td-Dft Study. *Chemical Physics Letters* **2007**, *433*, 305-311.

40. Umari, P.; Pasquarello, A., Car-Parrinello Molecular Dynamics in a Finite Homogeneous Electric Field. *AIP Conference Proceedings* **2003**, *677*, 269-275.

41. Berry, M. V., Quantal Phase Factors Accompanying Adiabatic Changes. *Proceedings of the Royal Society of London. Series A, Mathematical and Physical Sciences* **1984**, *392*, 45-57.

42. Putrino, A.; Sebastiani, D.; Parrinello, M., Generalized Variational Density Functional Perturbation Theory. *The Journal of Chemical Physics* **2000**, *113*, 7102-7109.

CHAPTER 5: MECHANISM OF NONLINEAR OPTICAL ENHANCEMENT OF SUPRAMOLECULAR Zn^{+2} AND Cd^{+2} SULFATES WITH PYRIDINE-4-ALDOXIME LIGANDS

5.1 Introduction

The rational selection of metal centers and organic ligands with suitable shape, functionality, flexibility, and symmetry plays a key role in producing metal–organic materials (MOMs) with desired structures and properties[1-7]. The versatile coordination abilities of Zn(II) and Cd(II)allow a wide variety of architectures resulting from the self-assembly of these metals with organic ligands.[8-13] Organic bridging ligands, which contain adjustable flexibility and connectivity information, play crucial role in construction and structural variations of coordination polymers (CP).[14-16]

The phenomenon of supramolecular isomerism (SI) in MOMs was first generalized by Moulton and Zaworotko in 2001.[17] For the past decade it has been disclosed in and enriched by a series of low and high dimensional MOMs. Although the origin of this phenomenon is not completely understood, and the generation of supramolecular isomers occurs primarily serendipitously, the interest to this event continues to

grow, and some reports declare the preparation of supramolecular isomers by design.[18-22]

Recent examples demonstrate SI in individual Zn(II) and Cd(II)series,[23-27] and although it was suggested that the similar in electronic d^{10} configuration, but different in the radii Zn(II) and Cd(II) ions contribute to forming different coordination networks, these metals are also capable to produce from the same starting materials alongside the isomorphous crystal structures the supramolecular isomers distinguished either by the conformation of the bridging ligands or by the crystal packing of the identical coordination arrays.[28-30]

Nonlinear optical (NLO) properties of MOMs are being investigated in relation to several technological applications, including optical communications and up conversion lazing.[31] Third order nonlinearities, such as two-photon absorption (2PA) present special interest, as they are not limited to non-centrosymmetric structures, unlike second harmonic generation and other second-order nonlinear optical properties.

Several studies indicated[32-33] that 2PA properties are enhanced by metal coordination in MOMs, when compared to free ligands. The mechanism of this enhancement is not well

understood. Supramolecular isomerism provides an excellent opportunity to investigate the role of ligand organization in the coordination sphere on 2PA materials design. Ligand assembly in MOM is more robust and well defined than non-covalent aggregation of the chromophores, which was shown (both in crystalline phase[34] and in aqueous solution[35]) to result in the coupling of the excited states of the monomers.

In a dimer, this coupling produces symmetric and antisymmetric combinations, shifted up and down in energy with respect to the monomeric states. Since selection rules for 1PA and 2PA absorption differ, the blue shift on the linear absorption spectra is accompanied by the red shift on 2PA spectrum and vice versa. These findings were recently reported[34-35] and confirmed.

The sulfate anion, as a simple tetrahedral oxo-anion, has versatile coordination modes including monodentate, bidentate bridging, bidentate chelating, tridentate bridging, and even tetradentate bridging, thus providing extensions of structures. We have recently demonstrated that the combination of Zn(II) or Cd(II) sulfates with 2-pyao resulted in a series of MOMs through the successive substitution of water molecules by sulfate bridges in the metal coordination environments.[36] From the crystal engineering viewpoint, this

gave rise to the hybrid solids of different dimensionalities, including mono-, binuclear, and 1D polymeric materials, whose interest for the materials science and primarily for NLO applications might arise from the acentricity of the synthetized 1D polymeric materials, $[Zn(SO_4)(2\text{-pya})(H_2O)_2]n$ and $[Cd(SO_4)(2\text{-pya})(H_2O)]n$, with the less amount of water in favor of sulfate anions in the metal coordination cores. Herein, the structures predicted NLO properties for these new crystalline solids is presented.

5.2 Methods

In order to rationalize the conformational differences between Zn and Cd complexes in position of the oxime ligands, the density functional theory calculations were performed using Gaussian09.[37] The polarizable continuum model[38-39] (PCM) was used, and a dielectric constant of 2 was used in order to simulate the crystalline environment. The M05-QX exchange-correlation functional (formerly known as M05-11/4X)[40] obtained by interpolation between M05 and M05-2X functionals[41] and including 35% of the exact exchange. We used SDD Stuttgart effective core potentials for the metal atoms[42] and D95 basis set for the other atoms.[43]

Prediction of the linear absorption spectra using linear response time dependent density functional theory[44] (TD-DFT) nowadays is routine.[45-47] Optimization and the acquisition of the minimum energy pathway of the excited state potential surface made it possible recently to predict emission spectra[45, 48] (including dual emission[36, 49-50]) and photochemical reaction processes.[51-53] In order to predict 2PA cross section profiles, we employed a posteriori Tamm-Dancoff approximation[54] (ATDA) to second order coupled electronic oscillator formalism,[55-56] applied at the TD-DFT level.

In this approximation, the excitation energies ω_{0X} and transition densities ξ_X between the ground and excited states are obtained as solutions to the habitual linear response TD-DFT equations. Therefore, transition dipoles are calculated as a convolution of the dipole moment operator μ with respective transition densities. At the same time, Tamm-Dancoff formulas are used to predict state-to-state transition dipoles μ and the differences between the permanent and ground state dipole moments since they are not available in linear response TD-DFT Both permanent[57] and state-to-state transition dipoles75 calculated this way were validated previously by comparison with the high theory level coupled cluster results. These values are then used in the Sum over States

(SOS) expression[58] to predict the two-photon transition matrix elements. All this formalism is implemented in an in a local version of Gaussian 09 code.

5.3 Discussion

The theoretical studies were performed on pyridine-4-aldoxime (4-pyao) and Pyridine-4-amidoxime (4-pyamo) ligands and on the crystal structures synthesized by our collaborator. The molecular structure of the ligands and the monomeric complex units of these crystal is shown in figure 15

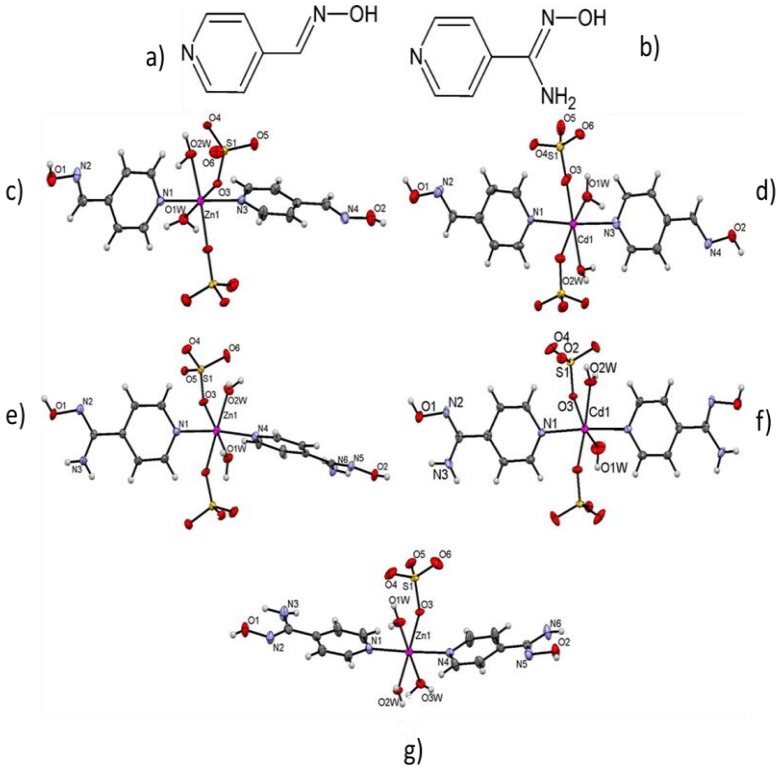

Figure 16 Ligands Used in This Study: (a) Pyridine-4-aldoxime (4-pyao); (b) Pyridine-4-amidoxime (4-pyamo) monomeric complex units 1–5 with the partial atom labeling: (c) 1, (d) 2, (e) 3, (f) 4, and (g) 5.

Since some of the crystals reported in this contribution belong to the centrosymmetric space groups, the second order nonlinearities vanish in crystals 1, 3, and 4 but can be observed in crystals 2 and 5 that belong to the acentric space groups.

However, the optical nonlinearity of all the crystals studied may reveal itself in the third order of external field, such as the two photon absorption. Simultaneous absorption of two photons have important technological implications such as optical power limiting,[53] up-conversion lasing,[59] and chemical and biological sensing.[60-61] However, 2PA process has a relatively low probability, and molecular design, leading to enhancement of 2PA cross sections is attracting considerable interest.

Recently, Cd-,[33] Zn-,[62-63] Ru-,[64] and Pt-based[65] MOMs had been reported with high two photon absorption cross-sections. Therefore, it is reasonable to question on whether crystals 1–5 may be found to be efficient two-photon absorbing materials. Here, we used the structure of the crystals 1–5 in order to answer this question, and, perhaps, more importantly, to formulate the principles of MOM optimization

for the purposes of enhancing their nonlinear optical properties.

Before we present our estimates for the crystals 1–5, one has to note that experimental investigation of 2PA spectra presents considerable challenge.[66] For that reason, such investigation extends beyond the scope of present work. Also, one has to be careful when selecting the representative fragment of the crystal for the purposes of 2PA spectra prediction, as crystalline environment may affect the NLO properties.

Investigation of the effect of the environment has been studied both experimentally[34] and theoretically[67-68] and found that stacking interactions of the conjugated π-systems, leading to H-aggregation[35] in the solid state, affect the optical properties to a much greater degree than the herringbone (T-shaped) interactions of the phenyl rings.

Table 4 Properties of Free Ligands 4-Pyao and 4-Pyamo, Model Complexes Calculated at the TD-DFT Level M05XQ*

System	σ	E	λ	μ(gf)	Δμ(f)	μ(gi)	μ(if)
4-pyao	3	5.00	248	1.12	0.3	1.72	0.84
4-pyamo	6	4.51	275	1.23	2.28	0.26	0.88
[Zn(4-pyao(H_2O)$_5$]	10	4.82	257	2.15	1.78		
[Cd(4-pyao(H_2O)$_5$]	11	4.88	254	2.14	1.98		
[Zn(4-pyamo(H_2O)$_5$]	12	3.71	334	1.35	2.93		
[Cd(4-pyamo(H_2O)$_5$]	12	3.95	314	1.24	2.98		

*The 2PA cross sections σ (in GM), excitation energies E (in eV), and absorption wavelengths λ (in nm) are reported. Also shown are the permanent dipole moments difference between 2PA absorbing (final, f) and ground (g) states, as well as transition dipole moments μ (in atomic units) from the ground to final, ground to intermediate (i, one photon absorbing) state, and intermediate to final states, respectively

Table 5 Properties of the Monomer Complexes 1m-5m with Three Exchange-Correlation Functionals: M05-QX, B3LYP, and CAM-B3LYP*

Functional	B3LYP			M05QX			CAM-B3LYP		
System	σ	E	λ	σ	E	λ	σ	E	λ
1m	27	4.67	266	22	4.87	255	15	5.04	246
2m	20	4.47	277	13	4.69	264	9	4.84	256
	18	4.69	264	16	4.90	253	11	5.07	245
3m	9	3.43	362	12	3.75	331	11	4.21	294
	19	3.6	344	14	3.92	316	15	4.31	288
4m	24	3.62	322	26	4.05	306	21	4.39	282
5m	12	3.59	346	10	3.99	311	11	4.33	287
	15	3.69	336	14	4.10	302	13	4.44	279

*The 2PA cross sections σ (in GM), excitation energies E (in eV), and absorption wavelengths λ (in nm) are reported. Also shown are the permanent dipole moments difference between 2PA absorbing (final, f) and ground (g) states, as well as transition dipole moments μ (in atomic units) from the ground to final, ground to intermediate (i, one photon absorbing) state, and intermediate to final states, respectively

Among the structures reported in this work, the largest stacking overlap is found in crystal 5. Comparison of 2PA cross sections for the monomeric complex and their stacking dimer found in the crystals of 5 demonstrates insignificant shifts in both pick position and this height. For this reason, we only report 2PA results for the monomeric complexes in crystals 1–5 in figure 15

As one can see from the Table 4, two-photon absorption cross sections of the complexes 1m–5m is in the range of 18–25 GM, similar to that of green fluorescent protein chromophore.[69] These values present considerable enhancement compared to 2PA cross sections of the 4-pyao and 4-pyamo ligands (3 and 6 GM, respectively). Comparison with the model complexes shows that if one of the two organic ligands is substituted with the water molecule, 2PA efficiency is reduced by half, and still exceeds the 2PA cross section of the isolated ligand by 2–3-fold.

In order to further investigate the origin of this enhancement, we analyzed 4-pyamo in greater details. The HOMO–LUMO transition in this molecule corresponds to the singlet excited state with large oscillator strength and 2PA cross section. According to two-state model for the polar chromophores, this cross section is proportional to the

squared change of the permanent dipole moment upon excitation and squared transition dipole moment to the ground state. These permanent and transition dipole moments are also listed in Table 4.

After Zn(II) coordination, the LUMO remains localized on the ligand, but it is somewhat destabilized and polarized toward the metal, so that the dipole moment change upon excitation is increased from 2.3 and 2.9 D. As the result, the resonant 2PA cross section of this state nearly doubles. Addition of the second ligand in orthogonal conformation and formation of the complex 3m results in appearance of another as shown in table 4, nearly degenerate state, localized on this added ligand, with a similar 2PA cross section. The two peaks overlap on 2PA spectrum and increase the resulting cross section by ~50%.

The situation is somewhat different for the complex 4m, however. Here the essential states, localized on two ligands, mix. Resulting symmetric combination has high oscillator strength and is somewhat stabilized. Antisymmetric combination, on the other hand, has zero oscillator strength and is slightly destabilized in energy (J-aggregate type state coupling). According to the three-state model for symmetric chromophores, 2PA cross section for this state is

proportional to the squared product of two transition dipole moments: one between ground to intermediate 1PA state, and another one is 1PA to the final 2PA state. Resulting 2PA cross section of antisymmetric combination more than doubles compared to the initial ligand localized states.

In order to test sensitivity of out 2PA predictions to the exchange-correlation functional used, we report the results obtained with widely used functionals B3LYP and CAM-B3LYP in table 5 as well. The functionals contain 20% and up to 60% of the Hartree–Fock exchange, respectively, as compared to 35% of HF exchange in M05-QX. One can see that B3LYP and CAM-B3LYP shift the 2PA resonance almost uniformly (by ~10 nm) to the longer and shorter wavelengths, respectively.

The 2PA cross sections are also increased or decreased by ~25% and (in the case of two 2PA bands) their intensity is slightly redistributed. These variations, however, do not change our quantitative conclusions on the mechanisms of 2PA enhancements upon the complex formation. In order to analyze the differences in conformations between Zn and Cd complexes, we performed the potential surface scan at M05-QX/SDD theory level. A model complexes 6m and 7m were built, where octahedral coordination around Zn (6m) or Cd (7m) was

saturated by four water molecules in the equatorial plane, while two axial positions were occupied by two 4-pyao molecules. The torsion angles between the pyridine rings were fixed at values between 0.0° and 180.0°, with 10° step size. All other degrees of freedom were optimized.

The resulting potential curves were found to have minima at nearly perpendicular conformations in 6m, and at coplanar conformations for 7m. The rotation barrier in both cases was found to be close to 1.4 kcal/ mol. This difference was attributed to the lower energy level of the Cd 4d-orbitals, which allow them to participate more effectively in the conjugation with both π-systems of the oxime ligands.

This conformational energy preference is fairly small, but apparently sufficient to result in different packing modes of analogous complexes in crystal.

5.4 Conclusion

The set of complexes were investigated as potential two-photon absorbing chromophores. TD-DFT calculations predict that metal coordination considerably enhances nonlinear optical response of the conjugated ligands. Detailed analyses of the electronic structure reveals the mechanism of this

enhancement. Metal coordination polarizes the LUMO, increasing the permanent dipole moment of the excited state, and its 2PA cross section. Coplanar coordination of the two ligands in Cd(II) complex more than doubles the 2PA cross section due to J-aggregate type state coupling.

Nonplanar conformation of the two ligands in Zn(II) complexes results in less pronounced enhancement of NLO properties. Our continuous efforts are aimed at the further modifications of these solids by consecutive substitution of water molecules by sulfate ligands in the metal coordination environment.

Computational predictions reported herein, should assist in design of new coordination polymers with expected nonlinear optical properties. Coordination polymers 1–3 also reveal ligand-based luminescence properties in the solid state.

5.5 Copyright Acknowledgment

5.6 List of References

1. Cui, Y.; Yue, Y.; Qian, G.; Chen, B., Luminescent Functional Metal-Organic Frameworks. *Chemical Reviews* **2012**, *112*, 1126-1162.

2. Cunha, D.; Ben Yahia, M.; Hall, S.; Miller, S. R.; Chevreau, H.; Elkaim, E.; Maurin, G.; Horcajada, P.; Serre, C., Rationale of Drug Encapsulation and Release from Biocompatible Porous Metal-Organic Frameworks. *Chemistry of Materials* **2013**, *25*, 2767-2776.

3. Eddaoudi, M.; Moler, D. B.; Li, H. L.; Chen, B. L.; Reineke, T. M.; O'Keeffe, M.; Yaghi, O. M., Modular Chemistry: Secondary Building Units as a Basis for the Design of Highly Porous and Robust Metal-Organic Carboxylate Frameworks. *Accounts of Chemical Research* **2001**, *34*, 319-330.

4. Horike S.; Kitagawa, S., Design of Pororus Coordination Polymers/Metal-Organic Frameworks: Past, Present, and Future. In Metal-Organic Frameworks: Applications from Catalysis to Gas Storage;. *Wiley-VCH VErlag GmbH & Co. KgaA* **2011**.

5. Janiak, C., Engineering Coordination Polymers Towards Applications. *Dalton Transactions* **2003**, 2781-2804.

6. Kreno, L. E.; Leong, K.; Farha, O. K.; Allendorf, M.; Van Duyne, R. P.; Hupp, J. T., Metal-Organic Framework

Materials as Chemical Sensors. *Chemical Reviews* **2012**, *112*, 1105-1125.

7. Robin, A. Y.; Fromm, K. M., Coordination Polymer Networks with O- and N-Donors: What They Are, Why and How They Are Made. *Coordination Chemistry Reviews* **2006**, *250*, 2127-2157.

8. Erxleben, A., Structures and Properties of Zn(Ii) Coordination Polymers. *Coordination Chemistry Reviews* **2003**, *246*, 203-228.

9. Liu, H.-Y.; Ma, J.-F.; Liu, Y.-Y.; Yang, J., A Series of Zn(Ii) and Cd(Ii) Coordination Polymers Based on Flexible Bis- (Pyridyl)-Benzimidazole Ligand and Different Carboxylates: Syntheses, Structures, and Photoluminescent Properties. *Crystengcomm* **2013**, *15*, 2699-2708.

10. Lu, W. G.; Jiang, L.; Feng, X. L.; Lu, T. B., Three 3d Coordination Polymers Constructed by Cd(Ii) and Zn(Ii) with Imidazole-4,5-Dicarboxylate and 4,4 '-Bipyridyl Building Blocks. *Crystal Growth & Design* **2006**, *6*, 564-571.

11. Wang, L.; You, W.; Huang, W.; Wang, C.; You, X.-Z., Alteration of Molecular Conformations, Coordination Modes, and Architectures for a Novel 3,8-Diimidazol-1,10-Phenanthroline Compound in the Construction of Cadmium(Ii) and Zinc(Ii) Homochiral Coordination Polymers Involving an

Auxiliary Chiral Camphorate Ligand. *Inorganic Chemistry* **2009**, *48*, 4295-4305.

12. Withersby, M. A.; Blake, A. J.; Champness, N. R.; Cooke, P. A.; Hubberstey, P.; Li, W. S.; Schroder, M., Solvent Control in the Synthesis of 3,6-Bis(Pyridin-3-Yl)-1,2,4,5-Tetrazine-Bridged Cadmium(Ii) and Zinc(Ii) Coordination Polymers. *Inorganic Chemistry* **1999**, *38*, 2259-2266.

13. Yoshida, J.; Nishikiori, S.-i.; Kuroda, R.; Yuge, H., Three Polymorphic Cdii Coordination Polymers Obtained from the Solution and Mechanochemical Reactions of 3-Cyanopentane-2,4-Dione with Cdii Acetate. *Chemistry-a European Journal* **2013**, *19*, 3451-3457.

14. Bu, X. H.; Chen, W.; Lu, S. L.; Zhang, R. H.; Liao, D. Z.; Bu, W. M.; Shionoya, M.; Brisse, F.; Ribas, J., Flexible Meso-Bis(Sulfinyl) Ligands as Building Blocks for Copper(Ii) Coordination Polymers: Cavity Control by Varying the Chain Length of Ligands. *Angewandte Chemie-International Edition* **2001**, *40*, 3201-+.

15. Carlucci, L.; Ciani, G.; Proserpio, D. M.; Rizzato, S., Coordination Networks from the Self-Assembly of Silver Salts and the Linear Chain Dinitriles Nc(Ch2)(N)Cn (N = 2 to 7): A Systematic Investigation of the Role of Counterions and of

the Increasing Length of the Spacers. *Crystengcomm* **2002**, 413-425.

16. Wang, X. L.; Chao, Q.; Wang, E. B.; Lin, X.; Su, Z. M.; Hu, C. W., Interlocked and Interdigitated Architectures from Self-Assembly of Long Flexible Ligands and Cadmium Salts. *Angewandte Chemie-International Edition* **2004**, *43*, 5036-5040.

17. Moulton, B.; Zaworotko, M. J., From Molecules to Crystal Engineering: Supramolecular Isomerism and Polymorphism in Network Solids. *Chemical Reviews* **2001**, *101*, 1629-1658.

18. Abourahma, H.; Moulton, B.; Kravtsov, V.; Zaworotko, M. J., Supramolecular Isomerism in Coordination Compounds: Nanoscale Molecular Hexagons and Chains. *Journal of the American Chemical Society* **2002**, *124*, 9990-9991.

19. Bourne, S. A., Supramolecular Isomerism. In *Supramolecular Chemistry*, John Wiley & Sons, Ltd: 2012.

20. Hennigar, T. L.; MacQuarrie, D. C.; Losier, P.; Rogers, R. D.; Zaworotko, M. J., Supramolecular Isomerism in Coordination Polymers: Conformational Freedom of Ligands in Co(No3)(2)(1,2-Bis(4-Pyridyl)Ethane)(1.5) (N). *Angewandte Chemie-International Edition* **1997**, *36*, 972-973.

21. Zhang, J.-P.; Huang, X.-C.; Chen, X.-M., Supramolecular Isomerism in Coordination Polymers. *Chemical Society Reviews* **2009**, *38*, 2385-2396.

22. Deng, D.; Liu, L.; Ji, B.-M.; Yin, G.; Du, C., Temperature, Cooling Rate, and Additive-Controlled Supramolecular Isomerism in Four Pb(Ii) Coordination Polymers with an in Situ Ligand Transformation Reaction. *Crystal Growth & Design* **2012**, *12*, 5338-5348.

23. Tong, M. L.; Hu, S.; Wang, J.; Kitagawa, S.; Ng, S. W., Supramolecular Isomerism in Cadmium Hydroxide Phases. Temperature-Dependent Synthesis and Structure of Photoluminescent Coordination Polymers of Alpha- and Beta-Cd-2(Oh)(2)(2,4-Pyda). *Crystal Growth & Design* **2005**, *5*, 837-839.

24. Tian, Z.; Lin, J.; Su, Y.; Wen, L.; Liu, Y.; Zhu, H.; Meng, Q.-J., Flexible Ligand, Structural, and Topological Diversity: Isomerism in Zn(No3)(2) Coordination Polymers. *Crystal Growth & Design* **2007**, *7*, 1863-1867.

25. Chen, D.-S.; Sun, L.-B.; Liang, Z.-Q.; Shao, K.-Z.; Wang, C.-G.; Su, Z.-M.; Xing, H.-Z., Conformational Supramolecular Isomerism in Two-Dimensional Fluorescent Coordination Polymers Based on Flexible Tetracarboxylate Ligand. *Crystal Growth & Design* **2013**, *13*, 4092-4099.

26. Cui, P.; Wu, J.; Zhao, X.; Sun, D.; Zhang, L.; Guo, J.; Sun, D., Two Solvent-Dependent Zinc(Ii) Supramolecular Isomers: Rare Kgd and Lonsdaleite Network Topologies Based on

a Tripodal Flexible Ligand. *Crystal Growth & Design* **2011**, *11*, 5182-5187.

27. Tan, Y. S.; Sudlow, A. L.; Molloy, K. C.; Morishima, Y.; Fujisawa, K.; Jackson, W. J.; Henderson, W.; Halim, S. N. B. A.; Ng, S. W.; Tiekink, E. R. T., Supramolecular Isomerism in a Cadmium Bis(N-Hydroxyethyl, N-Isopropyldithiocarbamate) Compound: Physiochemical Characterization of Ball (N=2) and Chain (N = Infinity) Forms of {Cd S2cn(Ipr)Ch2ch2oh (2)Center Dot Solvent}(N). *Crystal Growth & Design* **2013**, *13*, 3046-3056.

28. Croitor, L.; Coropceanu, E. B.; Jeanneau, E.; Dementiev, I. V.; Goglidze, T. I.; Chumakov, Y. M.; Fonari, M. S., Anion-Induced Generation of Binuclear and Polymeric Cd(Ii) and Zn(Ii) Coordination Compounds with 4,4 '-Bipyridine and Dioxime Ligands. *Crystal Growth & Design* **2009**, *9*, 5233-5243.

29. Croitor, L.; Coropceanu, E. B.; Siminel, A. V.; Kravtsov, V. C.; Fonari, M. S., Polymeric Zn(Ii) and Cd(Ii) Sulfates with Bipyridine and Dioxime Ligands: Supramolecular Isomerism, Chirality, and Luminescence. *Crystal Growth & Design* **2011**, *11*, 3536-3544.

30. Croitor, L.; Coropceanu, E. B.; Siminel, A. V.; Kulikova, O.; Zelentsov, V. I.; Datsko, T.; Fonari, M. S., 1,2-Cyclohexanedionedioxime as a Useful Co-Ligand for Fabrication of One-Dimensional Zn(Ii) and Cd(Ii) Coordination

Polymers with Wheel-and-Axle Topology and Luminescent Properties. *Crystengcomm* **2012**, *14*, 3750-3758.

31. Yu, J.; Cui, Y.; Xu, H.; Yang, Y.; Wang, Z.; Chen, B.; Qian, G., Confinement of Pyridinium Hemicyanine Dye within an Anionic Metal-Organic Framework for Two-Photon-Pumped Lasing. *Nature Communications* **2013**, *4*.

32. Nie, C.; Zhang, Q.; Ding, H.; Huang, B.; Wang, X.; Zhao, X.; Li, S.; Zhou, H.; Wu, J.; Tian, Y., Two Novel Six-Coordinated Cadmium(Ii) and Zinc(Ii) Complexes from Carbazate Beta-Diketonate: Crystal Structures, Enhanced Two-Photon Absorption and Biological Imaging Application. *Dalton Transactions* **2014**, *43*, 599-608.

33. Xu, D.; Yang, M.; Wang, Y.; Cao, Y.; Fang, M.; Zhu, W.; Zhou, H.; Hao, F.; Wu, J.; Tian, Y., New Dyes with Enhanced Two-Photon Absorption Cross-Sections Based on the Cd(Ii) and 4-(4- 4-(Imidazole)Styryl Phenyl)-2,2:6,2-Terpyridine. *Journal of Coordination Chemistry* **2013**, *66*, 2992-3003.

34. Hu, H., et al., Two-Photon Absorption Spectrum of a Single Crystal Cyanine-Like Dye. *Journal of Physical Chemistry Letters* **2012**, *3*, 1222-1228.

35. Passier, R.; Ritchie, J. P.; Toro, C.; Diaz, C.; Masunov, A. E.; Belfield, K. D.; Hernandez, F. E., Thermally Controlled

Preferential Molecular Aggregation State in a Thiacarbocyanine Dye. *Journal of Chemical Physics* **2010**, *133*.

36. Croitor, L.; Coropceanu, E. B.; Siminel, A. V.; Masunov, A. E.; Fonari, M. S., From Discrete Molecules to One-Dimensional Coordination Polymers Containing Mn(Ii), Zn(Ii) or Cd(Ii) Pyridine-2-Aldoxime Building Unit. *Polyhedron* **2013**, *60*, 140-150.

37. Frisch, M. J., et al. *Gaussian 09, Revision D.01*, Gaussian, Inc.: Wallingford CT, 2009.

38. Improta, R.; Barone, V.; Scalmani, G.; Frisch, M. J., A State-Specific Polarizable Continuum Model Time Dependent Density Functional Theory Method for Excited State Calculations in Solution. *Journal of Chemical Physics* **2006**, *125*.

39. Scalmani, G.; Frisch, M. J., Continuous Surface Charge Polarizable Continuum Models of Solvation. I. General Formalism. *Journal of Chemical Physics* **2010**, *132*.

40. Mikhailov, I. A.; Bondar, M. V.; Belfield, K. D.; Masunov, A. E., Electronic Properties of a New Two-Photon Absorbing Fluorene Derivative: The Role of Hartree-Fock Exchange in the Density Functional Theory Design of Improved Nonlinear Chromophores. *Journal of Physical Chemistry C* **2009**, *113*, 20719-20724.

41. Zhao, Y.; Schultz, N. E.; Truhlar, D. G., Exchange-Correlation Functional with Broad Accuracy for Metallic and Nonmetallic Compounds, Kinetics, and Noncovalent Interactions. *Journal of Chemical Physics* **2005**, *123*.

42. Andrae, D.; Haussermann, U.; Dolg, M.; Stoll, H.; Preuss, H., Energy-Adjusted Ab-Initio Pseudopotentials for the 2nd and 3rd Row Transition-Elements. *Theoretica Chimica Acta* **1990**, *77*, 123-141.

43. Dunning Jr., T. H. H., P. J., *Modern Theoretical Chemistry*, III ed., 1977.

44. Casida, M. E.; Huix-Rotllant, M., Progress in Time-Dependent Density-Functional Theory. *Annual Review of Physical Chemistry, Vol 63* **2012**, *63*, 287-323.

45. Masunov, A. E., Theoretical Spectroscopy of Carbocyanine Dyes Made Accurate by Frozen Density Correction to Excitation Energies Obtained by Td-Dft. *International Journal of Quantum Chemistry* **2010**, *110*, 3095-3100.

46. Jacquemin, D.; Mennucci, B.; Adamo, C., Excited-State Calculations with Td-Dft: From Benchmarks to Simulations in Complex Environments. *Physical Chemistry Chemical Physics* **2011**, *13*, 16987-16998.

47. Laurent, A. D.; Jacquemin, D., Td-Dft Benchmarks: A Review. *International Journal of Quantum Chemistry* **2013**, *113*, 2019-2039.

48. Toro, C.; Thibert, A.; De Boni, L.; Masunov, A. E.; Hernandez, F. E., Fluorescence Emission of Disperse Red 1 in Solution at Room Temperature. *Journal of Physical Chemistry B* **2008**, *112*, 929-937.

49. Moreshead, W. V.; Przhonska, O. V.; Bondar, M. V.; Kachkovski, A. D.; Nayyar, I. H.; Masunov, A. E.; Woodward, A. W.; Belfield, K. D., Design of a New Optical Material with Broad Spectrum Linear and Two-Photon Absorption and Solvatochromism. *Journal of Physical Chemistry C* **2013**, *117*, 23133-23147.

50. Ganin, E. V.; Masunov, A. E.; Siminel, A. V.; Fonari, M. S., Preparation, Characterization, and Electronic Structure of Asymmetric Isonaphthalimide: Mechanism of Dual Fluorescence in Solid State. *Journal of Physical Chemistry C* **2013**, *117*, 18154-18162.

51. De Boni, L.; Toro, C.; Masunov, A. E.; Hernandez, F. E., Untangling the Excited States of Dr1 in Solution: An Experimental and Theoretical Study. *Journal of Physical Chemistry A* **2008**, *112*, 3886-3890.

52. Patel, P. D.; Mikhailov, I. A.; Belfield, K. D.; Masunov, A. E., Theoretical Study of Photochromic Compounds, Part 2: Thermal Mechanism for Byproduct Formation and Fatigue Resistance of Diarylethenes Used as Data Storage Materials. *International Journal of Quantum Chemistry* **2009**, *109*, 3711-3722.

53. Masunov, A. E. M., I. A., Theory and Computations of Two-Photon Absorbing Photochromic Chromophores. *Eur. J. Chem.* **2010**, *1*, 142-161.

54. Mikhailov, I. A.; Tafur, S.; Masunov, A. E., Double Excitations and State-to-State Transition Dipoles in Pi-Pi* Excited Singlet States of Linear Polyenes: Time-Dependent Density-Functional Theory Versus Multiconfigurational Methods. *Physical Review A* **2008**, 77.

55. Chernyak, V.; Mukamel, S., Density-Matrix Representation of Nonadiabatic Couplings in Time-Dependent Density Functional (Tddft) Theories. *Journal of Chemical Physics* **2000**, *112*, 3572-3579.

56. Tretiak, S.; Mukamel, S., Density Matrix Analysis and Simulation of Electronic Excitations in Conjugated and Aggregated Molecules. *Chemical Reviews* **2002**, *102*, 3171-3212.

57. Mikhailov, I. A.; Musial, M.; Masunov, A. E., Permanent Dipole Moments and Energies of Excited States from Density

Functional Theory Compared with Coupled Cluster Predictions: Case of Para-Nitroaniline. *Computational and Theoretical Chemistry* **2013**, *1019*, 23-32.

58. Ohta, K.; Kamada, K., Theoretical Investigation of Two-Photon Absorption Allowed Excited States in Symmetrically Substituted Diacetylenes by Ab Initio Molecular-Orbital Method. *Journal of Chemical Physics* **2006**, *124*.

59. Perry, J. W., et al., Organic Optical Limiter with a Strong Nonlinear Absorptive Response. *Science* **1996**, *273*, 1533-1536.

60. Taki, M.; Wolford, J. L.; O'Halloran, T. V., Emission Ratiometric Imaging of Intracellular Zinc: Design of a Benzoxazole Fluorescent Sensor and Its Application in Two-Photon Microscopy. *Journal of the American Chemical Society* **2004**, *126*, 712-713.

61. Belfield, K. D.; Bondar, M. V.; Frazer, A.; Morales, A. R.; Kachkovsky, O. D.; Mikhailov, I. A.; Masunov, A. E.; Przhonska, O. V., Fluorene-Based Metal-Ion Sensing Probe with High Sensitivity to Zn2+ and Efficient Two-Photon Absorption. *Journal of Physical Chemistry B* **2010**, *114*, 9313-9321.

62. Easwaramoorthi, S., et al., Structure-Property Relationship for Two-Photon Absorbing Multiporphyrins: Supramolecular Assembly of Highly-Conjugated

Multiporphyrinic Ladders and Prisms. *Journal of Physical Chemistry A* **2008**, *112*, 6563-6570.

63. Ikeda, C.; Yoon, Z. S.; Park, M.; Inoue, H.; Kim, D.; Osuka, A., Helicity Induction and Two-Photon Absorbance Enhancement in Zinc(Ii) Meso-Meso Linked Porphyrin Oligomers Via Intermolecular Hydrogen Bonding Interactions. *Journal of the American Chemical Society* **2005**, *127*, 534-535.

64. Hanczyc, P.; Norden, B.; Samoc, M., Two-Photon Absorption of Metal-Organic DNA-Probes. *Dalton Transactions* **2012**, *41*, 3123-3125.

65. Rogers, J. E., et al., Platinum Acetylide Two-Photon Chromophores. *Inorganic Chemistry* **2007**, *46*, 6483-6494.

66. Dasari, R. R.; Sartin, M. M.; Cozzuol, M.; Barlow, S.; Perry, J. W.; Marder, S. R., Synthesis and Linear and Nonlinear Absorption Properties of Dendronised Ruthenium(Ii) Phthalocyanine and Naphthalocyanine. *Chemical Communications* **2011**, *47*, 4547-4549.

67. Suponitsky, K. Y.; Masunov, A. E., Supramolecular Step in Design of Nonlinear Optical Materials: Effect of Pi ... Pi Stacking Aggregation on Hyperpolarizability. *Journal of Chemical Physics* **2013**, *139*.

68. Suponitsky, K. Y.; Masunov, A. E.; Antipin, M. Y., Computational Search for Nonlinear Optical Materials: Are

Polarization Functions Important in the Hyperpolarizability Predictions of Molecules and Aggregates? *Mendeleev Communications* **2009**, *19*, 311-313.

69. Drobizhev, M.; Makarov, N. S.; Hughes, T.; Rebane, A., Resonance Enhancement of Two-Photon Absorption in Fluorescent Proteins. *Journal of Physical Chemistry B* **2007**, *111*, 14051-14054.

CHAPTER 6: THEORETICAL STUDIES OF TWO-PHOTON EXCITED PHOSPHORESCENT PORPHYRINS BASED SENSORS FOR OXYGEN IMAGING AND OTHER BIOLOGICAL APPLICATIONS

6.1 Introduction

Currently there is a great endeavor in finding efficient sensors, and this is due to their versatility of applications. The extensive search for efficient two photon absorbing materials is essential due to the potential innovative applications. Chromophores with high two-photon absorption cross-sections are useful for certain applications such a as microscopy[1], bioimaging[2-10], sensing.[11-15] among many others.

It is of great interest to aim these potential applications toward the biomedical field, because this sensors can aid in visualizing the cellular environment.[16-20] In order to visualize this environment, it is important to note that the biological tissue optical window lies in the range of 600-1300 nm. This implies that linear absorption sensors are not useful for these biological applications, due to the high amount energy that needs to be used to bring these sensors to the desired excited state. Consequently this increases that probability of damaging the biological tissue.[21-24]

In order to be inside this wavelength range two photon absorbing materials must be designed and optimized. The simplest description of the two photon absorption process is: 1) the chromophoric material is excited to a higher state by simultaneous Absorption of two photons, 2) this is followed by internal conversion (IC) to the lowest singlet excited state S_1 and then, 3) the excited singlet may decay back to the ground state S_0 by emitting fluorescence.

The common approach taken to design new two photon absorbing sensors consist on building a molecule with excitation affinity that is able to achieve a competitive cross section and quantum yield. In the purpose of aiding the effort to find an efficient sensor to image the brain, we propose to find the mechanism of two photon absorption, and enhance its cross-section. The quality of the 2PA cross-section is highly associated with the extent of the conjugation length, this is due to its contribution to enhance the transition dipole moment. This is clearly seem when analyzing the essential HOMO to LUMO orbitals in which transition occurs.[25-29] The transitions on this type of sensors have a change in fluorescence intensity in their bound states due to intramolecular electron transfer quenching.[30]

This type of material can also be engineered to act as efficient photosensitizer. The process starts by excitation mediated by absorption of two photon to a higher state followed by internal conversion (IC) to the lowest singlet excited state S_1, and this excited singlet may decay back to the ground state S_0 by emitting fluorescence. However the goal is to engineering molecules that are more likely to undergo $S_1 \rightarrow T_n$ intersystem crossing (ISC) to the triplet state.

The highest triplet state T_n then decays to T_1 and eventually returns to S_0 by emitting phosphorescence, which is a relatively slow process. In order to control this process, the system is introduced to the presence of molecules that induce triplet annihilation process (direct transfer of triplet excitation energy or quenching) to reduce the quantum yield of phosphorescence, this process is shown in figure 16.

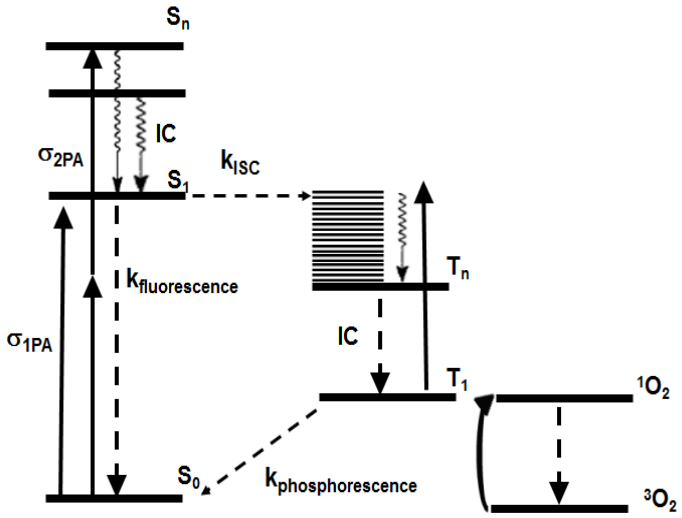

Figure 17 Jablonski energy diagram for the two photon absorption photophysical process which undergoes intersystem crossing toward the triplet state. After the triplet state the system relaxes media phosphorescence or energy transfer toward a quencher molecule.

For a long time porphyrins have been used as for photodynamic therapy (PDT) as photosensitizer.[31] Porphyrin molecules consists of four aromatic pyrrole rings joined by methyne groups in a conjugated heterocycle as shown in figure 17.

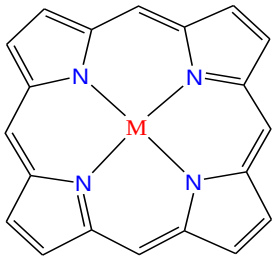

Figure 18 Porphyrin molecule consists of four aromatic pyrrole rings joined by methyne groups in a conjugated heterocycle. Porphyrin dianion can form a tetradentate complex with transition metal M^{2+}.

The porphyrin base molecule contain a closed-conjugated aromatic 18 π-electron system, which planarity can be

modulated by the interaction of substituents in the meso position. Gourterman's four orbital model describes the absorption properties of porphyrin to be caused by transitions within the two occupied molecular orbitals (HOMO) and the two lowest unoccupied molecular orbitals (LUMO).[32] It is know that the absorption spectra for one photon absorption is composed of a Soret band (an intense band found around the 400nm range and a set of Q-band found between 500 and 650nm that intensity decreases as the wavelength increases.[33]

Porphyrins has been found to have resonance enhancement of 2PA when the excitation wavelength is tuned close to the one photon allowed Q-band transition and when porphyrins are substituted by means of symmetrical or asymmetrical fashion, the cross-sections is known to be enhanced in the near IR region.[34-35] The excitation of free base porphyrin molecule leads to internal conversion to the lowest singlet excited state S_1. After that, about 5% of the Molecules decay back to the ground state S_0 by emitting fluorescence, while ~90% of them undergo $S_1 \rightarrow T_1$ intersystem crossing (ISC) to the lowest triplet state.[36] The T_1 then decays into S_0 by emitting phosphorescence, which is a relatively slow process as shown in figure 18.

The absorption (both 1PA and 2PA) into higher singlet is followed by vibrational relaxation into the lowest singlet, which is converted to triplet by intersystem crossing (ISC), followed by phosphorescence. This phosphorescence is strongly quenched by oxygen molecules, and serves as an indicator for O_2 concentration. High triplet quantum yield makes porphyrin complexes useful for a number of applications, including optical imaging of the oxygen concentration in biological tissues.[14-15, 37-39]

Light propagation in biological tissues is a complex function of scattering and absorption, which in turn, are dependent on cellular structure and molecular composition. Scattering originates from inhomogeneity in tissue, determined by refractive index discontinuities occurring both between and within cells. The spectral region between 600-1300 nm is considered to be the tissue optical window since both absorption and scattering losses are minimal through this interval.[21]

Two-photon excited phosphorescence is perfectly suited for deep tissue imaging for two reasons: (1) both excitation and emission wavelengths fit this optical window, and (2) a quadratic dependence in the intensity of light, which limits the electronic excitation and subsequent processes to the

tightly localized focal point of the laser beam. The design of the porphyrin chromophores with large two-photon absorption cross-sections is critically important for high-sensitivity imaging of oxygen concentrations in tissue.[37]

Phosphorescent imaging probes based on porphyrin dendrimers are functional macromolecules purposely designed to mimic heme-containing proteins, in which hemes are buried deep inside polypeptide macrostructures and protected from direct interactions with solvent and solutes. In porphyrin-based oxygen probes, dendrimers serve to provide well defined nano-environments for optically active cores (Pt or Pd porphyrins), and in order to control the sensor excitation after radiation has been applied to the system and to create an interface between phosphorescent cores of the probes in biological systems.[14-15, 38-40] This is a property needed for tuning the sensitivity and the dynamic range of the oxygen measurement method [41]

Biological systems can be measured optically by the phosphorescence quenching method using probes with controllable quenching parameters and defined bio-distributions. Such probes are delivered directly into the medium of interest, where they serve as molecular sensor for

oxygen. This technique can be modified to transfer the energy to other chromophores in order to obtain more contrast.

6.2 Methods

The synthetic procedure for the metal porphyrins was described previously[42]. All quantum chemical calculations were performed using the Gaussian 2009 suite of programs.[43] Density Functional Theory (DFT) was used with M05-QX exchange-correlation functional, which was derived[44] by interpolation between M05 and M05-2X functionals.[45] It includes 35% of the exact exchange and it predicts the energies of the electronic states with higher charge transfer character more accurately when compared to the commonly used functionals (such as B3LYP).

The SDD Stuttgart effective core potentials was chosen for the metal atoms[46] and D95 basis set[47] with no diffusion functions was used for the other elements in order to prevent the artificial Rydberg contributions into the valence excited states[25, 48]. The energies and oscillator strengths, necessary for the prediction of the linear absorption spectra were calculated using time dependent density functional theory[49] (TDDFT).

In order to predict the resonant 2PA cross sections, we combined 2PA matrix element sum-over-state formalism[50] with *a posteriori* Tamm-Dancoff approximation[51] (ATDA) to the second order coupled electronic oscillators formalism.[52-53] ATDA uses CIS formulas for the permanent dipole moments of the excited states, and transition dipole moments between the exited states. It was recently validated to produce accurate values for both and 2PA cross-sections,[25] and permanent dipoles of the excited states.[27] The ATDA method has been implemented in the local version of Gaussian 09 code.

Its predictions were found to be in close agreement with experimental 2PA profiles for a wide range of NLO chromophores.[11-13, 26, 54-59] The Gaussian lineshapes of 0.1 eV width was used to simulate the spectral profiles.

6.3 Discussion

Multiple Porphyrin derivatives were synthesized by our collaborators,[42] and two specific cases are analyzed and reported: 1) a case in which the substituents of the pyrrole ring are 1,2-dicarboxylic acid di-isononyl ester, **Pttchp(CO_2Bu)$_8$** and 2) a case in which the pyrrole ring is substituted with 1,2-Benzenedicarboxylic Acid, di-isononyl

ester **Pttbp$(CO_2Bu)_8$** as shown in figure 18. The purpose of our theoretical work is to investigate the effect of the aromatic ring in the porphyrin derivative and to describe the behavior of the transition dipole moments in respect to the absorption in the Soret band.

It has been shown before that when porphyrin derivatives have no aromatic substituent on the pyrrole ring may undergo distortion.[33] This distortion is caused by electronic vibrations, and these electronic vibrations are known to alter the allowed transitions in optical processes by breaking the symmetry of the wave function.

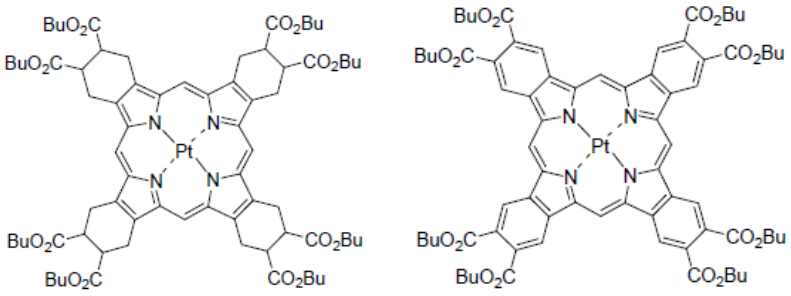

Figure 19 Molecular structure of a) Pttchp$(CO_2Bu)_8$ and b) Pttbp$(CO_2Bu)_8$

In order to take into account the distortion due to the molecular vibrations in Pttchp$(CO_2Bu)_8$, its geometry of the excited state was optimized and then the force constants, the displacement resulting from vibrational frequencies,and their intensities are calculated using the keyword: **Freq**. The range of coordinate change concerning the stretching and

compression of the bonds was then added to the initial optimized structure. All the vibrational modes were calculated as expressed in the methods section and the electronic absorption spectra were predicted for the vibrational mode of Pttchp($CO_2Bu)_8$ which followed experimental data.

The selected vibrational mode which corresponds with the experimental spectra consist on major coordinate changes in the Pt tetradendate and on the four cyclohexane substituent located in the pyrrole regions. On the cyclohexane the mayor regions undergoing distortion are positions 1 and 2 which contains the (CO_2Bu) groups. Both the experimental and predicted spectra are shown in figure 19.

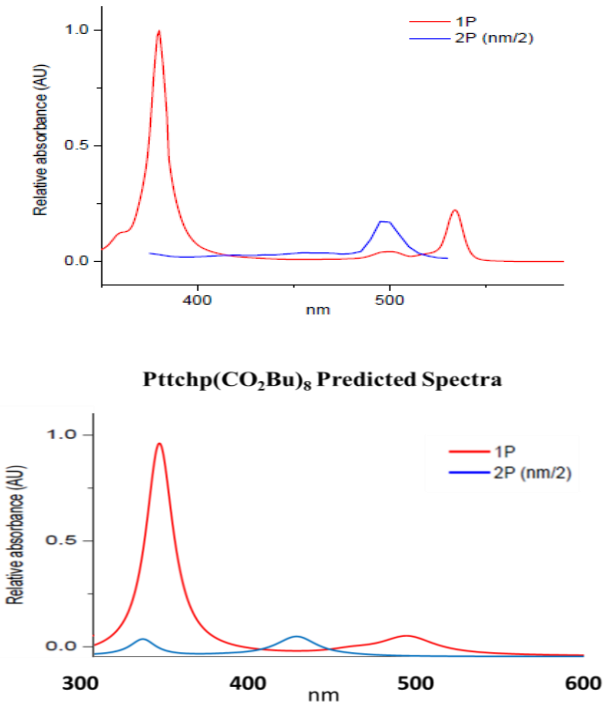

Figure 20 a) Experimental spectra of Pttchp$(CO_2Bu)_8$ b) Predicted absorption electronic spectra of Pttchp$(CO_2Bu)_8$ using TD-M05QX theory level

The experimental electronic spectra as shown in figure 19a, contains an intense absorption peak in the 380nm and a smaller one at 534nm corresponding to one photon spectra. It also contains a small two photon absorbing peak at the 490nm range. The predicted spectra as shown in figure 19b, is in agreement with experimental, except for the usual shift to the blue side consistent with a translation of about 40nm. In the case of one photon absorption the very intense peak lies in the 348nm and it is generated by the absorption of two symmetric

excited states with oscillator strength of 1.456 and 1.52 as shown in table 6a.

The transitions generating this peak corresponds to excited state 8 HOMO to LUMO+1 and 9 HOMO-1 to LUMO+1 essential Kohn-Sham orbitals are shown in figure 20. However the nature of this transition consist in a charge transfer originating from the pyrrole groups toward the Pt and the methyne linkers.

The small absorption peak is located at 496nm and it has an oscillator strength of 0.237 from the first excited state generate by a HOMO to LUMO transition also shown in figure 20. The nature of this transition concerns a charge transfer from the pyrrole to the metal. The two-photon absorption peak is located in the 430nm region is generated by the 4^{th} excited state, which receives contribution by the transition dipole moment multiplication of excited state 1 and 2. The nature and leading configuration of this transition is a HOMO-2 to LUMO local charge transfer in which the charge delocalized all over the aromatic system and the metal also shown in figure 20.

Table 6 a) Relevant parameters of the lowest 9 excited singlet states and b) calculated transition dipoles leading to two-photon absorption in Pttchp(CO_2Bu)$_8$

State	λ, nm	Oscillator	2PA
1	496	0.237	0.008
2	463	0.045	0.024
3	460	0.003	0.327
4	430	0.000	12.603
5	388	0.000	0.290
6	377	0.000	0.018
7	357	0.020	0.007
8	348	1.456	0.007
9	346	1.252	0.029

2PA State	Source State	Transition Dipole Moment (Debye)			Dipole Strength
		x	y	z	
4	1	-0.5674	-0.0016	-0.0032	0.3220
	2	-0.0006	0.001	-0.4483	0.2010

State	Leading Configuration	Amplitude	Wavelength	Oscillator	2PA
1	HOMO → LUMO	0.6507	496 nm	0.237	0.008
2	HOMO-1 → LUMO	0.5603	463 nm	0.045	0.024
4	HOMO-2 → LUMO	0.6890	430 nm	0.000	12.603
8	HOMO → LUMO+1	0.5655	348 nm	1.456	0.007
9	HOMO-1 → LUMO+1	0.6431	346 nm	1.252	0.029

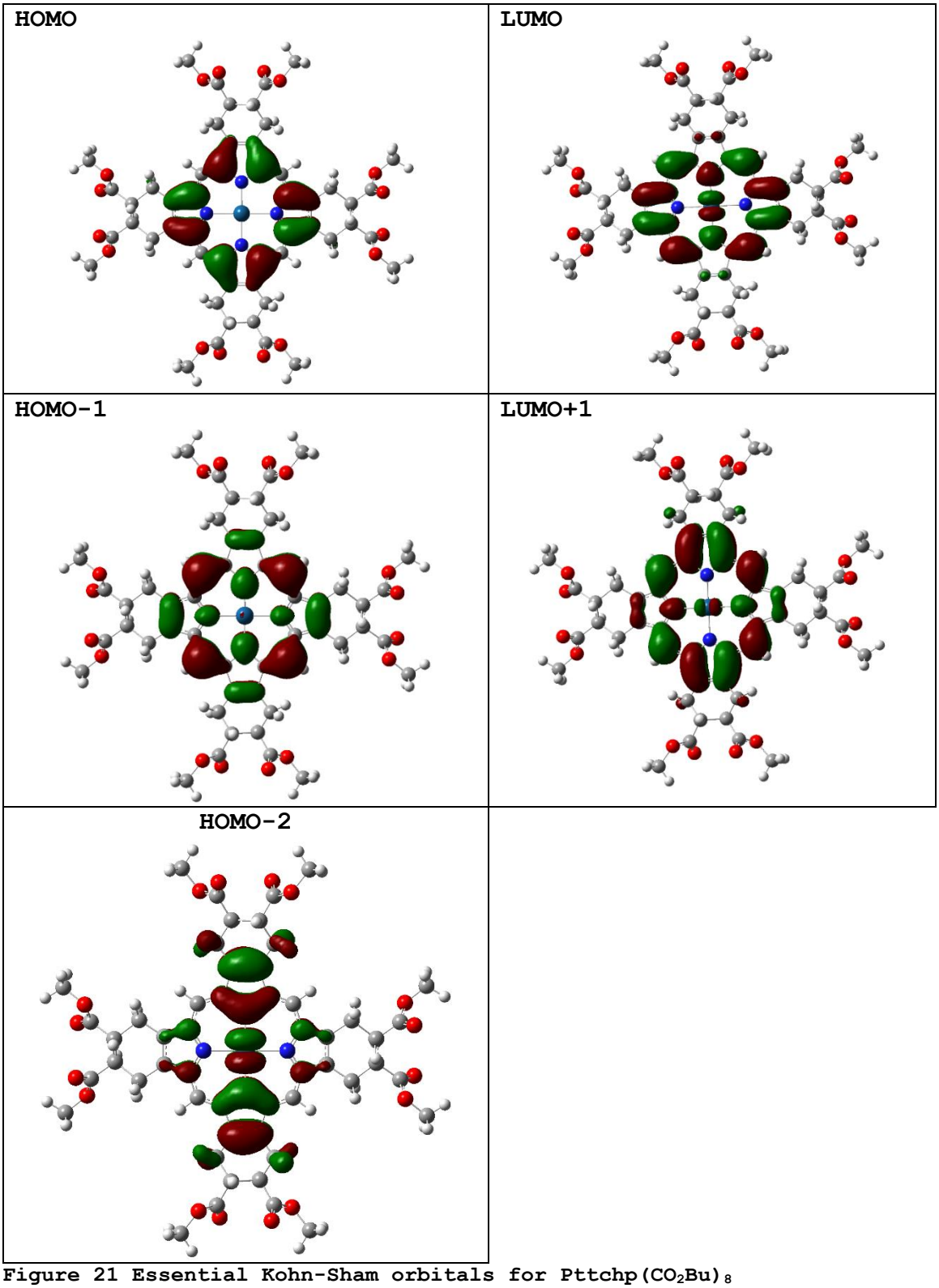

Figure 21 Essential Kohn-Sham orbitals for Pttchp(CO_2Bu)$_8$

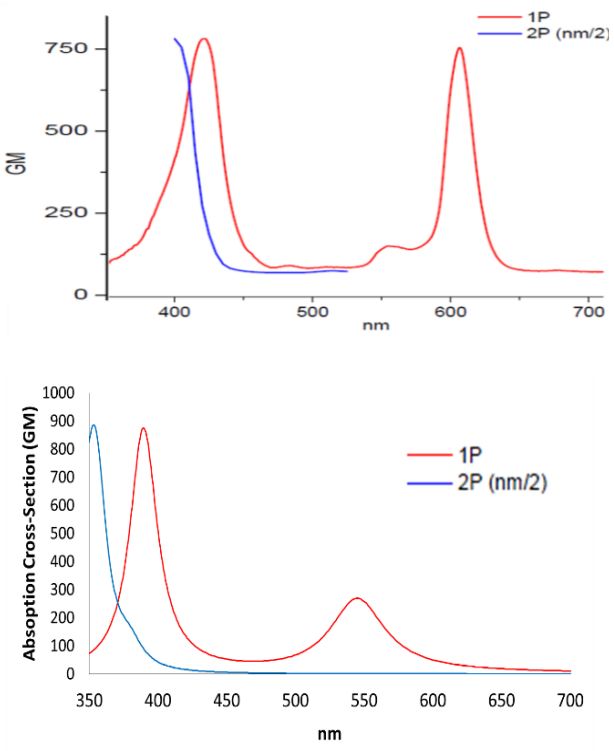

Figure 22 a) Experimental spectra of Pttbp$(CO_2Bu)_8$ b) Predicted absorption electronic spectra of Pttbp$(CO_2Bu)_8$ using TD-M05QX theory level

The experimental electronic spectra of Pttbp$(CO_2Bu)_8$ as shown in figure 21a contains an intense absorption peak in the 422nm and a smaller one at 606nm corresponding to one photon spectra. It also contains an intense two photon absorbing peak at the 400nm range. Our prediction are once again in close agreement with the experimental measurement. Our prediction is shown in figure 21b and is described as follows: for the case of one photon absorption the very intense peak lies in the 389nm and it is generated by the absorption of two symmetric excited states 4 and 5 with oscillator strength

of 1.55 (as shown in table 7a) and the nature of this transition correspond to a charge delocalization from the aromatic substituents into the metal center originating from the HOMO-1 to LUMO orbitals as shown by the essential Kohn-Sham orbitals described in figure 22. This transition is stabilized by the methoxy substituent of the benzene ring.

The small absorption peak is located at 545nm and it has an oscillator strength of 0.466 and it also correspond to the contribution of excited states 1 HOMO to LUMO and excited state 2 HOMO to LUMO+1 (symmetric states) and its mechanism correspond of LMCT stabilized later by the methoxy groups also shown in figure 22. The two-photon absorption peak is located in the 354nm region is generated by the 8^{th} excite state with a HOMO to LUMO+2 transition. This transition receives contribution by the transition dipole moment multiplication of multiple lower excited states as shown in table 7b. The nature of its transition is a MLCT from the Pt tetradendate complex toward the aromatic substituent stabilized by the methoxy substituents.

Table 7a) Relevant parameters of the lowest 9 excited singlet states in Pttbp($CO_2Bu)_8$, b) calculated transition dipoles leading to two-photon absorption and c) leading configurations of absorbing states.

State	λ, nm	Oscillator	2PA
1	545.6	0.4667	0
2	545.6	0.4666	0
3	391.06	0.0001	0
4	389.62	1.5554	0.0003
5	389.62	1.5551	0.0005
6	380.28	0	58.5814
7	379.75	0	23.0898
8	354.83	0	783.1727

2PA State	Source State	Transition Dipole Moment (Debye)			Dipole Strength
		x	y	z	
8	1	1.6565	0.0054	1.318	4.4811
	2	1.318	0.0043	-1.6561	4.4798
	4	-0.7762	-0.0026	0.6888	1.0769
	5	0.6889	0.0023	0.776	1.0768

State	Leading Configuration	Amplitude	Wavelength	Oscillator	2PA
1	HOMO → LUMO	0.65068	545 nm	0.466	0
2	HOMO → LUMO+1	0.65066	545 nm	0.466	0
4	HOMO-1 → LUMO	0.63124	389 nm	1.555	0
5	HOMO-1 → LUMO	0.63125	389 nm	1.555	0
8	HOMO → LUMO+2	0.59524	354 nm	0	783

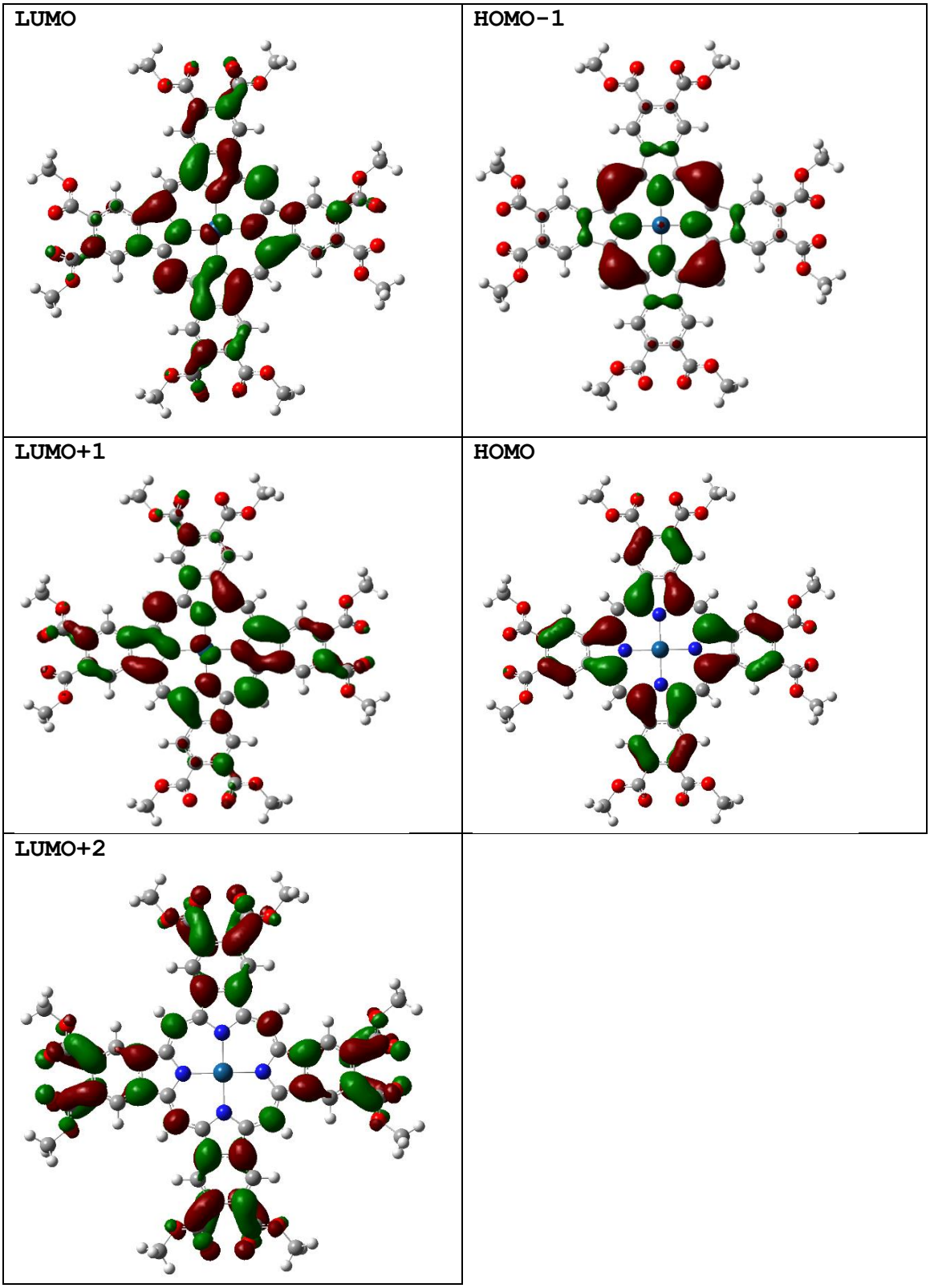

Figure 23 Essential Kohn-Sham Orbitals for in Pttbp(CO_2Bu)$_8$

6.4 Conclusion

Among the porphyrin derivatives studied, two specific phorphyrins were further investigated in order to find the effects of the aromatic substituents adjacent to the pyrrole ring. In Pttchp($CO_2Bu)_8$ the vibrational contributions allowed enough distortion which resulted in having an allowed transition for 2PA absorption. The mechanism of this transition is a Metal to ligand charge transfer. Theoretical predictions of both 1PA and 2PA spectra are found to be in close agreement with experimental measurements.

For Pttbp($CO_2Bu)_8$ the mechanism of 2PA was confirmed by our calculations to be related due to eight alkylcarboxy substituents which performed a drastic enhancement of the 2PA cross-sections in the range of wavelengths studied. Detailed analysis of the electronic structure (indicates that 2PA absorbing state is eights excited singlet (S8). It consists of mostly HOMO to LUMO+2 transition, and is coupled to strongly 1PA allowed Soret (S4/S5) and Q-bands (S1/S2) by large transition dipoles.

Although similar states are found in other porphyrins studied, alkylcarboxy substituents stabilize the LUMO+2 orbital by their strong π-acceptor effect, lowering the transition energy to the observable wavelengths range.

6.5 List of References

1. Fan, Y.; Liu, H.; Han, R.; Huang, L.; Shi, H.; Sha, Y.; Jiang, Y., Extremely High Brightness from Polymer-Encapsulated Quantum Dots for Two-Photon Cellular and Deep-Tissue Imaging. *Scientific Reports* **2015**, *5*.

2. Andrade, C. D.; Yanez, C. O.; Rodriguez, L.; Belfield, K. D., A Series of Fluorene-Based Two-Photon Absorbing Molecules: Synthesis, Linear and Nonlinear Characterization, and Bioimaging. *Journal of Organic Chemistry* **2010**, *75*, 3975-3982.

3. Zhang, Q., et al., Dual-Functional Analogous Cis-Platinum Complex with High Antitumor Activities and Two-Photon Bioimaging. *Biochemistry* **2015**, *54*, 2177-2180.

4. Bravaya, K. B.; Grigorenko, B. L.; Nemukhin, A. V.; Krylov, A. I., Quantum Chemistry Behind Bioimaging: Insights from Ab Initio Studies of Fluorescent Proteins and Their Chromophores. *Accounts of Chemical Research* **2012**, *45*, 265-275.

5. Feng, X. J.; Wu, P. L.; Bolze, F.; Leung, H. W. C.; Li, K. F.; Mak, N. K.; Kwong, D. W. J.; Nicoud, J.-F.; Cheah, K. W.; Wong, M. S., Cyanines as New Fluorescent Probes for DNA Detection and Two-Photon Excited Bioimaging. *Organic Letters* **2010**, *12*, 2194-2197.

6. Hayek, A.; Bolze, F.; Nicoud, J. F.; Baldeck, P. L.; Mely, Y., Synthesis and Characterization of Water-Soluble Two-Photon Excited Blue Fluorescent Chromophores for Bioimaging. *Photochemical & Photobiological Sciences* **2006**, *5*, 102-106.

7. Li, L.; Ge, J.; Wu, H.; Xu, Q.-H.; Yao, S. Q., Organelle-Specific Detection of Phosphatase Activities with Two-Photon Fluorogenic Probes in Cells and Tissues. *Journal of the American Chemical Society* **2012**, *134*, 12157-12167.

8. Picot, A.; D'Aleo, A.; Baldeck, P. L.; Grichine, A.; Duperray, A.; Andraud, C.; Maury, O., Long-Lived Two-Photon Excited Luminescence of Water-Soluble Europium Complex: Applications in Biological Imaging Using Two-Photon Scanning Microscopy. *Journal of the American Chemical Society* **2008**, *130*, 1532-+.

9. Wang, X., et al., Assembly, Two-Photon Absorption, and Bioimaging of Living Cells of a Cuprous Cluster. *Chemistry of Materials* **2012**, *24*, 954-961.

10. Yao, S.; Belfield, K. D., Two-Photon Fluorescent Probes for Bioimaging. *European Journal of Organic Chemistry* **2012**, 3199-3217.

11. Belfield, K. D.; Bondar, M. V.; Frazer, A.; Morales, A. R.; Kachkovsky, O. D.; Mikhailov, I. A.; Masunov, A. E.;

Przhonska, O. V., Fluorene-Based Metal-Ion Sensing Probe with High Sensitivity to Zn2+ and Efficient Two-Photon Absorption. *Journal of Physical Chemistry B* **2010**, *114*, 9313-9321.

12. Belfield, K. D.; Bondar, M. V.; Hernandez, F. E.; Masunov, A. E.; Mikhailov, I. A.; Morales, A. R.; Przhonska, O. V.; Yao, S., Two-Photon Absorption Properties of New Fluorene-Based Singlet Oxygen Photosensitizers. *Journal of Physical Chemistry C* **2009**, *113*, 4706-4711.

13. Webster, S., et al., Near-Unity Quantum Yields for Intersystem Crossing and Singlet Oxygen Generation in Polymethine-Like Molecules: Design and Experimental Realization. *Journal of Physical Chemistry Letters* **2010**, *1*, 2354-2360.

14. Brinas, R. P.; Troxler, T.; Hochstrasser, R. M.; Vinogradov, S. A., Phosphorescent Oxygen Sensor with Dendritic Protection and Two-Photon Absorbing Antenna. *J. Am. Chem. Soc.* **2005**, *127*, 11851-11862.

15. Dunphy, I.; Vinogradov, S. A.; Wilson, D. F., Oxyphor R2 and G2: Phosphors for Measuring Oxygen by Oxygen-Dependent Quenching of Phosphorescence. *Anal. Biochem.* **2002**, *310*, 191-198.

16. Schneider, H.-J.; Kato, K.; Strongin, R. M., Chemomechanical Polymers as Sensors and Actuators for

Biological and Medicinal Applications. *Sensors* **2007**, *7*, 1578-1611.

17. Kim, K.; Ha, Y.; Kaufman, L.; Churchill, D. G., Labile Zinc-Assisted Biological Phosphate Chemosensing and Related Molecular Logic Gating Interpretations. *Inorganic Chemistry* **2012**, *51*, 928-938.

18. Kamiya, M.; Asanuma, D.; Kuranaga, E.; Takeishi, A.; Sakabe, M.; Miura, M.; Nagano, T.; Urano, Y., Beta-Galactosidase Fluorescence Probe with Improved Cellular Accumulation Based on a Spirocyclized Rhodol Scaffold. *Journal of the American Chemical Society* **2011**, *133*, 12960-12963.

19. Carter, K. P.; Young, A. M.; Palmer, A. E., Fluorescent Sensors for Measuring Metal Ions in Living Systems. *Chemical Reviews* **2014**, *114*, 4564-4601.

20. Bae, S. K.; Heo, C. H.; Choi, D. J.; Sen, D.; Joe, E.-H.; Cho, B. R.; Kim, H. M., A Ratiometric Two-Photon Fluorescent Probe Reveals Reduction in Mitochondrial H2s Production in Parkinson's Disease Gene Knockout Astrocytes. *Journal of the American Chemical Society* **2013**, *135*, 9915-9923.

21. Tromberg, B. J.; Shah, N.; Lanning, R.; Cerussi, A.; Espinoza, J.; Pham, T.; Svaasand, L.; Butler, J., Non-

Invasive in Vivo Characterization of Breast Tumors Using Photon Migration Spectroscopy. *Neoplasia* **2000**, *2*, 26-40.

22. Pawlicki, M.; Collins, H. A.; Denning, R. G.; Anderson, H. L., Two-Photon Absorption and the Design of Two-Photon Dyes. *Angewandte Chemie-International Edition* **2009**, *48*, 3244-3266.

23. Kim, H. M.; Cho, B. R., Two-Photon Probes for Intracellular Free Metal Ions, Acidic Vesicles, and Lipid Rafts in Live Tissues. *Accounts of Chemical Research* **2009**, *42*, 863-872.

24. Meier, H., Conjugated Oligomers with Terminal Donor-Acceptor Substitution. *Angewandte Chemie-International Edition* **2005**, *44*, 2482-2506.

25. Nayyar, I. H.; Masunov, A. E.; Tretiak, S., Comparison of Td-Dft Methods for the Calculation of Two-Photon Absorption Spectra of Oligophenylvinylenes. *Journal of Physical Chemistry C* **2013**, *117*, 18170-18189.

26. Mikhailov, I. A.; Belfield, K. D.; Masunov, A. E., Dft-Based Methods in the Design of Two-Photon Operated Molecular Switches. *Journal of Physical Chemistry A* **2009**, *113*, 7080-7089.

27. Mikhailov, I. A.; Musial, M.; Masunov, A. E., Permanent Dipole Moments and Energies of Excited States from Density

Functional Theory Compared with Coupled Cluster Predictions: Case of Para-Nitroaniline. *Computational and Theoretical Chemistry* **2013**, *1019*, 23-32.

28. Masunov, A. M.; Tretiak, S., Prediction of Two-Photon Absorption Properties for Organic Chromophores Using Time-Dependent Density-Functional Theory. *Journal of Physical Chemistry B* **2004**, *108*, 899-907.

29. Albota, M., et al., Design of Organic Molecules with Large Two-Photon Absorption Cross Sections. *Science* **1998**, *281*, 1653-1656.

30. Pond, S. J. K.; Tsutsumi, O.; Rumi, M.; Kwon, O.; Zojer, E.; Bredas, J. L.; Marder, S. R.; Perry, J. W., Metal-Ion Sensing Fluorophores with Large Two-Photon Absorption Cross Sections: Aza-Crown Ether Substituted Donor-Acceptor-Donor Distyryl Benzenes. *Journal of the American Chemical Society* **2004**, *126*, 9291-9306.

31. Bonnett, R., Photosensitizers of the Porphyrin and Phthalocyanine Series for Photodynamic Therapy. *Chemical Society Reviews* **1995**, *24*, 19-33.

32. Gouterman, M., Spectra of Porphyrins. *Journal of Molecular Spectroscopy* **1961**, *6*, 138-163.

33. Greco, J. A.; Shima, S.; Wagner, N. L.; McCarthy, J. R.; Atticks, K.; Brückner, C.; Birge, R. R., Two-Photon

Spectroscopy of the Q-Bands of Meso-Tetraphenyl-Porphyrin and -Chlorin Framework Derivatives. *The Journal of Physical Chemistry C* **2015**, *119*, 3711-3724.

34. Drobizhev, M.; Stepanenko, Y.; Dzenis, Y.; Karotki, A.; Rebane, A.; Taylor, P. N.; Anderson, H. L., Understanding Strong Two-Photon Absorption in Pi-Conjugated Porphyrin Dimers Via Double-Resonance Enhancement in a Three-Level Model. *Journal of the American Chemical Society* **2004**, *126*, 15352-15353.

35. Drobizhev, M.; Stepanenko, Y.; Dzenis, Y.; Karotki, A.; Rebane, A.; Taylor, P. N.; Anderson, H. L., Extremely Strong near-Ir Two-Photon Absorption in Conjugated Porphyrin Dimers: Quantitative Description with Three-Essential-States Model. *Journal of Physical Chemistry B* **2005**, *109*, 7223-7236.

36. Perun, S.; Tatchen, J.; Marian, C. M., Singlet and Triplet Excited States and Intersystem Crossing in Free-Base Porphyrin: Tddft and Dft/Mrci Study. *Chemphyschem* **2008**, *9*, 282-292.

37. Finikova, O. S.; Lebedev, A. Y.; Aprelev, A.; Troxler, T.; Gao, F.; Garnacho, C.; Muro, S.; Hochstrasser, R. M.; Vinogradov, S. A., Oxygen Microscopy by Two-Photon-Excited Phosphorescence. *ChemPhysChem* **2008**, *9*, 1673-1679.

38. Rozhkov, V.; Wilson, D.; Vinogradov, S., Phosphorescent Pd Porphyrin-Dendrimers: Tuning Core Accessibility by Varying the Hydrophobicity of the Dendritic Matrix. *Macromolecules* **2002**, *35*, 1991-1993.

39. Ziemer, L. S.; Lee, W. M. F.; Vinogradov, S. A.; Sehgal, C.; Wilson, D. F., Oxygen Distribution in Murine Tumors: Characterization Using Oxygen-Dependent Quenching of Phosphorescence. *J. Appl. Physiol.* **2005**, *98*, 1503-1510.

40. Mani, T.; Niedzwiedzki, D. M.; Vinogradov, S. A., Generation of Phosphorescent Triplet States Via Photoinduced Electron Transfer: Energy and Electron Transfer Dynamics in Pt Porphyrin–Rhodamine B Dyads. *The Journal of Physical Chemistry A* **2012**, *116*, 3598-3610.

41. Lee, C. C.; MacKay, J. A.; Frechet, J. M. J.; Szoka, F. C., Designing Dendrimers for Biological Applications. *Nat Biotech* **2005**, *23*, 1517-1526.

42. Esipova, T. V.; Vinogradov, S. A., Synthesis of Phosphorescent Asymmetrically Pi-Extended Porphyrins for Two-Photon Applications. *Journal of Organic Chemistry* **2014**, *79*, 8812-8825.

43. Frisch, M. J., et al. *Gaussian 09, Revision D.01*, Gaussian, Inc.: Wallingford CT, 2009.

44. Mikhailov, I. A.; Bondar, M. V.; Belfield, K. D.; Masunov, A. E., Electronic Properties of a New Two-Photon Absorbing Fluorene Derivative: The Role of Hartree-Fock Exchange in the Density Functional Theory Design of Improved Nonlinear Chromophores. *J. Phys. Chem. C* **2009**, *113*, 20719-20724.

45. Zhao, Y.; Schultz, N. E.; Truhlar, D. G., Design of Density Functionals by Combining the Method of Constraint Satisfaction with Parametrization for Thermochemistry, Thermochemical Kinetics, and Noncovalent Interactions. *J. Chem. Theory Comput.* **2006**, *2*, 364-382.

46. Andrae, D.; Haussermann, U.; Dolg, M.; Stoll, H.; Preuss, H., Energy-Adjusted Abinitio Pseudopotentials for the 2nd and 3rd Row Transition Elements. *Theoretica Chimica Acta* **1990**, *77*, 123-141.

47. Dunning Jr., T. H.; Hay, P. J., Modern Theoretical Chemistry. *Schaefer, H. F. III (Ed.)* **1977**, *3*, 1-21.

48. Masunov, A. E. M., I. A. , Theory and Computations of Two-Photon Absorbing Photochromic Chromophores. *Eur. J. Chem.* **2010**, *1*, 142-161.

49. Casida, M. E.; Huix-Rotllant, M., Progress in Time-Dependent Density-Functional Theory. *Annual Review of Physical Chemistry, Vol 63* **2012**, *63*, 287-323.

50. Ohta, K.; Kamada, K., Theoretical Investigation of Two-Photon Absorption Allowed Excited States in Symmetrically Substituted Diacetylenes by Ab Initio Molecular-Orbital Method. *Journal of Chemical Physics* **2006**, *124*.

51. Mikhailov, I. A.; Tafur, S.; Masunov, A. E., Double Excitations and State-to-State Transition Dipoles in Pi-Pi* Excited Singlet States of Linear Polyenes: Time-Dependent Density-Functional Theory Versus Multiconfigurational Methods. *Physical Review A* **2008**, *77*.

52. Tretiak, S.; Mukamel, S., Density Matrix Analysis and Simulation of Electronic Excitations in Conjugated and Aggregated Molecules. *Chemical Reviews* **2002**, *102*, 3171-3212.

53. Chernyak, V.; Mukamel, S., Density-Matrix Representation of Nonadiabatic Couplings in Time-Dependent Density Functional (Tddft) Theories. *Journal of Chemical Physics* **2000**, *112*, 3572-3579.

54. Moreshead, W. V.; Przhonska, O. V.; Bondar, M. V.; Kachkovski, A. D.; Nayyar, I. H.; Masunov, A. E.; Woodward, A. W.; Belfield, K. D., Design of a New Optical Material with Broad Spectrum Linear and Two-Photon Absorption and Solvatochromism. *Journal of Physical Chemistry C* **2013**, *117*, 23133-23147.

55. Kuchma, M. H.; Komanski, C. B.; Colon, J.; Teblum, A.; Masunov, A. E.; Alvarado, B.; Babu, S.; Seal, S.; Summy, J.; Baker, C. H., Phosphate Ester Hydrolysis of Biologically Relevant Molecules by Cerium Oxide Nanoparticles. *Nanomedicine-Nanotechnology Biology and Medicine* **2010**, *6*, 738-744.

56. Luchita, G.; Bondar, M. V.; Yao, S.; Mikhailov, I. A.; Yanez, C. O.; Przhonska, O. V.; Masunov, A. E.; Belfield, K. D., Efficient Photochromic Transformation of a New Fluorenyl Diarylethene: One- and Two-Photon Absorption Spectroscopy. *Acs Applied Materials & Interfaces* **2011**, *3*, 3559-3567.

57. Peceli, D., et al., Enhanced Intersystem Crossing Rate in Polymethine-Like Molecules: Sulfur-Containing Squaraines Versus Oxygen-Containing Analogues. *Journal of Physical Chemistry A* **2013**, *117*, 2333-2346.

58. Toro, C.; De Boni, L.; Yao, S.; Ritchie, J. P.; Masunov, A. E.; Belfield, K. D.; Hernandez, F. E., Linear and Nonlinear Optical Characterizations of a Monomeric Symmetric Squaraine-Based Dye in Solution. *Journal of Chemical Physics* **2009**, *130*.

59. Croitor, L.; Coropceanu, E. B.; Masunov, A. E.; Rivera-Jacquez, H. J.; Siminel, A. V.; Fonari, M. S., Mechanism of Nonlinear Optical Enhancement and Supramolecular Isomerism in 1d Polymeric Zn(Ii) and Cd(Ii) Sulfates with Pyridine-4-

Aldoxime Ligands. *Journal of Physical Chemistry C* **2014**, *118*, 9217-9227.

APPENDIX A: COPYRIGHT CLEARANCE CONTENTS ON CHAPER 2

APPENDIX B: COPYRIGHT CLEARANCE CONTENTS CHAPTER 5

APPENDIX C: LIST OF PUBLICATIONS

1. **Molecular Packing in Organic Solar Cell Materials: Insights from the Emission Lineshapes of P3HT/PCBM Polymer Blend Nanoparticles**, Crotty A., Gizzi A., Rivera-Jacquez H.J., A.E. Masunov, Hu Z., Geldmeier J., Gesquire A.J., J. Phy. Chem. C.(2014),118(34), pp199975-19984

2. **Mechanism of Nonlinear Optical Enhancement and Supramolecular Isomerism in 1D Polymeric Zn(II) and Cd(II) Sulfates with Pyridine-4-aldoxime Ligands,** Croitor L., Coropceanu E., Masunov A.E., Rivera-Jacquez H.J., Siminel A., Fonari M., Phy. Chem. C.(2014),118(17), pp9217-9227

3. **Polymeric Luminescent Zn(II) and Cd(II) Dicarboxylates Decorated by Oxime Ligands: Tuning the Dimensionality and Porosity** Croitor L., Coropceanu E. B., Masunov A. E., Rivera-Jacquez H. J., Siminel A.V., Zelentsov V. I., Datsko T., Fonari M. S. Cryst. Growth Des., 2014, 14 (8), pp 3935−3948

4. **Robust Packing Patterns and Luminescence Quenching in Mononuclear [Cu(II)(phen)2] Sulfates** Melnic E., Coropceanu E., Kulikova O., Siminel A., Anderson D., Rivera-Jacquez H.J, Masunov A.E., Fonari M., Kravtsov V., J.Phy. Chem.C(2014),118, pp30087-30100

5. **New two-photon BODIPY-based fluorescent probe: Linear photophysics, stimulated emission and ultrafast spectroscopy** Belfield K., Bondar M.V., Sui B., Anderson D., Rivera-Jacquez H.J., Masunov A.E. **Submitted**

6. **From Pink to Blue and Back to Pink Again: Changing the Co(II) Ligation in a Two-Dimensional Coordination Network upon Desolvation** Chisca D., Croitor L., Coropceanu E.B., Petuhov O., Baca S., Liu S.X., Decurtins S., Rivera-Jacquez H. J., Masunov A.E., Fonari M.S. **Submitted**

7. **One- and Two-Photon Absorption Properties of Phosphorescent p-Extended Porphyrins** Esipova T.V., Rivera-Jacquez H.J., Masunov A.E., Weber B, Vinogradov S.A., **Submitted**

8. **Understanding the Response Mechanism Leads to Redesign of Aza-Crown Multi-Chromophoric Non-Linear Optical Sensor** Rivera-Jacquez H.J., Masunov A.E. **Manuscript in Preparation**